Andrea Salomon

Regulation of transcription factor HIVEP1 by inflammatory cytokines and statins

-2012-

Biologie

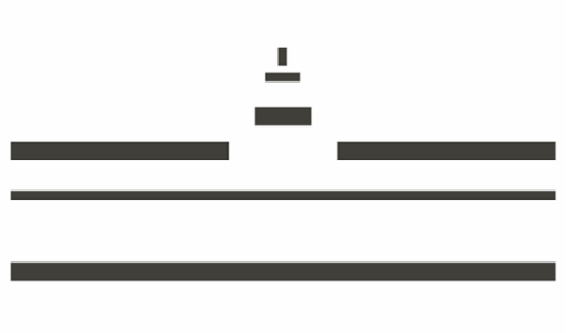

Regulation of transcription factor HIVEP1 by inflammatory cytokines and statins

Regulation des Transkriptionsfaktors HIVEP1
durch inflammatorische Cytokine und Statine

Inaugural-Dissertation

zur Erlangung des Doktorgrades

der Naturwissenschaften im Fachbereich Biologie

der Mathematisch-Naturwissenschaftlichen Fakultät

der Westfälischen Wilhelms-Universität Münster

vorgelegt von

Andrea Salomon

aus Hamm (Westf.)

- 2012 -

Dekan:	Univ.-Prof. Dr. Dirk Prüfer
Erster Gutachter:	Univ.-Prof. Dr. Dr. med. Stefan-Martin Brand
Zweiter Gutachter:	Univ.-Prof. Dr. Bruno Moerschbacher
Datum der mündlichen Prüfung:	06.07.2012
Datum der Promotion:	13.07.2012

„Man liebt das, wofür man sich müht,

und man müht sich für das, was man liebt."

Erich Fromm (1900-80)

Meinen Eltern

TABLE OF CONTENTS

ABBREVIATIONS

AP-2α	Activator Protein-2α
ARE	Adenylate-uridylate Rich Element
AS	Antisense Strand
ATP	Adenosine Triphosphate
BRE	TFIIB Recognition Element
CAD	Coronary Artery Disease
CHD	Coronary Heart Disease
ChIP	Chromatin Immunoprecipitation
COX	Cyclooxygenase
CVD	Cardiovascular Disease
Cys	Cysteine
DPE	Downstream Promoter Element
DVT	Deep Vein Thrombosis
EA.hy926	Human vascular endothelial cells
e.g.	for example
eGFP	enhanced Green Fluorescent Protein
EGR1	Early Growth Response factor 1
EMSA	Electrophoretic Mobility Shift Assay
FARIVE	FActeurs de RIsque et de récidives de la maladie thromboembolique VEineuse study
FI	Fold Induction
FPP	Farnesyl-Pyrophosphate
GAAP1	Gatekeeper of Apoptosis Activating Proteins 1
GGPP	Geranylgeranyl-Pyrophosphate
GTFs	General Transcription Factors
GTP	Guanosine Triphosphate
GWA	Genome-Wide Association study
H3/4	Histone 3/4
HAT	Histone Acetyltransferase
HDL	High-Density Lipoprotein
HEK293T	Human Embryonic Kidney cells
HeLa	Human cervix carcinoma cells

HEPG2	Human Hepatocellular carcinoma cells
His	Histidine
HIV-1	Human Immunodeficiency Virus type-1
HIVEP1	Human Immunodeficiency Virus type 1 Enhancer binding Protein 1
HMG-CoA	3-Hydroxy-3-Methylglutaryl Coenzyme A
HuH-7	Human Hepatocarcinoma cells
HUVEC	Human Umbilical Vein Endothelial Cells
i.e.	id est
ICAM-1	Intercellular Adhesion Molecule-1
IFN-β/γ	Interferon-β/γ
IκB	Inhibitor of kappa B
IKK	IκB Kinase
IL-1β/4/5/8/10/13	Interleukin-1β/4/5/8/10/13
Inr	Initiator element
IRF-1	Interferon Regulatory Factor-1
K	Lysine
LD	Linkage Disequilibrium
(ox)LDL	(oxidized) Low-Density Lipoprotein
LUC	Luciferase gene
MARTHA	MARseille THrombosis Association study
MEGA	Multiple Environmental and Genetic Assessment study
MG63	Osteosarcoma cells
miRNA	microRNA
MMPs	Matrix Metalloproteinases
MolHap	Molecular Haplotype
MolProMD	Münster Molecular Functional Profiling for Mechanism Detection study
MPs	Microparticles
ncRNA	noncoding RNA
NELF	Negative Elongation Factor
NEMO	NF-κB Essential Modifier
NF-kB	Nucelar Factor kappa-light-chain-enhancer of activated B cells
NFR	Nucleosome-Free Regions
NLS	Nuclear Location Signal
NO	Nitric Oxide

NOS	NO Synthase
ns	not significant
PAGE	SDS-Polyacrylamide Gel Electrophoresis
PAI-1	Plasminogen Activator Inhibitor-1
PDGF	Plateled-Derived Growth Factor
PE	Pulmonary Embolism
PEST	Proline Glutamic acid Serine Threonine
PIC	Preinitiation Complex
PMA	Phorbol 12-Myristate 13-Acetate
Pol II	RNA Polymerase II
RISC	RNA-Induced Silencing Complex
RLU	Relative Light Units
ROS	Reactive Oxygen Species
RP27	Ribosomal Protein 27
RT	Room Temperature
Saos-2	Human Osteosarcoma cells
shRNA	short hairpin RNA
siRNA	small interfering RNA
SNP	Single Nucleotide Polymorphism
SP1	Specificity Protein 1
SS	Sense Strand
SV40	Simian vacuolating Virus 40
TAF1/2/6/9	TBP-Associated Factors 1/2/6/9
TBP	TATA-Binding Protein
TF	Transcription Factor
TFBS	Transcription Factor Binding Site
TFIIA/B/D/E/F/H	Transcription Factor IIA/B/D/E/F/H
THP1	Human acute monocytic leukemia cells
TNFα	Tumor Necrosis Factor α
TNFαRI	TNFα type I Receptor
TSS	Transcription Start Site
TXA2	Thromboxane A2
U937	Human leukemic monocyte lymphoma cells
UTR	Untranslated Region

VD	Vascular Disease
VSMC	Vascular Smooth Muscle Cell
VT	Venous Thrombosis
VTE	Venous Thromboembolism
wt	wild type
WT1	Wilms' Tumor protein 1
Zn	Zinc

ABSTRACT

The human immunodeficiency virus type 1 enhancer binding protein 1 (HIVEP1) binds to the NF-κB consensus sequence and is therefore suggested to be involved in inflammatory signaling cascades. We recently identified two tagging SNPs, positioned 90 kb upstream (rs169713) and within exon 4 (rs2228220) of the *HIVEP1* gene, to be replicatively associated with venous thrombosis in a multistage study following GWAs (Morange et al., 2010; Germain et al., 2011). Venous thrombosis, like other vascular diseases, is a common multifactorial trait involving various pathophysiological processes. In the current work, we analyzed the impact of distinct proinflammatory stimuli on endogenous *HIVEP1* expression and found that TNFα and IL-1β increased *HIVEP1* expression in endothelial cells (EA.hy926) and monocytes (THP1). The TNFα-induced *HIVEP1* expression could be dose-dependently decreased by simvastatin and to a lesser extent by rosuvastatin and atorvastatin, but not by pravastatin or aspirin. We demonstrated the exclusive nuclear localization of HIVEP1 using western blot analyzes and immunofluorescence. Investigation of the transcriptional regulation of *HIVEP1* revealed the strongest transcriptional activity residing between positions -1650 and -1241 (from the transcription start site) in both, endothelial and monocytic cells, while an intronic modulator affected *HIVEP1* expression in a cell type-specific manner. In addition, we observed a potential enhancer capacity of a 319 bp region harbouring the rs169713 T allele in EA.hy926 and THP1 cells. Screening of 5 kb of the *HIVEP1* 5'-flanking region in 57 patients with cardiovascular disease (MolProMD study) led to the identification of ten common genetic variants. Individual subcloning and resequencing of a region encompassing three adjacent SNPs in the strong transcriptional activity portion (-1060 to -953) revealed the existence of four molecular haplotypes (MolHaps): MolHap1 (A^{-1060}-C^{-1037}-A^{-953}), MolHap2 (A^{-1060}-G^{-1037}-A^{-953}), MolHap3 (A^{-1060}-G^{-1037}-C^{-953}) and MolHap4 (T^{-1060}-G^{-1037}-C^{-953}). Using reporter gene assays, we observed a significantly decreased (~50%) transcriptional activity of MolHap4 compared to MolHap1 ($p<0.001$). To identify transcription factors involved in *HIVEP1* regulation, we performed cotransfection, ChIP and EMSA experiments and found a transcription factor module comprising the zinc finger proteins SP1, WT1 and EGR1 to be involved in *HIVEP1* expression regulation. Our analyses also suggest the involvement of the inflammatory transcription factor NF-κB in HIVEP1 expression, which is modulated by simvastatin. Our results indicate that HIVEP1 is differentially regulated by transcription factors and proinflammatory cytokines, and that it may serve as a potential pharmacological target of statins' pleiotropic pharmacologic actions. Animal and clinical studies should follow to evaluate a potential causal relationship between HIVEP1 expression and development of venous thrombosis.

1 INTRODUCTION

1.1 Studying genetic diseases

The predisposition of an individual to a disease often depends on both, environmental factors, such as nutrition, smoking and physical exercise, and genetic susceptibility. Classical twin studies, comparing monozygotic (identical) and dizygotic (fraternal) twins, are a method to analyze the contribution of environmental versus genetic factors to disease development, first published by Galton (Galton, 1875). Thereby, differences in phenotypes of monozygotic twins imply that the observed differences are due to environmental instead of genetic factors. By contrast, if a disease is influenced by heritable factors, the disease concordance would be greater in monozygotic than in dizygotic twins, postulated by Siemens in 1924, termed the twin rule of pathology (Boomsma et al., 2002). Twin studies revealed that lipoprotein(a) levels (Austin et al., 1992), the susceptibility to certain cancers, such as prostate cancer (Grönberg, 2003; Ahlbom et al., 1997), and death from coronary heart disease (CHD) at younger ages (Marenberg et al., 1994) are genetically determined.

The genetic component of a disease is based on genetic variants, i.e. a variation in the human sequence, such as single nucleotide polymorphisms (SNPs), deletions or insertions, in a single gene (monogenic “Mendelian” disease) as well as by common variants located in several genes (polygenic disease). Monogenic diseases, such as cystic fibrosis (Kerem et al., 1989) and Huntington disease (Gusella et al., 1983), are rare diseases due to evolutionary selection. Polygenic diseases are complex diseases, in which each common variant (minor allele frequency >1%) contributes moderately to disease development, termed the “common variant-weak effect-common disease” model (Cambien and Tiret, 2007). Complex diseases, such as cardiovascular disease (CVD), diabetes mellitus and dementia, are to a great extent responsible for human morbidity and mortality, pointing to the necessity to reveal the genetic mechanisms of complex diseases (Buckland, 2006).

Two strategies exist to elucidate genetic patterns that contribute to or cause disease phenotypes: Family approaches (linkage analyses) and case-control studies (association studies). Both approaches can be subdivided into the candidate gene approach and the genome-wide approach, while family approaches are classical performed using the candidate gene approach (Brand-Herrmann, 2008). If the pathophysiology of a disease is well described, association studies focus on genetic variants within genes known to be involved in the relevant pathophysiological processes (candidate gene approach). Since the human genome has been sequenced (Venter et al., 2001; Lander et al., 2001) and

costs of high throughput methods have decreased considerably, genome-wide association studies (GWAs) become increasingly popular in studying complex diseases, 1183 studies to date (http://www.genome.gov/gwastudies/). This non-hypothesis driven approach has already led to the identification of variants located in genes or intergenic regions with often unknown contribution to the disease.

1.1.1 Linkage analyses

Linkage analyses are based on genotype and phenotype data of disease-unaffected and -affected family members in different generations. It addresses the question whether a genetic marker is accumulated in affected family members, thus cosegregates with the trait of interest with higher frequency than expected by chance (Cambien and Tiret, 2007). Biostatistical algorithms combine marker, phenotype and pedigree data to identify genetic variants associated with the analyzed trait. Confirmation of the association can be conducted by a second linkage analysis comprising a higher density of genetic markers (fine mapping). Linkage analyses are often limited by the small number of affected family members and are in the need of well-defined phenotypes. Linkage analyses have been used successfully to provide information on high risk variants associated with rare disorders (Arnett et al., 2007). For example, the susceptibility gene for familial Alzheimer disease, *apolipoprotein E (ApoE)* (Pericak-Vance et al., 1991), or for early-onset breast cancer, *breast cancer 1 early-onset (BRCA1)* (Hall et al., 1990), was identified by linkage analysis.

1.1.2 Association studies

Association studies are based on different frequencies of SNPs or copy number variants (CNVs) and haplotypes in cases compared to controls. A haplotype displays the allele combination of physically close SNPs on the same chromosome, which are inherited together based on linkage disequilibrium (LD), i.e. two alleles occur on the same chromosome more often than if they were unlinked. To identify a SNP or haplotype, which is significantly associated with the trait of interest, the frequency of SNPs or haplotypes in case and control samples are compared, while statistical differences between these groups reveal the association of a SNP or haplotype with the analyzed disorder (Arnett et al., 2007). Instead of testing millions of SNPs, GWAs are performed using so-called “tagging SNPs”. The genotype of a tagging SNP predicts those of cosegregating SNPs, if both SNPs are found in LD. Since the genome can be subdivided into LD segments, a set of well-chosen tagging SNPs is able to deliver information about most common genomic

variants (Hirschhorn and Daly, 2005). A limitation of GWAs is the heterogeneity of populations, while the advantage of GWAs is the independence from a prior biological hypothesis. Individual GWAs revealed a large number of CVD-associated SNPs. Schunkert and collegues (Schunkert et al., 2011) found 13 new susceptibility loci for coronary artery disease (CAD) and validated association of previously found loci to CAD. Several loci were identified and subsequently confirmed by GWA to influence blood pressure (Newton-Cheh et al., 2009; Levy et al., 2009; Ehret et al., 2011) as well as myocardial infarction (Kathiresan et al., 2009). A follow up study of a GWA, comprising cases with a documented history of venous thromboembolism (VTE), including deep vein thrombosis (DVT), pulmonary embolism (PE) or both, and controls of the MARseille Thrombosis Association study (MARTHA), FActeurs de RIsque et de récidives de la maladie thromboembolique VEineuse (FARIVE) study and Multiple Environmental and Genetic Assessment (MEGA) study, identified a susceptibility locus for venous thrombosis on chromosome 6p24.1, the *HIVEP1* locus (Morange et al., 2010).

1.2 Vascular diseases

1.2.1 Inflammatory background of multifactorial diseases

The final goal of the acute inflammatory response, consisting of inducers (microbial infections, malfunctionaling tissue), sensors (Toll-like receptors) and mediators (tumor necrosis factor α [TNFα], interleukin-1 [IL-1]), which affect the target tissue to react in an appropriate manner, is to restore normal functionality of the affected tissue, at least by the resolution of inflammation (Medzhitov, 2008). Once the resolution of inflammation fails, e.g. due to incomplete trigger elimination, an acute inflammatory state is transformed to chronic inflammatory conditions. Thus, persistence of allergens, unrepaired tissue damage, indigestible pathogens or inadequate production of resolution mediators may cause chronic inflammation. Nonresolving inflammation leading to the development of chronic inflammatory states is involved in the pathogenesis of a variety of human diseases, such as multiple sclerosis, asthma, cancer, obesity, neurodegenerative disease, rheumatoid arthritis, type 2 diabetes mellitus or vascular diseases such as atherosclerosis (Tedgui and Mallat, 2006; Nathan and Ding, 2010).

1.2.2 Endothelial function and dysfunction

Blood vessels display a characteristic three layer, consisting of the outermost adventitia, predominantly containing elastic and collagen fibers, the media, characterized by smooth muscle cells, and the innermost intima, comprising endothelial cells (Fanghänel et al., 2003). Venous vessels usually are composed of a thinner media and a thicker adventitia compared to arteries (Fanghänel et al., 2003). The vascular endothelium, composed of a single layer of endothelial cells, builds the primary physical barrier between blood and tissue in both types of vessels. Located at this position, the endothelial cells are sensitive to changes in plasma and interstitial fluid and therefore harbouring a pivotal role in modulating the function of organs (Deanfield et al., 2007). Although the 6×10^{13} human endothelial cells, which build an area of approximately 7000 m^2 in humans (Simionescu, 2007), are heterogenic due to their tissue location, e.g. artery or vein, they share common functions, such as transport of macromolecules and solutes across the endothelium, regulation of vascular tone, contributing to coagulation, providing of an antithrombotic surface and aiding during immune response (Pober et al., 2009). Von Willebrand factor, thrombomodulin and tissue factor pathway inhibitor are coagulation regulating molecules, which are produced by the endothelium. Fibrinolysis can be activated by tissue-plasminogen activator, whose activity is in turn controlled by plasminogen activator inhibitor-1 (PAI-1) (Pober et al., 2009). Furthermore, prostacyclin and nitric oxide (NO) are important inhibitors of platelet activation and aggregation as well as inducers of vasorelaxation. Endothelial cells constitutively generate NO from L-arginine by the NO synthase (NOS). An increase in blood pressure leading to shear stress results in release of NO, that diffuses to vascular smooth muscle cells (VSMCs), thereby altering artery stiffnes by influencing the VSMC tone (Wilkinson et al., 2004). Besides its vasodilator property and suppressing effect on platelet activation, NO inhibits adhesion of monocytes at the endothelial surface by suppressing the expression of adhesion molecules and decreases low-density lipoprotein (LDL) oxidation. In clinical practice, NO is measured to reflect the state of the endothelial function (Deanfield et al., 2007).

Endothelial dysfunction in venous and arterial vessels is triggered by mechanical or chemical stress leading to decreased NOS protein expression, loss of antithrombotic properties and increased expression of cell adhesion molecules of the endothelium. These changes in endothelial properties result in vascular stiffness, platelet activation and aggregation as well as leukocyte adhesion with subsequent penetration (Celermajer, 1997; Saha et al., 2011). The molecular basis of vascular diseases (VD), such as atherosclerosis and venous thrombosis, has its basis in an early endothelial “dysfunction” (a term which is more often related to arterial disease).

1.2.3 Pathophysiology of atherosclerosis

Atherosclerosis describes a complex, multifactorial, progressive, chronic inflammatory disease of large and medium-sized arteries, exhibiting formation of plaques within the arterial walls. Artherosclerotic plaques consist of necrotic cores and lipid accumulations, calcified regions, leukocytes, endothelial and foam cells as well as activated VSMCs (Galkina and Ley, 2009). Atherosclerosis is the primary cause of CVD comprising CAD and cerebrovascular disease, the most common forms of CVD (Lusis, 2000). CVD causes 16.7 million deaths each year, therefore being the leading cause of mortality worldwide (Dahlöf, 2010).

One of the first steps in the development of atherosclerotic lesions is endothelial dysfunction caused by multiple factors, such as elevated plasma levels of oxidatively modified LDL or homocysteine, infection, increased blood pressure, smoking induced production of free radicals or genetic factors, followed by transcytosis of lipoproteins into the subendothelium (Ross, 1999) (Figure 1, 1). Accumulated lipoproteins undergo physico-chemical modifications, such as oxidation and proteo- or lipolysis, which leads to activation of endothelial cells resulting in enhanced production of cytokines and chemokines as well as endothelial cell surface adhesion molecules (E- and P-selectin, intercellular adhesion molecule-1 [ICAM-1] or vascular cell adhesion molecule-1 [VCAM-1]) (Hansson, 2005; Hansson and Hermansson, 2011) (Figure 1, 2/3). In particular, released proinflammatory cytokines, such as TNFα and IL-10, in turn activate VSMCs (Raines and Ferri, 2005) and released chemoattractant substances, such as monocyte chemoattractant protein-1 (MCP-1) and IL-8, lead to adherence of monocytes at sites of activated endothelium and subsequent migration into the subendothelium (Simionescu, 2007). Here, endothelial-released macrophage colony-stimulating factor (M-CSF) mediates differentiation of monocytes into macrophages (Hansson, 2005; Smith et al., 1995) (Figure 1, 4). Activated macrophages express scavenger receptors, which unlike LDL receptors lead to immense uncontrolled uptake of oxLDL causing transformation of macrophages into foam cells (Ross, 1993) (Figure 1, 5). The so-called “fatty streaks”, consisting of lipid-laden foam cells, endothelial lipid accumulation and T-cells, are characteristic for early atherosclerotic lesions (Hansson and Hermansson, 2011). The progress of plaque formation is mediated by cytokines, growth factors, tissue factor and interferon-γ (IFN-γ) causing proliferation and infiltration of VSMCs from the media through the internal elastic lamina into the intima of the artery (Plutzky, 2003). Subsequently, VSCMs generate extracellular matrix proteins such as collagen. In this way, a fibrous cap is developed by several VSMCs embedded in layers of connective tissue, e.g. elastic fibers and collagen, to cover the lipid and necrotic core of the atherosclerotic plaque (Plutzky, 2003; Ross, 1995) (Figure 1, 6/7). Plaque progression

and continuous thickening by infiltration of patrolling T cells, macrophages and mast cells at the shoulder of the plaque, synthesizing proinflammatory mediators (TNFα, IFNγ, IL-4) and enzymes (proteases) (Hansson and Robertson, 2006), are characteristic for later stages of atherosclerotic lesions (Figure 1, 8).

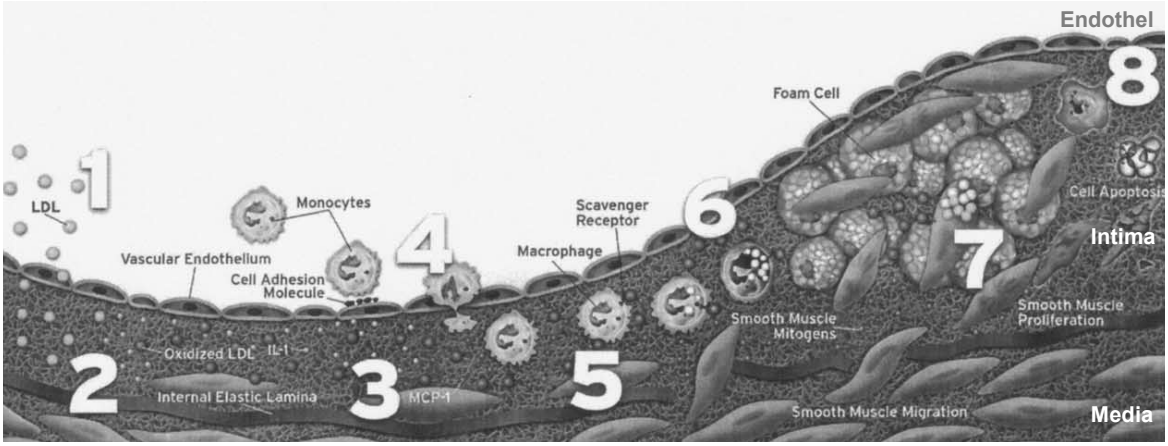

Figure 1: Stages of the atherosclerotic lesion (1) LDL particles accumulate at the surface of the endothelium. Subsequently, transcytosis and oxidation of LDL trigger the production of proinflammatory cytokines (IL-1) and chemokines (MCP-1) (2). (3) Expression of cell surface adhesion molecules and chemokines leads to attachment of monocytes, followed by migration into the subendothelium and to differentiation into macrophages (4). (5) Massive uptake of oxLDL by scavenger receptor expressing macrophages results in foam cell formation (fatty streaks). (6 and 7) Release of cytokines and growth factors mediates activation and proliferation of VSMCs, migrating out of the media into the intima. VSMCs produce extracellular matrix, which contributes to formation of a fibrous cap. (8) Later stages of atherosclerotic lesions are characterized by infiltration of patrolling T cells, mast cells and further macrophages, leading to an atherosclerotic plaque, containing a lipid and necrotic core. LDL, low-density lipoprotein; IL-1, interleukin-1; MCP-1, monocyte chemoattractant protein-1; VSMCs, vascular smooth muscle cells (adapted and printed with permission from Plutzky 2003).

The stability of an atherosclerotic plaque depends on the balance between matrix synthesis and degradation, numbers of infiltrating cells at the plaque's shoulders as well as on hemodynamic forces, especially at arterial branches (Shah, 2003). Clinical symptoms may already occur before plaque rupture, since growing atherosclerotic plaques narrow the vessels lumen (Hansson and Hermansson, 2011). Once a plaque rupture occurs due to fissuring, erosion or ulceration, the highly thrombotic substances of the plaque’s lipid core are exposed and thrombus formation is immediately initiated at the vessel’s surface by platelet aggregation and humoral coagulation. Thus, atherothrombosis in peripheral, coronary or cerebral arteries provokes gangrene, myocardial infarction or stroke, respectively, by critically reducing any further blood flow at sites of thrombus formation or in distal regions due to embolus formation (Hansson and Hermansson, 2011).

1.2.4 Venous thrombosis

In contrast to arterial thrombosis, venous thrombosis (VT) arises in the venous system, initiated primarily at the venous valves (Esmon, 2009). The incidence of symptomatic and objectively confirmed VTE is 2 to 3 per thousand inhabitants and varies strongly with age from 0.1 in adolescence to 8 per 1000 in ≥80-year-olds (Naess et al., 2007). Deep injury of the vessel wall may not be a common feature in VT as in arterial thrombosis, though mechanical (stretch or surgery) or chemical (sepsis) stress may activate the endothelium leading to an increased expression of cytokines and procoagulant proteins (tissue factor) as well as adhesion molecules, promoting thrombus formation (Saha et al., 2011). Since inflammation decreases endothelial production of antithrombotic thrombomodulin and PAI-1, while increasing tissue factor and fibrinogen, inflammation is thought to influence thrombogenesis (Wakefield et al., 2008). The initial trigger of thrombus formation in the venous system is under debate. However, in 1856 already, Virchow postulated a triad of causes, which lead to the development of VT: 1) changes in blood coagulability, as shown for alterations in genes, which lead to increased blood coagulation, such as factor V Leiden, prothrombin or factor VII (Zee et al., 2009), 2) alterations in the vessel wall, as one thrombosis initiating factor is trauma-derived injury of the vein wall leading to endothelial damage, and 3) stasis, occurring primarily at venous valves inducing hypoxia due to hemoglobin desaturation, leading to endothelial activation (Lopez et al., 2004). Activated endothelial cells express the cell surface adhesion molecules E- and P-selectin to recruit leukocytes or tissue factor-rich microparticles (MPs) to the region of stasis, where they initiate the thrombus formation cascade. MPs are phospholipid vesicles derived from leukocytes, platelets or endothelial cells. Tissue factor-bearing MPs express P-selectin-glycoprotein ligand-1 (PSGL-1) on their surface to interact with the activated endothelium or with platelets (Polgar et al., 2005; Myers et al., 2003). Subsequently, release of tissue factor to the endothelial cells triggers the coagulation reactions on the phosphaditylserine-rich activated endothelial cell surface (Figure 2). The coagulation cascade starts by the zymogen X, which is converted by the serine protease VIIa to the active enzyme Xa. Fusion of Xa and Va mediates conversion of prothrombin (II) to thrombin (IIa) (Lopez et al., 2004). The prothrombotic protease thrombin in turn leads to activation of further coagulation factors, such as XIa or VIIIa, platelet activation and fibrin formation. Fibrin deposition occurs and platelets, arriving at the fibrin clot, contribute to thrombus growth (Wu and Thiagarajan, 1996), leading to clinical manifestations such as DVT, which may cause PE.

Thrombus resolution involves recruitment of neutrophils and leukocytes, mediating fibrinolysis and collagenolysis as well as phagocytosis (Wakefield et al., 2008).

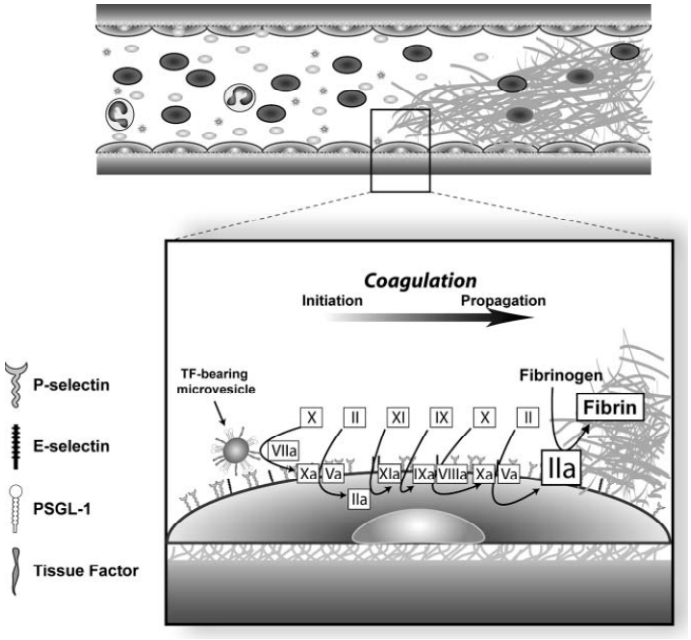

Figure 2: Model for venous thrombosis The activated endothelium upregulates expression of P- and E-selectin. Leukocyte-derived tissue factor-loaden microvesicles attach to the cell surface by interaction of PSGL-1 and endothelial selectins. Release of tissue factor to endothelial cells triggers the activation of the enzymatic coagulation cascade, resulting in thrombin synthesis and fibrin accumulation. PSGL-1, P-selectin glycoprotein ligand-1; TF, tissue factor; factor II, prothrombin; IIa, thrombin (with permission from Lopez et al., 2004).

1.2.5 Therapeutic effects of antiinflammatory drugs

In this work, we concentrated on two main drugs for the therapy of chronic inflammatory disorders: acetylsalicylic acid (e.g. aspirin) and 3-hydroxy-3-methylglutaryl coenzyme A (HMG-CoA) reductase inhibitors (statins).

Aspirin is an antiinflammatory cyclooxygenase (COX) inhibitor, which mediates its antiinflammatory property in part by inhibition of the nuclear factor kappa-light-chain-enhancer of activated B cells (NF-kB) activation, an important mediator of inflammation (Yin et al., 1998).

Large clinical trials demonstrated the beneficial effects of drug treatment with statins in the primary and secondary prevention of CHD, a major manifestation of atherosclerosis (Liao and Laufs, 2005). As HMG-CoA reductase inhibitors, statins lower the cholesterol synthesis by binding to the active site of the HMG-CoA-reductase, the rate limiting enzyme in hepatic cholesterol biosynthesis (Istvan and Deisenhofer, 2001; Goldstein and Brown, 1990). Reduced cellular cholesterol levels lead to upregulation of the LDL receptor, followed by an increased hepatic uptake of apolipoprotein B-containing lipoproteins (very-low-density lipoproteins [VLDL], intermediate-density lipoproteins [IDL],

LDL), thereby positively modifying the balance between antiatherogenic high-density lipoprotein (HDL) and atherogenic LDL through an elevation of HDL (Sposito and Chapman, 2002). Since the cholesterol level is associated with CHD (Klag et al., 1993), the positive effect of statins on the risk for CHD is attributed to their cholesterol, thus LDL lowering capacity. Clinically used statins are lovastatin, pravastatin, simvastatin, fluvastatin, atorvastatin, cervistatin, pitastatin and rosuvastatin. The various statins share the HMG-like moiety, while they differ in their tissue permeability, metabolism and efficiency to inhibit extrahepatic HMG-CoA reductase (Liao and Laufs, 2005).

Besides the cholesterol lowering effect of statins, several so-called “pleiotropic”, cholesterol-independent effects (Figure 3) have been described, which are in part based on the inhibition of the synthesis of the isoprenoid intermediates geranylgeranyl-pyrophosphate (GGPP) and farnesyl-pyrophosphate (FPP), mevalonic acid downstream products, among the endproduct cholesterol (Hansson, 2005). By a process termed prenylation, GGPP and FPP are attached to proteins, for which prenylation is necessary to attach to the cell membrane and their biological functionality. As statins are able to decrease the prenylation, they subsequently inhibit activation of the small guanosine triphosphate (GTP)-binding protein Ras and Ras-like proteins, such as Rho (Guijarro et al., 1998). Reduction of active Rho leads to reduction of NF-kB activity (Sposito and Chapman, 2002). Furthermore, animal studies have shown that statins inhibit recruitment of monocytes by downregulation of surface adhesion molecules, e.g. P-selectin, due to restorage of NO production (Lefer et al., 1999; Scalia et al., 2001), demonstrating additional antiinflammatory properties of statins. In addition, in clinical studies, such as the Cholesterol and Recurrent Events (CARE) study or the Air Force/Texas Coronary Atherosclerosis Prevention Study (AFCAPS/TexCAPS), statin treatment resulted in decreased levels of C-reactive protein, a clinical marker for systemic inflammation (Mizuno et al., 2011). The endothelial function is improved by statin use, since statins enhance the mRNA stability of endothelial NOS (Laufs and Liao, 1998), thereby increasing the endothelial production of NO, which permitts vasodilatation. Statins also decrease endothelin-1 expression, a potent vasoconstrictor, and the synthesis of reactive oxygen species (ROS) (Takemoto and Liao, 2001). The antiproliferative property of statins is attributed to the above mentioned accumulation of inactive Rho and Ras, which are involved in cell cycle regulation, as well as to the statin-mediated inhibition of VSMC proliferation, which in turn improves plaque stability (Liao and Laufs, 2005). Statins have been shown to mediate plaque stability, since they - besides their lipid lowering effect - have been shown to inhibit expression of matrix metalloproteinases (MMPs), which degrade the plaque matrix (Aikawa et al., 2001). Several statins modulate thrombogenesis by suppressing expression of tissue factor, the initiator of intravascular thrombus

formation (cf. chapter 1.2.4) (Colli et al., 1997). The coagulation activity of factor VII and the factor V dependent prothrombin activation are reduced upon statin application (Undas et al., 2001), while tissue plasminogen activator expression is increased in contrast to downregulation of its inhibitor (PAI-1) by endothelial cells (Bourcier and Libby, 2000). Additionally, platelet aggregation can be suppressed by statins, possibly by decreasing the cholesterol amount in the platelet membrane in combination with a reduced thromboxane A2 (TXA2) production (Sposito and Chapman, 2002), all together pointing to an antithrombotic property of statins.

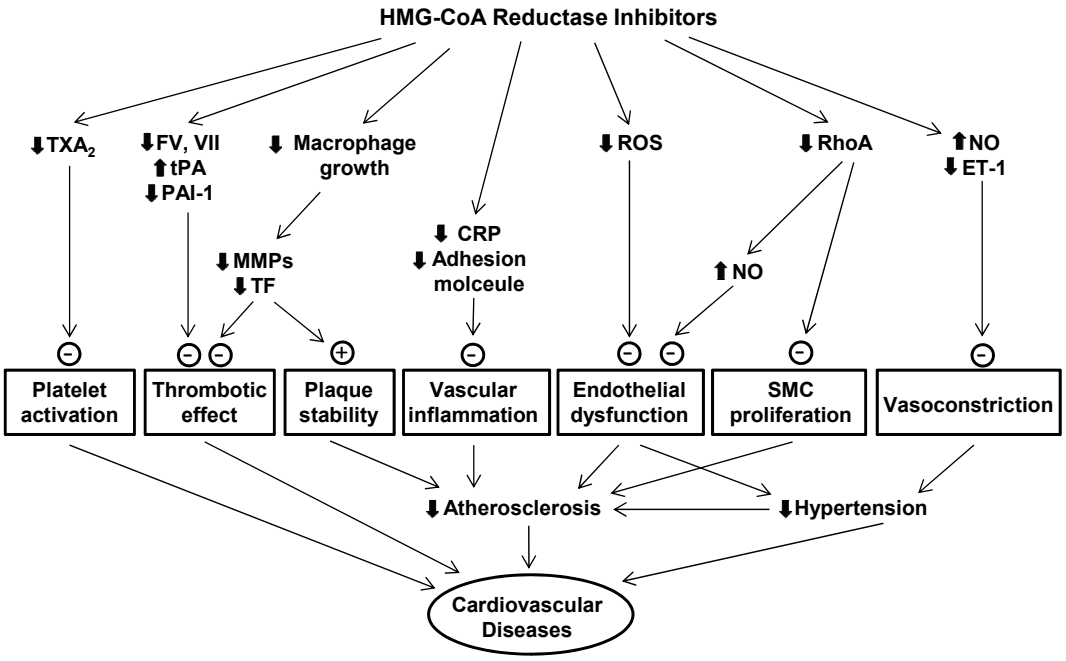

Figure 3: Pleiotropic effects of statins Overview of the cholesterol-independent impact of statins on vascular wall cells, which reduces the risk for cardiovascular diseases. Statins inhibit platelet activation, promote fibrinolysis and strengthen the plaque stability. Vascular inflammation is diminished, endothelial function is improved, and vasoconstriction as well as proliferation of vascular SMCs is suppressed by statins. TXA2, thromboxane A2; FV or VII, coagulation factor V or VII; tPA, tissue plasminogen activator; PAI-1, plasminogen activator inhibitor-1; MMPs, matrix metalloproteinases; TF, tissue factor; CRP, C-reactive protein; ROS, reactive oxygen species; NO, nitric oxide; SMC, smooth muscle cell; ET-1, endothelin-1 (modified from Takemoto and Liao, 2001).

1.3 Control of eukaryotic gene expression

The sequence of the human genome is known since 2001 (Venter et al., 2001; Lander et al., 2001). Approximately 1.5% of the genome was discovered to be protein coding, 45% to be repetitive DNA, while the function of the remaining approximately 50% of the genome is still subject to scientists' work. However, a large body of evidence suggests involvement of these noncoding sequences in gene expression regulation, harbouring important *cis*-regulatory elements, which are recognized by diverse transcription factors (Heintzman and Ren, 2009). The precise interplay of *trans*-acting factors is essential for the proper spatial and temporal gene expression in order to provide accurate execution of biological processes (Maston et al., 2006). Eukaryotic transcription can be controlled at different levels: accessibility of DNA sequence, transcription initiation and elongation, mRNA processing, transport and stability, and translation.

1.3.1 *Cis*-active transcriptional regulatory elements

Transcriptional *cis*-regulatory elements are subdivided into two classes: proximal or core regulatory elements and distal regulatory elements, such as enhancer, silencer and insulator. These regulatory elements harbour binding sites for the molecular machinery encompassing basic or general transcription factors (GTFs), activators and coactivators (Maston et al., 2006).

1.3.1.1 Core promoter – proximal regulatory elements

The core promoter surrounds the transcription start site (TSS) and defines the direction of transcription. The regulatory elements, which are required for assembling of the preinitiation complex, guiding the RNA Polymerase II upstream of the TSS to transcribe the gene, are located in the core promoter (Smale and Kadonaga, 2003). Several characteristic core promoter elements (TATA box, Inr, DPE, BRE, MTE) are located in a ~100 bp zone surrounding the TSS and are recognized by GTFs (Ohler and Wassarman, 2010) (Figure 4). Not all of the core promoter elements are present in every core promoter, the TATA box, for example, is only found in 10-16% of vertebrates' promoters and the initiator (Inr) is the most common core element, represented in 55% of promoters (Heintzman and Ren, 2007; Table 1).

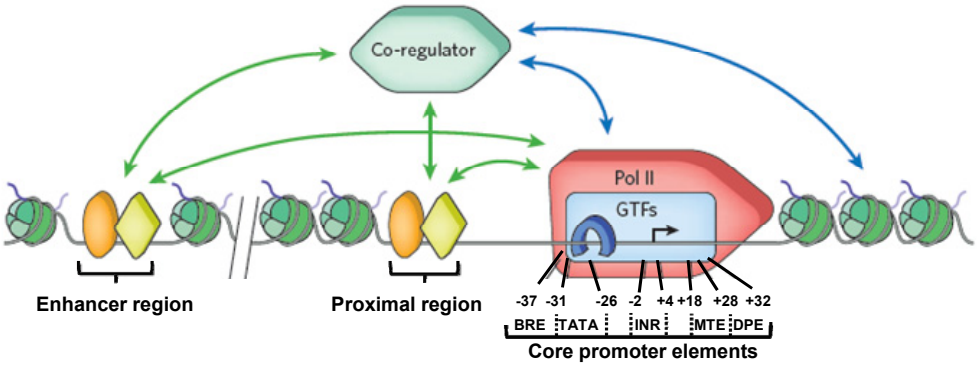

Figure 4: Transcription regulatory elements General transcription factors (GTFs) interact with specific core promoter elements (TFIIB recognition element [BRE], TATA box [TATA], initiator [Inr], motif ten element [MTE], downstream promoter element [DPE]), surrounding the transcription start site (TSS, black arrow). Numbers indicate position of core promoter elements relative to the TSS (counted in bp). Activators (orange oval and yellow diamond) bind to specific consensus sites in proximal or distal enhancer regions and interact (green arrows) with GTFs (blue rectangle and horseshoe) and coregulators (green hexagon). Coregulators may interact (blue arrows) with the general transcription machinery, chromatin-modifiers or nucleosomes (green). Pol II, RNA Polymerase II (adapted and printed with permission from Fuda et al., 2009).

Table 1: Sequences and frequencies of core promoter elements
(adapted from Heintzman and Ren 2007)

Core element	Position relative to TSS*	Consensus sequence**	Frequency in promoters	
			Flies	Vertebrates
TATA	approx. -31 to -26	TATAWAAR	33-43%	10-16%
Inr	-2 to +4	YYANWYY	69%	55%
DPE	+28 to +32	RGWYV	40%	48%
BRE	approx. -37 to -32	SSRCGCC	-	12-62%
MTE	+18 to +29	CSARCSSAACGS	8.5%	-

* Transcription start site (TSS) is assigned to position +1.
**Degenerate nucleotides represented using IUPAC codes.

The first identified core promoter element was the TATA box, an A/T-rich sequence positioned 26-31 bp upstream of the TSS and bound by a subunit of the transcription factor IID (TFIID), the TATA-binding protein (TBP) (Burley, 1996). Independent of the TATA box, the TSS surrounding Inr is able to trigger accurate transcription (Smale and Baltimore, 1989), while TATA box and Inr work synergistically, when they exist together in one core promoter (Smale et al., 1990). The Inr consensus sequence is bound by subunits of TFIID, TBP-associated factors 1/2 (TAF1 and TAF2) (Chalkley and Verrijzer, 1999). A third core promoter element, primarily present in TATA-less promoters, is the downstream promoter element (DPE), located 28-32 bp downstream of the TSS. The DPE is recognized by TAF6 and TAF9 and is, like the TATA box, suggested to be able to

communicate with enhancer regions (Butler and Kadonaga, 2001). The element first identified to be situated upstream of the TATA box, at positions -37 to -31 relative to TSS and recognized by TFIIB instead of TFIID, is the TFIIB recognition element (BRE) (Lagrange et al., 1998). But further studies found the BRE element to be located either up-or downstream of the TATA box (BRE^u and BRE^d), the position determining its repressive or active function (Deng and Roberts, 2006). Another core element is the motif ten element (MTE), at positions +18 to +29 downstream of the TSS, which needs to interact with the Inr motif to promote transcription and is able to compensate the function of mutated TATA box or DPE (Lim et al., 2004).

Beside these core elements, the existence of stretches (0.5 to 2 kb) of the CG dinucleotide, termed “CpG islands”, is a common feature in many often TATA-less promoters (Blake et al., 1990). The highest GC content was shown to be distributed to the 5’-untranslated region (5’-UTR), the TSS and the first 1000 bp upstream of the TSS. Housekeeping genes are mostly driven by CpG islands promoters, while differently regulated genes rather harbour TATA-boxes in their promoter region (Jaksik and Rzeszowska-Wolny, 2012). The majority, i.e. approximately 70% (Saxonov et al., 2006), of mammalian genes is under the control of CpG island promoters, while the minority is regulated by TATA-box comprising promoters (Carninci et al., 2006). Metyhlation occurs at CG dinucleotides, while CpG islands are predominantly nonmethylated and recruit proteins to provide an accessible chromatin state for transcription initiation. However, metyhlation of CpG islands resulting in gene silencing may occur during cell differentiation and is considered to be involved in the development of cancer (Deaton and Bird, 2011).

1.3.1.2 Distal regulatory elements

The distal regulatory elements encompass enhancer, silencer and insulator. Enhancers mostly harbour clusters of transcription factor binding sites (TFBS) and action in a distance- and orientation-independent manner (Maston et al., 2006). Thus, they may be located several hundreds of kilobase pairs up- or downstream of the TSS, as shown for the three interleukin genes *IL-4*, *IL-13* and *IL-5*, which are spread over 120 kb and are controlled by one regulatory element (Loots et al., 2000). The favored mechanism by which the distant enhancer element can interact with the core promoter region is “DNA-looping” (Vilar and Saiz, 2005). Enhancers possess different mechanisms to enhance transcription of the core promoter. First of all, enhancers may modify the chromatin structure. The basic unit of the chromatin is the nucleosom, which consists of ~146 bp of DNA wrapped around a histone octamer complex, harbouring two H2A-H2B dimers and one H3-H4 histone tetramer (Luger et al., 1997). By recruitment of the

nucleosome-remodeling complex comprising SWI//SNF proteins, the position of nucleosomes at the DNA is altered in an adenosine triphosphate (ATP)-dependent manner, allowing easier access of the transcription machinery to the core promoter to activate transcription (Kingston and Narlikar, 1999). A second mechanism to promote transcription is the recruitment of protein complexes, which leads to histone-acetylation, resulting in decondensation of the chromatin (Heintzman and Ren, 2009). At least, enhancers may interact with the mediator complex, connecting activators binding at the enhancer region with GTFs to initiate transcription (Myers and Kornberg, 2000).

Silencers, as enhancers, work in an orientation- and distance-independent manner, but repress gene transcription instead of enhancing it, thus containing consensus sites for repressors (Ogbourne and Antalis, 1998). An activator may switch to a repressor by interaction with repressive coactivators. Repressors inhibit transcription by competition with activators at consensus sites, as shown for specificity protein 1 and 3 (Li et al., 2004), or by direct inhibition of the activator (Harris et al., 2005). In contrast to enhancers, silencers may recruit complexes to mediate chromatin stability (Srinivasan and Atchison, 2004).

Insulators or boundary elements form a wall between neighboring genes and their gene-specific regulatory element to prevent that one gene is affected by the transcription machinery of the nearby gene (Maston et al., 2006). Insulators function in a position-dependent but orientation-independent manner. On the one hand, they are able to block the spread of repressive chromatin (heterochromatin-barrier activity). On the other hand, an insulator may inhibit activation of transcription by catching an activator and thereby preventing this factor from binding at its target promoter to enhance transcription, termed enhancer-blocking activity (Maston et al., 2006).

1.3.2 Eukaryotic transcription

1.3.2.1 Modification of the chromatin structure

The first rate limiting step of transcription is the access of the transcriptional machinery to the DNA sequence, whereby the local chromatin structure at promoters plays a pivotal role (Mellor, 2005). Studies in yeast demonstrated the association of active promoters with nucleosome-free regions (NFR) (Lee et al., 2004). Yuan et al. (Yuan et al., 2005) suggested the region ~150 to ~200 bp upstream of the start codon to be characterized by nucleosome depletion and flanked on both sides by nucleosomes. Heintzman and Ren (Heintzman and Ren, 2007) confirmed that NFR also exist in humans, which is in accordance to observations of increased chromatin accessibility at regulatory elements (Felsenfeld, 1996), pointing to an evolutionarily conserved mechanism of nucleosome

depletion at active promoters. In addition, histone modifications seem to be associated with regulatory and transcribed regions. A conserved mechanism, which comes along with active genetic regions, is acetylation of histone H3 and H4 (Roh et al., 2005). Acetylation of lysine residues of histones is a reversible modification conducted by histone acetyltransferases (HATs) and histone deacetylases (HDACs). As mentioned above, the transfer of HATs to regulatory regions is mediated by transcription factors and increased by enhancers. On the other hand, methylation of histones is executed by histone methyltransferases (HMTs), adding one to three methylgroups to lysine (K) residues. A 3' to 5' gradient of H3K4 methylation was observed within transcribed regions peaking in trimethylation at the 5'-end (Pokholok et al., 2005). Methylation also occurs in CpG islands by modification of cytosines. Depending on the methylated residue, methylation may result in activation or repression of transcription (Heintzman and Ren, 2007). Taken together, active promoter regions are characterized by NFR, H3/H4 acetylation and trimethylation of H3K4.

1.3.2.2 The transcription cycle

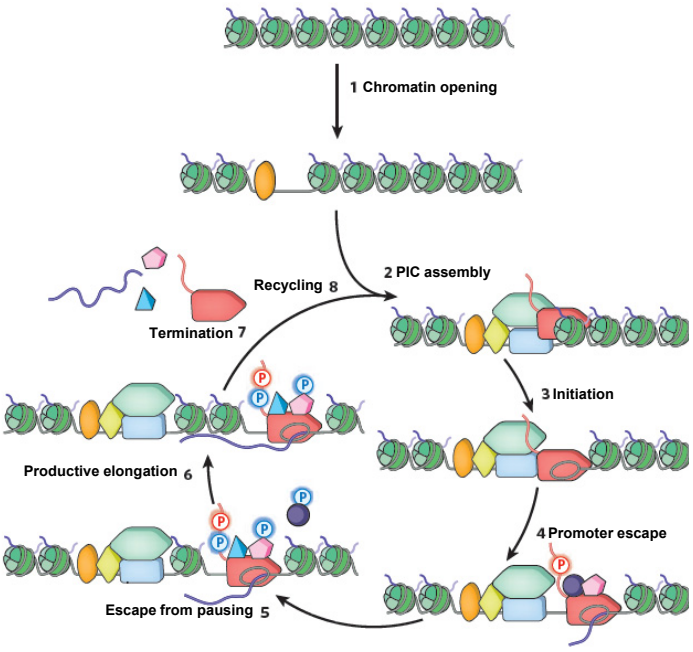

Figure 5: Steps of the eukaryotic transcription cycle (1) An activator (orange oval) recruits nucleosome remodellers to decondensate the chromatin. A second activator (yellow diamond) recruits GTFs (blue rectangle) and coactivators (green hexagon), leading to entry of Pol II (red rocket) and PIC assembling (2). (3) DNA is unwound at TSS, transcription is initiated. (4) Pol II escapes from the promoter, transcribes up to 50 bases (RNA, purple line) and is phosphorylated to pause, mediated by SPT4/5 (pink pentagon) and NELF (purple cycle). (5) Hyperphosphorylation by P-TEFb (blue triangle) results in escape from pausing. (6) Elongation, the entire gene is transcribed until termination (7) leads to release of Pol II, which can initiate a new transcription cycle (8). GTFs, general transcription factors; Pol II, RNA Polymerase II; PIC, preinitiation complex; NELF, negative elongation factor; P-TEFb, positive transcription elongation factor b (adapted and printed with permission from Fuda et al., 2009).

The eukaryotic transcription cycle can be subdivided into eight major steps (Figure 5), which may be controlled and influenced by activators to modulate the rate of transcription

(Fuda et al., 2009). First of all, the transcription machinery has to gain access to the DNA sequence, implying chromatin remodeling (step 1), as described above (cf. chapter 1.3.2.1). Then preinitiation complex (PIC) can be assembled (step 2), which may occur in two different ways: the sequential assembly pathway or the RNA Polymerase II (Pol II) Holoenzyme pathway (two-component). The sequential pathway starts with binding of TFIID to the TATA box. This interaction is stabilized by the following entry of TFIIA and TFIIB, leading to attachment of Pol II and TFIIF. At last TFIIE and TFIIH join the stable TFIID-TFIIA-TFIIB-Pol II/TFIIF-promoter complex to finish the PIC assembling (Thomas and Chiang, 2006). The two-component pathway suggests preformation of complexes harbouring GTFs and Pol II (for details refer to Thomas and Chiang, 2006). In the next step, the DNA surrounding the TSS is unwound, the transcription bubble is built and transcription is initiated by Pol II (step 3). Pol II then escapes from the core promoter, produces 20-50 bases of RNA downstream of the TSS (step 4) and pauses due to phosphorylation by the negative elongation factor (NELF). Further hyperphosphorylation and dissociation of NELF leads to escape of the Pol II from pausing in order to elongate transcription (step 5). Pol II transcribes the entire gene (step 6), following termination and consequent release of RNA and Pol II from the DNA (step 7), which can initiate a new transcription cycle (step 8) (Fuda et al., 2009).

1.3.2.3 Posttranscriptional control by microRNA

Eukaryotic gene expression can be controlled at different levels (cf. chapter 1.3). Besides the first control point, the accessibility of the transcription machinery to the DNA, eukaryotic gene expression can be regulated at last posttranscriptionally by small noncoding RNAs (ncRNAs), especially by microRNAs (miRNAs) (He and Hannon, 2004). miRNAs are small ncRNAs of 21 to 25 nucleotides, deriving from larger precursors, which are characterized by imperfect stem loop structures (Bartel, 2004). The mature miRNA is assembled in a RNA-induced silencing complex (RISC), containing Argonaute proteins, harbouring endonuclease activity for cleavage of the target mRNA. Usually, the 3'-UTR of a target gene is recognized by the RISC, which leads to mRNA degradation or translation inhibition. About 60% of protein coding genes are considered to be posttranscriptionally regulated by miRNAs (Esteller, 2011). The gene silencing effect of miRNAs is technically used to mediate a precise knockdown of the gene of interest. Thereby, miRNA can be synthetically produced as a small interfering RNA (siRNA) duplex, comprising 21 to 23 nucleotides complementary to the target mRNA, or as a vector based short hairpin RNA (shRNA) (Rao et al., 2009). siRNA duplexes are delivered by transfection as well as shRNA expression vectors, which continuously produce shRNA in the transfected cell.

1.4 Transcription factor human immunodeficiency virus type 1 enhancer binding protein 1 (HIVEP1)

1.4.1 Transcription factor families

Transcription factors (TFs) represent the largest most varying class of DNA-binding proteins. They are responsible for tissue- and stimuli-specific gene regulation in order to mediate cell growth, differentiation and development. TFs often harbour two domains: a DNA-binding domain and an activation domain, to act in response to certain stimuli, such as growth or inflammation. On the basis of their related primary sequence and three-dimensional structure of the DNA-binding domain, TFs are subdivided into diverse groups harbouring a specific DNA-binding-motif, such as the helix-turn-helix, helix-loop-helix, leucine zipper, homeodomain, steroid receptor or zinc finger motif (Pabo and Sauer, 1992; Latchman, 1997). Besides the diversity of DNA-binding motifs of TFs, some overall principles of site-specific recognition are suggested: 1) Contacts to the bases and DNA-backbone is essential, 2) hydrogen bonding is crucial for recognition, 3) side chains mediate the critical contacts, 4) protein folding and docking at the DNA severe correct position of side chains, 5) interactions take place into the major groove, especially with purines, 6) DNA-binding motifs often contain α-helices, fitting in the major groove, 7) hydrogen bonds and/or salt bridges mediate the contact to the DNA-backbone, 8) site-specific recognition implies multiple DNA-binding domains and 9) hydration and sequence-specific aspects of the DNA structure may be critical for recognition (Pabo and Sauer, 1992).

1.4.1.1 Zinc finger proteins

Zinc (Zn) finger containing proteins contribute to several cellular processes, such as development, differentiation and tumor suppression, and represent ~1% of all mammalian proteins, displaying the largest family of regulatory proteins in mammals (Iuchi, 2001). There exist 8 classes of Zn finger proteins, which differ in nature and distribution of their Zn-binding residues and their ability to bind DNA or RNA or to mediate protein-protein or protein-lipid interactions (Krishna et al., 2003). One single Zn finger domain is unable to bind to the DNA, resulting in the presence of at least two, but mostly multiple Zn fingers in one Zn finger protein. The Zn finger domain is characterized by one (or more) central Zn ion, which is (are) bound by conserved cysteine (Cys) or histidine (His) residues (Klug and Rhodes, 1987). The “classical” C2H2 Zn finger represents the major group of Zn fingers in the human genome, consisting of one Zn ion, that is bound by two Cys and two His residues (Miller et al., 1985). The C2H2 Zn finger was first identified in the *Xenopus* TFIIA

(Miller et al., 1985), and the consensus sequence described is Cys-X_{2-4}-Cys-X_{12}-His-X_{3-5}-His (Pabo and Sauer, 1992). The folded structure is composed of a 12 residue α-helix, harbouring the two His and a β-sheet hairpin, the two Cys residing in its turn (Pavletich and Pabo, 1991). To bind to the DNA, the N-terminus of the α-helix lies in the major groove and protein-DNA interactions may be executed by DNA phosphates, interacting with arginine and serine side chains as well as with the first Zn-coordinating His by hydrogen bond formation (Harrison, 1991). Additionally, a set of hydrogen bonds between guanine and arginine or histidine mediates the contact between the DNA and Zn finger (Pabo and Sauer, 1992).
Besides the common Zn finger motif, there exist several other DNA-binding domains, such as the Rel homology domain, characteristic for the NF-κB family.

1.4.1.2 Inflammatory transcription factors: The NF-κB family

Members of the NF-κB transcription factor family, which is conserved from the phylum Cnidaria to humans (Gilmore, 2006), coordinate the expression of a variety of genes involved in cell proliferation, apoptosis, immune response and inflammatory diseases, such as multiple sclerosis and rheumatoid arthritis (Li and Verma, 2002). In contrast to non-atherosclerotic vessels, activated NF-κB is found in SMCs and macrophages, infiltrating atherosclerotic lesions, linking activated NF-κB signaling to CVD (Brand et al., 1996).
The NF-κB family can be subdivided into two groups: NF-κB and Rel proteins. The “NF-κB subfamily” encompasses the two TFs p50 and p52, which arise from processed p105 and p100, respectively. p105 and p100 harbour copies of ankyrin repeats, inhibiting their function, while they share with “Rel proteins” (RelA (p65), c-Rel, and RelB) the N-terminal DNA-binding/dimerization Rel homology domain (RHD) (Gilmore, 2006). In addition, Rel proteins contain the transactivation domain (TAD) to interact with GTFs TBP or TFIIB and coactivators (Schmitz et al., 1995; Sheppard et al., 1999), positively mediating gene expression, while p50 and p52 need coactivators or another NF-κB member for initiating gene expression. The activity of NF-κB is strongly controlled, as inactive NF-κB is maintained in the cytoplasm in a complex with inhibitor of kappa B (IκB) proteins (IκBα, IκBβ or IκBε) or the precursor p100 or p105 (Hayden and Ghosh, 2008). IκBs are distributed to different tissues and distinct NF-κB dimers. IκBα, as an example, covers the nuclear location signal (NLS) and interacts with DNA binding sites (Gilmore, 2006). The recognition site (κB-site) of all NF-κB TFs consists of 9 to 10 bp and is highly variable (5’-GGGRNWYYCC-3’; R, purine; N, any nucleotide; W, A or T; Y, pyrimidine) (Hoffmann et al., 2006). All NF-κB proteins form homo- and heterodimers, except for RelB, which

generates only heterodimers, while the major heterodimer *in vivo* is p50-RelA (Gilmore 2006).

There are two major pathways leading to NF-κB activation: The canoncial (classic) and the non-canoncial pathway (Chen and Greene, 2004; Figure 6). Both pathways lead to activation of IκB kinases (IKKs) and finally to degradation of IκBs or p100/p105, which results in release and translocation of the NF-κB dimer into the nucleus to regulate gene expression. In the canonical pathway (Figure 6), NF-κB dimers, such as p50/RelA, are maintained in the cytoplasm associated to IκBα. Binding of ligands to their receptors, e.g. TNFα to the TNF-receptor, leads to recruitment of adaptors, as TNF receptor-associated factors (TRAFs), which play a central role in receptor-induced IKK activation (Devin et al., 2001). IKK1 and IKK2, also termed IKKα and IKKβ, are associated with the regulatory scaffold NF-κB essential modifier (NEMO) to form the IKK complex (Krappmann et al., 2000). Subsequently, IKK2 phosphorylates serine residues of IκBα, resulting in its ubiquitylation and subsequent degradation by the 26S proteasome, which leads to release and translocation of p50/RelA into the nucleus (Chen and Greene, 2004). The NF-κB dimer regulates transcription of various genes, including the IκBα gene, providing a negative feedback mechanism of the canoncial NF-κB activation pathway.

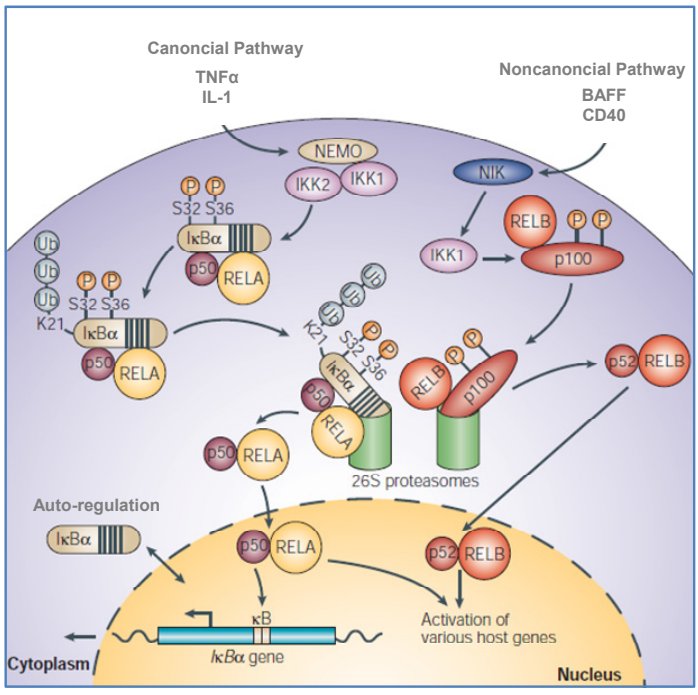

Figure 6: Pathways for NF-κB activation In the canoncial pathway, activation of the IKK complex (IKK1/2 and NEMO) by TNFα or IL-1 leads to phosphorylation, subsequent ubiquitylation and degradation of IκBα, resulting in the release and translocation of NF-κB dimer p50/RelA into the nucleus, mediating gene expression. Negative feedback regulation is executed by activation of the IκBα gene. NIK activation in the non-canoncial pathway by BAFF, for example, activates IKK1, which in turn phosphorylates the RelB/p100 dimer. The following p100 processing generates p52, and the p52/RelB dimer is translocated into the nucleus to promote target gene expression. TNFα, tumor necrosis factor α; IL-1, interleukin 1; IKK, IκB kinase; NEMO, NF-κB essential modifier; NIK, NF-κB-inducing kinase; BAFF, B-cell activating factor (adapted and printed with permission from Chen and Greene, 2004).

The non-canoncial pathway (Figure 6) mainly activates the p100/RelB complex and is mediated by certain receptors, such as B-cell activating factor (BAFF) or CD40 (Gilmore 2006). In this pathway, the IKK complex does not involve NEMO and only consists of IKK1. Ligand-binding activates the NF-κB-inducing kinase (NIK), which phosphorylates and activates IKK1, leading to phosphorylation of p100 of the p100/RelB dimer. Subsequent ubiquitylation and degradation of p100 results in p52 generation (Amir et al., 2004). In turn, the active p52/RelB heterodimer translocates into the nucleus to regulate target gene expression (Chen and Greene, 2004).

NF-κB target genes can be classified into two groups, depending on the chromatin structure of their promoter region. Chromatin remodeling is not necessary for constitutively and immediately accessible promoters, while stimulus-dependent genes require chromatin modification for gene expression (Natoli et al., 2005)**,** suggesting chromatin modification to be involved in NF-κB selectivity (Smale, 2011). As an example, IL1-β stimulation leads to acetylation of histone H4 in the granulocyte-macrophage colony-stimulating factor (GM-CSF) promoter, permitting access of Pol II and transcription initiation (Ito et al., 2000). Major target genes for NF-κB dimers are genes encoding proinflammatory cytokines, chemokines, adhesion molecules, inducible NOS, MMPs and COX2. It is still discussed, whether NF-κB increased proinflammatory gene expression is the result of or trigger for increased NF-κB activity (Li and Verma, 2002).

Besides IκB degradation and NF-κB transport into the nucleus, full activation of the NF-κB pathway requires distinct posttranslational modifications, including phosphorylation and acetylation (Chen and Greene, 2004). Phosphorylation of the NF-κB dimer enables the TF to interact with coactivators or directly enhances its transcriptional response. In case of RelA, phosphorylation of distinct serines enhances binding of the coactivators CREB-binding protein (CBP) and p300 to RelA, resulting in easier displacement of repressive histone deactylase complexes from promoter regions of target genes (Zhong et al., 2002). Thus, phosphorylation of RelA at several sites leads to recruitment of different coactivators, resulting in distinct patterns of gene expression (Chen and Greene, 2004). Directly increased transcriptional activity of RelA is also mediated by different serines, phosphorylated by various kinases, such as the mitogen- and stress-activated kinase-1 (MSK1) or protein kinase A (PKA_c) (Vermeulen et al., 2003; Zhong et al., 1997). In addition, acetylation of RelA occurs *in vivo* in response to TNFα or phorbol 12-myristate 13-acetate (PMA) (Rahman et al., 2002). The RelA-IκBα complex is disintegrated by acetylation of RelA at lysine 221, resulting in increased RelA activity (Chen and Greene, 2004). In conclusion, posttranslational modifications of NF-κB have a major impact on the intensity of the NF-κB response.

1.4.2 HIVEP1 - gene and protein

Besides NF-κB family members, the κB motif can be recognized by the neuronal κB binding factor (NKBF) (Moerman et al., 1999), developing brain factors (DBF1/2) (Cauley and Verma 1994), the brain-specific enhancer binding transcription activator (BETA) (Korner et al., 1989) or the HIVEP family (Hicar et al., 2001).

The *HIVEP* genes *HIVEP1*, *HIVEP2* and *HIVEP3* are characterized by one large exon of ~5.5 kb and by relatively small and nonconserved exons, spread over a large DNA region at the 5' end. The 3' region is more conserved, concerning exon size, exon-intron boundaries and sequence, since all *HIVEP* genes harbour a 176 bp exon, encoding most of their C-terminal Zn finger pair (Hicar et al., 2001). Proteins encoded by the *HIVEP* gene family are large proteins, comprising four to five Zn fingers and two ZAS domains, in which a characteristic pair of C2H2 Zn fingers is linked to an acidic-rich and serine/threonine-rich region (Wu et al., 1996). HIVEP proteins share only up to ~30% sequence similarity, but distinct protein regions, such as two Zn finger pairs, a putative NLS and the 5'-flanking proline- and glutamine/aspartate-rich region, including the immediately downstream serine-rich sequence, are highly conserved (Hicar et al., 2001).

The *HIVEP1 (MBP1/PRDII-BF/ZNF40)* gene is located on chromosome 6 (6p24), spanning ~152 kb and consisting of 9 exons (cf. chapter 4.2.2). The 6p24 locus has been shown to be associated with acute myeloid leukemia (AML) (Chen et al., 2000) and the schizophrenia susceptibility locus maps to chromosomal region 6p22-6p24 (Olavesen et al., 1997). However, no studies have observed the *HIVEP1* expression regulation up to now. The full length mRNA size of HIVEP1 is 8891 bp (NM_002114.2) and was detected by northern blots in several cell lines, including human cervix carcinoma (HeLa) cells, human B cell lines (X50-7, BJA-B), T cell line Jurkat, human retinal cell line and human fibroblasts (GM0010) (Baldwin et al., 1990). The full length HIVEP1 protein has a predicted size of 298 kDa and harbours two sets of C2H2 Zn finger pairs, which are widely separated by 1630 amino acids. Another Zn finger (C2X13HC) is located between the two pairs of C2H2 Zn fingers and an acidic putative transcription activation domain was found to be located downstream from the C-terminal Zn finger set (Fan and Maniatis, 1990). A possible phosphorylation site, rich of serine and threonine residues, and a putative NLS are positioned in the N-terminal part of HIVEP1 (Baldwin et al., 1990).

By electrophoretic mobility shift assays (EMSAs), recombinant HIVEP1 has been shown to bind NF-κB and related motifs within the enhancer element of human immunodeficiency virus type-1 (HIV-1) and promoter regions of immunoglobulin kappa (Igκ), major histocompatibility complex (MHC) class I, interleukin 2-receptor (IL-2R) and interferon-β (IFN-β) (Baldwin et al., 1990; Fan and Maniatis, 1990; Muchardt et al., 1992; Seeler et al., 1994). Thereby, Fan and Maniatis (Fan and Maniatis, 1990) demonstrated that each set of

Zn fingers is able to bind to NF-kB motifs independently. Two alternative *HIVEP1* splice products have been proposed with predicted protein sizes of 70 kDa and 200 kDa, lacking the first (exon 4) and second (exon 6) Zn finger pair respectively, while both splice products were not able to activate *HIV-1* gene expression (Muchardt et al., 1992), in contrast to recombinant full length HIVEP1 *in vitro* (Seeler et al., 1994). Instead, the 70 kDa alternative splice product of *HIVEP1*, designated gatekeeper of apoptosis activating proteins 1 (GAAP1), was found *in vitro* to increase the expression of interferon regulatory factor-1 (IRF-1) and p53 by binding to a novel regulatory element in their promoter regions, the IRF-1/p53 common sequence (IPCS) motif (Lallemand et al., 2002). An enhanced green fluorescent protein (eGFP)/GAAP1 fusion protein encoding plasmid was transfected into human hepatocarcinoma cells (HuH-7) and detected in both, the cytoplasm and nucleus. Notably, after deletion of a C-terminal PEST-like (i.e. rich in proline, glutamic acid, serine, threonine) sequence, GAAP1 was located exclusively in the nucleus (Lallemand et al., 2002). In this respect, Fan and Maniatis (Fan and Maniatis, 1990) reported exclusive nuclear localization of HIVEP1 in osteosarcoma cells (MG63), using an antibody, that targets the C-terminal residue of HIVEP1. Another HIVEP1 peptide, termed Cirhin interaction protein (Cirip), harbouring the C-terminal Zn finger pair and a NLS, was identified by yeast two-hybrid screening as well as coimmunoprecipitation to interact with the nucleolar protein Cirhin, which leads to increased Cirip action on the *HIV-1* enhancer (Yu et al., 2009). Mutation in *CIRH1A* led to amino acid change in Cirhin causing North American Indian Childhood Cirrhosis (NAIC) and weakens its positive regulatory effect on Cirip activity (Yu et al., 2009).

So far, studies investigating the DNA binding capacity of HIVEP1 were based on recombinant HIVEP1 and the cellular role of HIVEP1 in NF-κB signaling and proinflammatory or apoptotic processes is not well characterized.

1.5 Aim and design of the study

Since we recently identified the *HIVEP1* locus to be replicatively associated with VT, with at least two tagging SNPs, one positioned 90 kb upstream (rs169713) and one in exon 4 (rs2228220) of the *HIVEP1* gene (Morange et al., 2010; Germain et al., 2011), and HIVEP1 was suggested to regulate expression of genes involved in inflammatory processes by recognizing NF-κB motifs, the aim of the current thesis was to characterize the regulation of *HIVEP1* expression in a broader context, especially with respect to inflammatory conditions. As knowledge on *HIVEP1* gene regulation is rather scarce to date, we attempted to analyze the gene expression regulation of *HIVEP1* in endothelial and monocytic cells under basic and inflammatory conditions by semiquantitative PCR. Since statins harbour antiinflammatory properties, most likely via NF-κB singaling, we subsequently tested the potential impact of different clinically used statins on *HIVEP1* expression in endothelial cells under basic and inflammatory conditions. After investigation of the influence of inflammatory cytokines or statins on HIVEP1 mRNA expression, we analyzed the observed effects at the protein level using western blot. Since functionally active *HIVEP1* promoter regions and potential transcriptional regulators have not been yet characterized, we aimed at functionally analyzing the *HIVEP1* promoter structure, including a potential enhancer region encompassing rs169713. We thus performed reporter gene assays in both, monocytic and endothelial cells, to identify a putative cell type-specific *HIVEP1* promoter structure and function. In addition, we analyzed the 5'-flanking region of *HIVEP1* with respect to genetic variants and molecular haplotypes (MolHaps) and analyzed their influence on transcriptional activities. Subsequently, we conducted *in silico* analyses for prediction of potential TFs binding to the identified *HIVEP1* promoter or regulatory regions, to evaluate the impact of *trans*-acting factors on *HIVEP1* expression regulation. To demonstrate a potential impact of predicted TFs on *HIVEP1* promoter activity *in vitro*, we performed overexpression as well as EMSA analyses under stimulatory and basic conditions to identify differential binding patterns under distinct physiological conditions. Chromatin immunoprecipitation (ChIP) assays were performed to confirm binding of TFs to the *HIVEP1* promoter region *in vivo*.

2 MATERIAL

2.1 Chemicals

Chemical	Manufacturer
Acrylamide-Bisacrylamide 30% (37, 5:1) (AA/BA)	Merck, Darmstadt
Acetylsalicylic acid	Sigma-Aldrich, Steinheim
Agar (Bacto)	BD Bioscience, Heidelberg
Agarose	Biozym Scientific, Oldendorf
Ammonium persulfate (APS)	Sigma-Aldrich, Steinheim
Atorvastatin	Biomol, Hamburg
Betaine	Sigma-Aldrich, Steinheim
Blocking reagent, EMSA	Roche Diagnostics, Mannheim
Boridic acid	Roth, Karlsruhe
Bromphenol blue	Sigma-Aldrich, Steinheim
Calcium chloride ($CaCl_2$)	Sigma-Aldrich, Steinheim
Caseine	Sigma-Aldrich, Steinheim
Chloroform	Fluka Reidel.de Haën, Seelze
Coomassie Brilliant Blue R-250	Roth, Karlsruhe
Cobalt(II) chloride ($CoCl_2$)	Merck, Darmstad
Deoxycholic acid	Sigma-Aldrich, Steinheim
4',6-diamidino-2-phenylindole (DAPI)	Sigma-Aldrich, Steinheim
Dimethyl sulfoxide (DMSO)	Merck, Darmstadt
dNTPs (dATP, dCTP, dGTP, dTTP)	Fermentas, St. Leon-Rot
1,4 Dithiothreitol (DTT)	Roth, Karlsruhe
Ethanol	Merck, Darmstadt
Ethidium bromide	Roth, Karlsruhe
Ethylenediamine tetraacetic acid (EDTA)	Merck, Darmstadt
Ethyleneglycol-tetraacetic acid (EGTA)	Merck, Darmstadt
Ficoll	Fluka Reidel.de Haën, Seelze
Formaldehyde 37%	Roth, Karlsruhe
Gelatin	Sigma-Aldrich, Steinheim
Glacial acetic acid	Roth, Karlsruhe
L-Glutamine	Sigma-Aldrich, Steinheim
Glycerol	Roth, Karlsruhe
Glycine	Roth, Karlsruhe
4-(2-hydroxyethyl)-1-piperazineethanesulfonic acid (HEPES)	Roth, Karlsruhe
Imidazole	Roth, Karlsruhe
Interleukin-1β (IL-1 β)	Calbiochem, Darmstadt
Isopropylalcohol	Merck, Darmstadt
Lithium chloride (LiCl)	Merck, Darmstadt
Magnesium chloride hexahydrate ($MgCl_2$)	Roth, Karlsruhe
Manganese(II) chloride ($MnCl_2$)	Sigma-Aldrich, Steinheim
β-Mercaptoethanol	Serva, Heidelberg
Methanol	Roth, Karlsruhe
3-(N-Morpholino)propanesulfonic acid (MOPS)	Sigma-Aldrich, Steinheim
N',N',N',N'-Tetramethylendiamine (TEMED)	Roth, Karlsruhe
Nonidet P-40	Sigma-Aldrich, Steinheim
Paraformaldehyde, powder (95%) (PFA)	Sigma-Aldrich, Steinheim
Phenylmethylsulphonyl fluoride (PMSF)	Roth, Karlsruhe

Chemical	Manufacturer
Phorbol-12-myristate-13-acetate (PMA)	Sigma-Aldrich, Steinheim
Poly(dI•dC)	USB, Staufen
Potassium chloride (KCl)	Merck, Darmstadt
Pravastatin	Sigma-Aldrich, Steinheim
Protease inhibitor cocktail with EDTA (Complete)	Roche Diagnostics, Mannheim
Rosuvastatin	Biomol, Hamburg
Simvastatin	Sigma-Aldrich, Steinheim
Sodium acetate (NaAc)	Merck, Darmstadt
Sodium bicarbonate ($NaHCO_3$)	Sigma-Aldrich
Sodium chloride (NaCl)	Roth, Karlsruhe
Sodium deoxycholate	Simga-Aldrich
Sodium dodecyl sulfate (SDS)	Roth, Karlsruhe
Sodium heparin	Invitrogen, Karlsruhe
Spermidine	Fluka Riedel-de Haën
Tumor necrosis factor α (TNFα)	Cell Signaling, Frankfurt
Tris-(hydroxymethyl)-aminomethane (Tris-base)	Roth, Karlsruhe
Triton X-100	Roth, Karlsruhe
Tryptone (Bacto)	BD Bioscience, Heidelberg
Tween-20	Roth, Karlsruhe
Biotin-16-ddUTP	Roche Diagnostics, Mannheim
Xylene xyanole	Roth, Karlsruhe
Yeast (Bacto) extract	BD Bioscience, Heidelberg

2.2 Sera and media

Serum/medium	Manufacturer
Dulbecco's modified eagle's medium (DMEM)	Sigma-Aldrich, Steinheim
Dulbecco's phosphate buffered saline (PBS)	PAA, Pasching
Fetal bovine serum (conditioned) (FBS)	PAA, Pasching
Fetal calf serum (FCS), iron-supplemented	Cell Concepts, Umkirch
Roswell Park Memorial Institute 1640 medium (RPMI)	Sigma-Aldrich, Steinheim

2.3 Consumables and kits

Consumable/kit	Manufacturer
BCA Protein Assay Kit	Thermo Fischer, Bonn
CL-X Posure Film	Thermo Fischer, Bonn
Gateway LR Clonase II Enzyme Mix	Invitrogen, Karlsruhe
High Pure PCR Product Purification Kit	Roche Diagnostics, Mannheim
KAPA-HiFi PCR Kit	PEQLAB, Erlangen
Immobilon-P Transfer Membrane (PVDF)	Millipore, Bedford, USA
LightShift Chemiluminescent EMSA Detection Kit	Thermo Fischer, Bonn
LR Clonase II Enzyme Mix	Invitrogen, Karlsruhe
Luciferase Assay System	Promega, Mannheim
Magnetic Protein-G beads	Invitrogen, Karlsruhe
M-MuLV Reverse Transcriptase	Fermentas, St. Leon-Rot
Nanofectin	PAA, Pasching
NucleoSpin Plasmid	Macherey-Nagel, Düren

Consumable/kit	Manufacturer
NucleoSpin RNA II	Macherey-Nagel, Düren
Oligofectamine	Invitrogen, Karlsruhe
Passive Lysis Buffer (5 x)	Promega, Mannheim
pCR8/GW/TOPO TA Cloning	Invitrogen, Karlsruhe
PureLink HiPure Plasmid DNA Purification Kit	Invitrogen, Karlsruhe
QIAamp DNA Blood Mini Kit	Qiagen, Hilden
QIAquick Gel Extraction Kit	Qiagen, Hilden
siRNA duplex	Ambion, Carlsbad, USA
siRNA control duplex (low GC)	Invitrogen, Karlsruhe
SuperScript III Reverse Transcriptase	Invitrogen, Karlsruhe
SuperSignal West Chemiluminescent Substrate Pico/Femto	Thermo Fischer, Bonn
tRNA	Roche Diagnostics, Mannheim
Whatman Paper 3MM Chr.	Biometra, Göttingen
Pipette tips 0.1 µl - 1000 µl	Sarstedt, Nürnbrecht
Reaction tubes 0.2 ml - 2 ml	Eppendorf, Hamburg Biozym, Hess. Oldendorf
15 ml/50 ml tubes	Greiner, Kremsmünster Nunc, Wiesbaden
Petri dishes	Sarstedt, Nürnbrecht
Plastics for cell culture	Greiner, Kremsmünster
PCR plates, microtiter plates	Abgene, Hamburg

2.4 DNA and protein marker

Marker	Manufacturer
GeneRuler 100 bp DNA ladder	Fermentas, St. Leon-Rot
GeneRuler 1 kb DNA ladder	Fermentas, St. Leon-Rot
Precision Plus Protein Dual Color Standard Plus	BioRad, Munich
Precision Plus Protein Western C	BioRad, Munich

2.5 Enzymes and antibiotics

Enzyme/antibiotic	Manufacturer
Ampicillin	Roth, Karlsruhe
BigDye3.1	Applied Biosystems, Foster City, USA
GoTaq DNA Polymerase	Promega, Mannheim
Penicillin/Streptomycin	PAA, Pasching
Proteinase K	Fermentas, St. Leon-Rot
Restriction endonucleases	Fermentas, St. Leon-Rot
RiboLock	Fermentas, St. Leon-Rot
Shrimp Alkaline Phosphatase	Fermentas, St. Leon-Rot
Spectinomycin	Sigma-Aldrich, Steinheim
TdT terminal transferase	Roche Diagnostics, Mannheim
Trypsine-EDTA (0.05%)	Gibco, Karlsruhe

2.6 Antibodies

Antibody	Host	Manufacturer
β-actin	rabbit	Cell Signaling, Frankfurt am Main
EGR-1	rabbit	Cell Signaling, Frankfurt am Main
HIVEP1	mouse	Abcam, Cambridge, UK
SP1	rabbit	Millipore, Bedford, USA
WT1	mouse	Millipore, Bedford, USA
anti-mouse	sheep	GE Healthcare UK Ltd, Little Chalfont Buckinghamshire, UK
anti-rabbit	donkey	GE Healthcare UK Ltd, Little Chalfont Buckinghamshire, UK
anti-mouse, Cy3 - conjugated	donkey	Millipore, Bedford, USA

2.7 Plasmids and vectors

Plasmid/vector	Description	Manufacturer/gift of
pCR8/GW/TOPO	cloning vector	Invitrogen, Karlsruhe
pGL3-Basic	reporter gene vector	Promega, Mannheim
pGL3-Control	reporter gene vector	Promega, Mannheim
pGL3-Promoter	reporter gene vector	Promega, Mannheim
pRc/CMV	expression vector	Dr. Dimitris Kardassis, Heraklion, Greece
pSP1/CMV	expression vector	Dr. Dimitris Kardassis, Heraklion, Greece
pEGR1/CMV	expression vector	Dr. Dona Wong, Boston, USA
pWT1(-/-)/CMV	expression vector	Dr. Kerstin Duning, Münster
Bacterial aritifcal chromosome (BAC) RP11-456H18, AL157373.23	contains the 5'-end of *HIVEP1* and three CpG islands on chromosome 6	BACPAC Resource Center, Oakland, USA

2.8 Bacteria (*E. coli*)

Strain	Genotype	Manufacturer
Mach1	derivatives of *E.coli* W strains ΔrecA1398 endA1 tonA Φ80ΔlacM15 ΔlacX74 hsdR(rK- mK+)	Invitrogen, Karlsruhe

2.9 Eucaryotic cells

Line	Origin	Reference
EA.hy926	Human vascular endothelium	Edgell et al., 1983
HEK293T	Human embryonic kidney	ATCC no.: CRL-11268
HeLa	Human cervix carcinoma	DMSZ ACC57
HEPG2	Human hepatocellular carcinoma	ATCC no.: HB-8065
HUVEC	Human umbilical vein endothelium	-
Saos-2	Human osteosarcoma	DSMZ no.: ACC 243
THP1	Human monocytes	ATCC no.: TIB-202
U937	Human monocytes	ATCC no.: CRL-1593.2

2.10 Laboratory equipment

Instrument	Specification	Manufacturer
Autoclave	FVS-2 Systec VX-75	Fedegari, Albuzzano, Italy Systec, Wettenberg
Cell counter	Casy Model TT	Innovatis, Bielefeld
Centrifuge	Multifuge 3SR	Heraeus, Hanau
Centrifuge	5415C	Eppendorf, Hamburg
Centrifuge	5417R	Eppendorf, Hamburg
Centrifuge	5810R	Eppendorf, Hamburg
Centrifuge	J2-21M/E Beckman	Coulter, Krefeld
CO_2-Incubator (eukaryotic cells)	MCO-18AIC	Sanyo, Munich
Developing machine	Optimax	Protec, Oberstenfeld
Gel electrophoresis chamber	Mini PROTEAN	BioRad, Munich
Gel electrophoresis chamber	StarPhoresis	Starlab, Ahrensburg
Gel imaging	AlphaImagerEC	Alpha Innotech Corp, San Leandro, USA
Incubator shaker (bacteria)	Shaker Series 25	New Brunswick Scientific, Nürtingen
Luminometer	Sirius V12	Berthold Detection Systems, Pforzheim
Microbiological incubator	B 6120	Heraeus, Hanau
Microscope	Axiovert 40 CFL	Zeiss, Jena
Microscope	Axioplan 2	Zeiss, Jena
pH-Meter	Calimatic 766	Knick, Dülmen
Power supply	PowerPackBasic	BioRad, Munich
Spectrophotometer	Nanophotometer	Implen, Munich
Sequence detection system	7500 ABIprism	Applied Biosystems, Foster City, USA
Sonicator	Bioruptor UCD-200	Diagenode, Liège, Belgium
Sterile hood (bacteria)	Class II type EF	Clean air Techniek B.V., Woerden, The Netherlands
Sterile hood (eukaryotic cells)	HS 12	Heraeus, Hanau
Tank Blot chamber	Mini Trans-Blot Cell	BioRad, Munich
Thermocycler	PTC-225, DNA Engine Tetrad (2)	MJ Research, Miami, USA
UV-table	Transilluminator	Intas, Göttingen
Waterbath	GFL 1083	GFL, Großburgwedel

3 METHODS

3.1 Molecular biological methods

Standard molecular methods were performed as described in “Molecular Cloning” (Sambrook and Russel, 2001) or in manufacturers’ instructions. Modifications in protocols are indicated where appropriate.

3.1.1 Isolation of nucleic acids

3.1.1.1 Preparation of genomic DNA

Genomic DNA from white blood cells was extracted using the QIAamp DNA Blood Kit (Qiagen). EDTA-treated human whole blood (200 µL) was mixed with 20 µL proteinase K and 200 µL binding buffer, incubated at 56°C for 10 min, and loaded onto the spin columns, allowing the DNA to bind to the silica-gel membrane. The DNA was eluted after two washing steps in dH_2O (pH 7 - 8.5) or TE buffer and held at 4°C or stored at -20°C.

3.1.1.2 Preparation of total RNA

Total RNA was extracted from ~5 x 10^6 cultured cells using the NucleoSpin RNA II Kit (Macherey-Nagel) according to manufacturers’ protocol. Cells were lysed with 350 µL lysis buffer (1% β-mercaptoethanol). Subsequent clearance of the lysate was conducted by filtration through a filter column. Optimal binding conditions were achieved by addition of 350 µL ethanol. The lysate was loaded onto the RNA binding column, the membrane desalted and DNA digested by addition of DNase for 15 min. After three washing steps, RNA was eluted in RNase-free water and stored at -80°C.

3.1.1.3 Preparation of plasmid DNA

The NucleoSpin Plasmid Kit (Macherey-Nagel) was used for preparation of plasmid DNA from *E. coli* cultures (2 mL). Cells were spun down and the pellet lysed for 5 min at RT. Neutralization buffer was added, followed by a centrifugation step to clear the lysate. DNA was loaded and bound to silica membrane. After washing twice, plasmid DNA was eluted and held at 4°C or stored at -20°C.

Isolation of transfection grade endotoxin-free plasmid DNA from *E. coli* cultures was performed using the PureLink HiPure Plasmid DNA Purification Kit (Invitrogen) as described in manufacturers’ protocol. Cells from an overnight culture (100 mL) were spun

down and the pellet was resuspended in a RNase A containing buffer. After addition of lysis buffer for 5 min, lysate was cleared using precipitation buffer and centrifugation (12000 x g, 10 min, room temperature [RT]). The supernatant was cleared from bacterial endotoxins by additional incubation with Endotoxin Removal Buffer A and washing with Endotoxin Removal Buffer B. The cleared lysate were loaded onto a pre-equilibrated column, washed and eluted. DNA was precipitated by addition of isopropanol (70% v/v) and centrifugation (15000 x g, 30 min, 4°C). After washing with ethanol (70% v/v), DNA was air-dried and resuspended in TE buffer. Plasmid DNA was held at 4°C and stored at -20°C. In case of bacterial artificial chromosome (BAC) clone RP11-456H18, preparation was performed as described above except of addition of 1% NaCl to the washing buffer.

Endotoxin Removal Buffer A	Endotoxin Removal Buffer B
50 mM MOPS, pH 7.0	100 mM sodium acetate, pH 5.0
750 mM sodium chloride	750 mM sodium chloride
10% (w/v) Triton X-100	1% (w/v) Triton X-100
10% (v/v) isopropyl alcohol	

3.1.2 Photometric measurement of nucleic acid concentration

Measurement of concentration and purity of nucleic acids were performed photometrically using a nanophotometer (Implen). The particular elution buffer served as blank. An optical density (OD) of 1 at 260 nm indicates a concentration of 50 µg/mL of DNA or 40 µg/mL of RNA. The purity was indicated by the E_{260}/E_{280} ratio (1.9 pure DNA, >2.0 pure RNA).

3.1.3 Polymerase Chain Reaction (PCR)

The PCR is conducted to amplify DNA fragments *in vitro* with two specific oligonucleotides (primer) using a thermo resistant DNA polymerase as described by Mullis et al. (Mullis et al., 1986). GoTaq DNA polymerase (Promega) was used for standard PCRs. A proofreading enzyme was used (KAPAHiFi, PeqLab) to assure amplicon sequence identity to template DNA for cloning of transfection vectors.

Standard PCR reaction	Standard PCR program		
5 ng of genomic DNA	Initial denaturation	95°C, 5 min	
10 µM sense primer (SS)	Denaturation	95°C, 1 min	
10 µM antisense primer (AS)	Annealing*	x°C, 45 sec	25-38
200 µM of each dNTP	Elongation	72°C, 1 min/kb	cycles
1 M betaine	Terminal elongation	72°C, 10 min	
1x DNA polymerase buffer			
0.6 U DNA polymerase			
add nuclease-free H_2O to 25 µL			

*Annealing temperature (T_A) depended on primer melting temperature (T_M) and was calculated as $([T_{M(SS)} + T_{M(AS)}]/2) - 2 = T_A$.
T_M was calculated using the following algorithm (Nakano et al., 1999):
$T_M = (wA+xT)*2 + (yG+zC)*4 - 16.6*\log_{10}(0.050) + 16.6*\log_{10}([Na^+])$
(w,x,y,z are the number of the bases A,T,G,C in the sequence, respectively)

Two modifications were applied where necessary:

a) Touch down PCR

For enrichment of specific PCR products annealing temperature is gradually decreased, starting at 5-10°C over calculated primer annealing temperature. Annealing temperature was reduced by 2°C every second cycle until the calculated annealing temperature was reached, followed by 25 cycles at final annealing temperature.

b) Nested PCR

For generation of a higher amount and specificity of a weak PCR signal. Amplified PCR products from the first run were used as templates for a second run using a second set of primers located within the first amplicon. PCR products from the first run were extracted from agarose gels (cf. chapter 3.1.6) or directly used as templates.

3.1.4 Generation of cDNA

Synthesis of cDNA was performed using Superscript III (Invitrogen) or M-MuLV Reverse Transcriptase (Fermentas) according to manufacturers' instructions. Total RNA (0.5-1 µg) was mixed with 1 µL oligo(dT_{18-20}), 1-2 µL dNTPs (10 mM each), 20-40 U RNase Inhibitor (RiboLock, Fermentas; RNaseOUT, Invitrogen) and the particular reverse transcriptase. RNA was reversely transcribed into cDNA at 50°C (Superscript III) or at 37°C (M-MuLV)

for 60 min. Reaction was inactivated at 70°C for 15 min (Superscript III) or for 10 min (M-MuLV). Success of synthesis was routinely controlled by diagnostic PCR for human Ribosomal Protein 27 (RP27). To detect endogenous expression of HIVEP1, cDNA was used as template for amplification with specific primers (appendix, Table A1) in a semiquantitative PCR.

3.1.5 DNA-modifying reactions

3.1.5.1 Restriction of DNA

DNA (100-500 ng) was restricted using 1 U of the appropriate endonuclease. dH_2O and 10 x reaction buffer were added to a total volume of 20 µl, incubated for 1h at 37°C. Restriction enzyme was heat-inactivated at 70°C for 10 min. Restriction of DNA was checked by agarose gel electrophoresis (cf. chapter 3.1.6).

3.1.5.2 Dephosphorylation

Shrimp Alkaline Phosphatase (SAP) was used for dephosphorylation of 5'-ends to avoid religation of linearized plasmid DNA. Digestion reaction was mixed with 1 U SAP and 10 x reaction buffer. dH_2O was added to a total volume of 25 µL. Reaction mixture was incubated at 37°C for 30 min and heat-inactivated at 65°C for 10 min.

3.1.5.3 Labeling and annealing of single-stranded oligonucleotides

Single-stranded oligonucleotides (25-50 bp) for EMSA experiments were synthesized at a minimum coupling efficiency of >98.5% and purified twice by high pressure liquid chromatography (HPLC) (IBA, Göttingen). These oligonucleotides as well as double-stranded PCR products, were 3'-biotinylated with biotin-16-ddUTP (Roche) using TdT. In a reaction mix, containing 2 mM $CoCl_2$, 500 pmol biotin-16-ddUTP and 60 U TdT, 5 pmol of each probe were labeled at 37°C for 30 min. To remove excessive biotin molecules, labeled probes were chloroform-extracted and centrifuged twice (14000 x g, 2 min, RT). Oligonucleotides were labeled prior to annealing, since double-stranded blunt or recessed 3' termini are poor substrates for TdT. Taq polymerase (Promega) adds a protruding adenosine to the 3' end and was therefore used for PCR products. Annealing of oligonucleotides (20 fmol) was achieved by denaturation at 95°C for 10 min in 100 mM NaCl and a subsequent slow cool down over night to RT. Double-stranded unlabeled probes (competitors) were generated using 2 pmol of each unlabeled oligonucleotide. Annealing was controlled routinely by gel electrophoresis.

3.1.6 Agarose gel electrophoresis

Since DNA is negatively charged due to its phosphate backbone, DNA migrates in an electric field. Agarose concentrations of 0.8% to 2%, depending on fragment size, were applied in 1 x TAE buffer. Ethidium bromide was added to the gel solution at a concentration of 0.05 µg/mL to visualize DNA double-strands using the AlphaImager (Alpha Innotech Corporation) gel documentation system.

50 x TAE buffer	6 x loading buffer
40 mM Tris base	0.02% (w/v) bromphenole blue
1 mM EDTA	0.02% (w/v) xylene xyanole
5.71% glacial acetic acid	30% (v/v) glycerol
	20 mM Tris-HCl, pH 7.6
	2 mM EDTA

3.1.7 Purification of PCR products

Purification of DNA fragments for subsequent applications like sequencing or cloning was performed either by column wash, gel extraction or enzymatic reaction.

3.1.7.1 Column purification

Purification of PCR products was performed using the High Pure PCR Product Purification Kit (Roche). PCR reactions were mixed with binding buffer, loaded onto the silica membrane column and washed twice. DNA was eluted in 10 mM Tris-HCl (pH 8.5).

3.1.7.2 Gel extraction

Gel extraction was performed using the QIAquick Gel Extraction Kit (Qiagen). After resection from 0.8% agarose gels, DNA fragments were mixed with solubilization buffer QG (pH 7.5) and heated at 50°C for 10 min for dissolving of gel slices. Probes were mixed with one gel volume of isopropanol (100%) and loaded onto the silica membrane column. After two washing steps, DNA was eluted in buffer EB (10 mM Tris-HCl, pH 8.5).

3.1.7.3 DNA precipitation

Precipitation was performed to concentrate DNA in a sample. The sample was mixed with 1/10 volume of 3 M NaAc (pH 5.2) and one volume isopropanol (100%), incubated at -80°C for 2h and centrifuged twice (maximal speed, 20 min, 4°C). After two washing steps

with ice-cold ethanol (70%), the pellet was air-dried and the DNA resuspended in ~20 µL nuclease-free dH_2O.

3.1.7.4 ExoSAP clean-up

The ExoSAP-it protocol was used for rapid one-step PCR clean-up for sequencing reactions. A mixture of Exonuclease I (Exo) and Shrimp Alkaline Phosphatase (SAP) (both Fermentas) was used to digest small single-stranded fragments (e.g. primers) and to remove dNTPs. One µL of ExoSAP-it mixture was added to each PCR product (5 µL) and incubated at 37°C for 30 min. Inactivation of enzymes was performed at 80°C for 15 min.

ExoSAP mixture
20 U Exonuclease I (*E. coli*)
10 U Shrimp Alkaline Phosphatase (SAP)
add dH_2O to 100 µL

3.1.8 Construction of reporter gene plasmids

Promoter fragments were generated using DNA extracted from clone RP11-456H18, bearing *HIVEP1* wild type (wt) sequence, or patients' genomic DNA (MolProMD), bearing the respective variants, as template. Deletion constructs of the *HIVEP1* 5'-flanking region were amplified using one antisense primer at position +79 bp and sense primers (Table 2) generating constructs shown in Figure 7. Deletion constructs harbouring part of intron 1 were generated with one antisense primer at position +421 and deletion constructs sense primers (Table 2). A 412 bp fragment comprising exon 1 and part of intron 1 was generated with sense primer at position +10 and the antisense primer at position +421 (Table 2). The construct harbouring the rs169713 site was amplified using a sense primer at position -92387 (5'-CAGCTTTCACGTTCTCACCTG-3'), an antisense primer at position -92068 (5'-GCAGTGAGGTATGAGTGTGC-3') and genomic DNA, bearing the rs169713 C or T allele, as template. For all deletion constructs, genomic or BAC clone DNA representing the wt sequence was used as template. Each *HIVEP1* MolHap construct (1-4) was generated using the primer set for deletion construct -1650/+79 and the genomic DNA of a patient, harbouring the respective MolHap sequence, as template.
For transient transfection assays, synthesized PCR fragments were introduced in 5'-3'-orientation into the promoter-less luciferase reporter gene vector pGL3-Basic (Promega, Figure 8) (deletion constructs) or into the pGL3-Promoter vector (Promega,

Figure 8) (enhancer constructs), harbouring the Simian vacuolating virus 40 (SV40) promoter for PIC assembly, using the Gateway cloning system (Invitrogen). The site-specific recombination property of bacteriophage λ is the basis of this cloning technique (Landy, 1989). Recombination occurs at attachment sequences of phage DNA (*att*P) and bacteria DNA (*att*B). Initially, the gel extracted PCR fragment was cloned into the entry vector pCR8/GW/TOPO. The introduced PCR fragment was flanked by *att*L sequences. The vector was subsequently transformed into competent Mach1 (Invitrogen) bacterial cells (cf. chapter 3.3.1.3) and the plasmid isolated and purified (cf. chapter 3.1.1.3). The modified pGL3-Basic destination vector, bearing artificial *att*R sites, was mixed with the entry vector and incubated with the LR Clonase enzyme allowing the exchange of the Gateway cassette in combination with the insert of interest, e. g. the *HIVEP1* promoter fragment. For verification of accurate insert size and orientation (5'-3'), plasmids were double digested with sequence-specific endonucleases (cf. chapter 3.1.5.1) followed by agarose gel electrophoresis. Sequencing (cf. chapter 3.1.9) of generated plasmids for transfection assays was performed to guarantee sequence correctness and identity.

Standard pCR8/GW/TOPO cloning reaction

1 µL salt solution (1.2 M NaCl, 0.06 M $MgCl_2$)
1 µL pCR8/GW/TOPO cloning vector (10 ng/µL)
4 µL purified insert
incubation for 5 min at RT,
transformation in competent Mach1 bacterial cells

LR clonase reaction

100 ng entry vector
150 ng destination vector
2 µL LR Clonase
add TE buffer to 8 µL
incubation for 1h at 25°C
add 1 µL Proteinase K
incubation for 10 min at 37°C

Table 2: Oligonucleotide sequence for *HIVEP1* promoter deletion constructs

Description	Sequence 5'-3'	Position	Ref. Accession #
HIVEP1-4790 SS	ACAGTTTGGTCAAGGTGCCA	-4790	NC_000006.11
HIVEP1-2288 SS	GCATTATTTCATCGTAGGGTTAGC	-2288	NC_000006.11
HIVEP1-1650 SS	GGTCACACCTTGGTTCATGC	-1650	NC_000006.11
HIVEP1-1241 SS	CTGAGGAAACCCCCTTGGG	-1241	NC_000006.11
HIVEP1-1097 SS	ACTACGGCCCCGCCCGTC	-1097	NC_000006.11
HIVEP1-740 SS	CCCATCCAGTCCCTACACC	-740	NC_000006.11
HIVEP1-469 SS	GCTAAACGTGCCCTACTCTGC	-469	NC_000006.11
HIVEP1+79 AS	AACCTG CTGCCAGGACGCC	+79	NC_000006.11
HIVEP1+421 AS	GGGAAAGAAACCCACAAAGC	+421	NC_000006.11
HIVEP1+10 SS	GCCATCAGCAGCGCAGCTC	+10	NC_000006.11

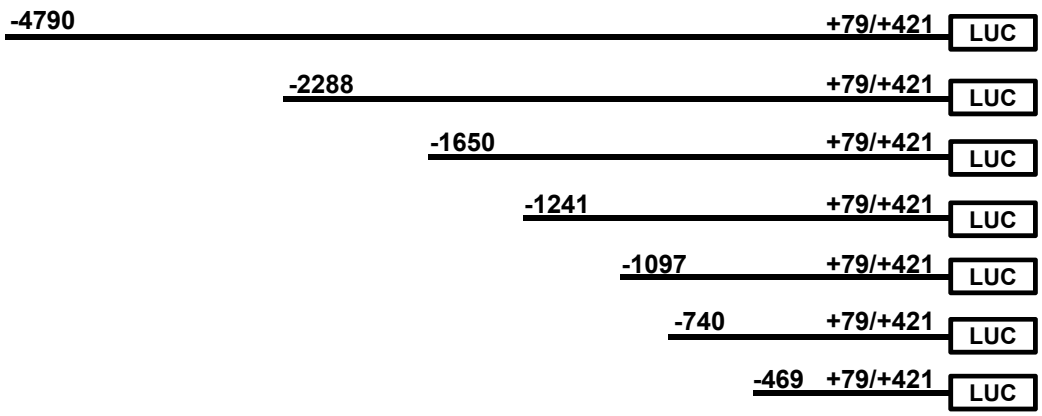

Figure 7: Schematic representation of *HIVEP1* promoter deletion constructs Deletion constructs were cloned into the pGL3 vector system (Promega). The pGL3-Basic vector contains a luciferase cassette adjacent to the multiple cloning site but lacks a promoter sequence. Transcriptionally active *HIVEP1* promoter fragments result in the expression of the luciferase protein, permitting assessment of promoter activity in relative light units. Sequence positions are shown according to TSS. LUC: *luciferase* gene.

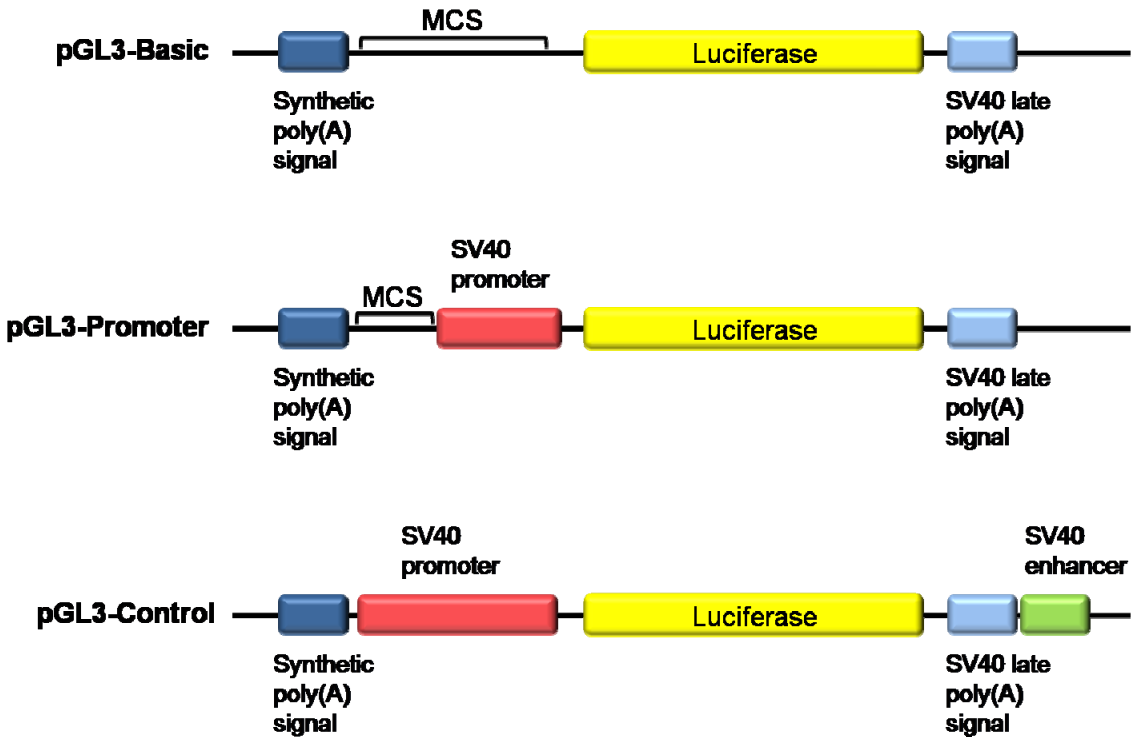

Figure 8: Schematic representation of the pGL3-Basic, pGL3-Promoter and pGL3-Control vector used in reporter gene assays The pGL3-Basic vector lacks eukaryotic promoter and enhancer sequences, the pGL3-Promoter vector contains a SV40 promoter upstream of the *luciferase* gene and the pGL3-Control vector possesses SV40 promoter and enhancer sequences. Putative promoter or enhancer sequences were introduced in 5'-3' orientation into the pGL3-Basic or pGL3-Promoter vector, respectively. MCS: Multiple cloning site.

3.1.9 Sequencing

For detection and localization of genetic variants in the MolProMD study and to ascertain sequence accuracy of DNA fragments and plasmid constructs samples were sequenced (both strains) using an automated ABI 3730 fluorescence sequencer with BigDye terminator chemistry (PE Applied Biosystems).

3.1.10 EMSA

EMSA experiments were performed to analyze DNA/protein interactions *in vitro.* In a native Gel, DNA/protein complexes migrate through the gel according to their size and charge. Protein binding to the applied oligonucleotide (Table 3) is visualized as a “shifted” band, representing a larger, less mobile DNA/protein complex compared to the free migrating unbound oligonucleotides. 3'-biotinylated oligonucleotides were detected with an anti-biotin antibody. Per reaction, 5 µg nuclear protein extracts were incubated in binding buffer with 500 ng presheared poly dI●dC as non-specific competitor, 250 mM betaine and a 200-fold molar excess of unlabeled oligonucleotide as specific competitor for 5 min at RT. After addition of the labeled probe, reactions were incubated for 20 min at RT. Probes and complexes were separated on a 6% native PAGE (cf. chapter 3.2.3) (0.5 x TBE, 100 V), followed by blotting onto a PVDF membrane (cf. chapter 3.2.5) (0.5 x TBE, 100 V, 60 min). Using UV-light (312 nm), DNA probes were cross-linked to the membrane for 15 min. Subsequently, the Chemiluminescent Nucleic Acid Detection Kit (Thermo Fischer) was used to visualize the blotted probes. Membranes were blocked, washed four times, equilibrated and incubated in substrate working solution (luminal/enhancer and peroxidase solution) followed by exposure to CL-X Posure Film (Thermo Fischer).

4 x binding buffer	6% PAGE	5 x TBE
20 mM $MgCl_2$	2 mL AA/BA, 30%	45 mM Tris base
240 mM KCl	1 mL 5 x TBE	45 mM boridic acid
40 mM HEPES/KOH, pH 7.9	83.7 µL APS, 10%	10 mM EDTA
5 mM spermidine	3.7 µL TEMED	
16% (w/v) Ficoll	add dH_2O to 10 mL	

Table 3: Oligonucleotide sequences of EMSA probes

Description	Sequence 5'-3'	Position	Reference
HIVEP1 intron 1 SS	CGTCCTGGCAGCAGGTTCGGCGCGGGCTC CGCGGCGGGGGCGCTGCAGCTGGGGAGGG CGGCGGGGCGGAGGGGGGGGGGGCAGG AGCACATCCCTTCGGCGGGCGGGGGGCGT GCGGGCGCGCGTGTGTGTGTGTG	+63	NC_000006.11
HIVEP1 intron 1 AS	CACACACACACACGCGCGCCCGCACGCCCC CCGCCCGCCGAAGGGATGTGCTCCTGCCCC CCCCCCCCTCCGCCCCGCCGCCCTCCCCAG CTGCAGCGCCCCCGCCGCGGAGCCCGCGC CGAACCTGCTGCCAGGACG	+63	NC_000006.11
HIVEP1 5'-flanking region SS	CTACACCCGGTCAGAGCTGGCGGCCGCGC CGGCCCAGCTGGGCCCCGGCGCCTGGGCG TCCCGCGCCCCTCGCCCCGGCCTCAACCCC AGCCCCCGCGGGGACGCCCCCTCCCCCGC CCACGCGTCGCCGCCCGCGGCCTCCCCTC CTCCCGCCCCCGGGGATCCCCTGCCGCCC CGCCCACCCGCGGGAAAGCCTCCGACCTTC GCCCTGCCTCCCCCGCGCCGCCCGGCCCG CGTTCCTCCCGCCGGCCCCAAAGACGCTAA AC	-728	NC_000006.11
HIVEP1 5'-flanking region AS	GTTTAGCGTCTTTGGGGCCGGCGGGAGGAA CGCGGGCCGGGCGGCGCGGGGGAGGCAG GGCGAAGGTCGGAGGCTTTCCCGCGGGTG GGCGGGGCGGCAGGGGATCCCCGGGGGC GGGAGGAGGGGAGGCCGCGGGCGGCGAC GCGTGGGCGGGGGAGGGGGCGTCCCCGC GGGGGCTGGGGTTGAGGCCGGGGCGAGGG GCGCGGGACGCCCAGGCGCCGGGGCCCAG CTGGGCCGGCGCGGCCGCCAGCTCTGACC GGGTGTAG	-728	NC_000006.11
NF-κB probe AB SS	TTCACAATGACTTTCCCCTTCCTTCTACGCG TTGCTGAGGAAACCCCCTTG	-1275	NC_000006.11
NF-κB probe AB AS	CAAGGGGGTTTCCTCAGCAACGCGTAGAAG GAAGGGGAAAGTCATTGTGAA	-1275	NC_000006.11
NF-κB probe A SS	TTCACAATGACTTTCCCCTTCCTTCTACGC	-1275	NC_000006.11
NF-κB probe A AS	AAGTGTTACTGAAAGGGGAAGGAAGATGCG	-1275	NC_000006.11
NF-κB probe B SS	TACGCGTTGCTGAGGAAACCCCCTTG	-1245	NC_000006.11
NF-κB probe B AS	ATGCGCAACGACTCCTTTGGGGGAAC	-1245	NC_000006.11
NF-κB consensus site	AGTTGAGGGGACTTTCCCAGGC	-	Lenardo & Baltimore, 1989

3.1.11 ChIP Assay

ChIP assays were performed to investigate the association of TF with the DNA of interest *in vivo* using a modified protocol (Boyd et al. 1998; Liu et al., 2000). The technique involves crosslinking of proteins with the DNA and precipitation of bound chromatin using selected specific antibodies. PCR was performed for identification of the DNA fragment associated with the protein. About 10^7 cells were fixed by addition of formaldehyde (final concentration 1%) for 20 min at RT. Fixation was stopped by addition of 140 µL/mL glycine (1 M) for 5 min at RT. Cells were washed twice with ice-cold PBS (Sigma) and lysed for 10 min at RT. After centrifugation, isolated nuclei were sonicated using a Bioruptor (Diagenode, intensity: high, interval: 0.5, 45 min) to result in an average chromatin length of ~500 bp. Size of chromatin fragments was routinely controlled using agarose gel electrophoresis. After centrifugation, the supernatant was incubated with rabbit pre-immune serum for 30 min at 4°C and subsequently incubated with freshly prepared magnetic Protein-G beads (blocked with BSA and tRNA 1h, 4°C) for 30 min at 4°C. After centrifugation, supernatant was transferred to low-binding tubes and 4 µg of specific antibody against SP1 (Upstate), EGR1 (Cell Signaling) or WT1 (Millipore) was added and incubated over night at 4°C. The next day, samples were incubated with freshly prepared magnetic Protein-G beads for 3h at 4°C. After several washing steps using wash buffer I, II and III, the antibody/protein/DNA complex was eluted from the beads. Crosslinks were reversed at 67°C over night and protein digested using proteinase K (2h, 37°C). DNA was extracted by phenol/chloroform/isoamyl alcohol extraction, resuspended in nuclease-free dH_2O and used for PCR analysis (oligonucleotide sequences in Table 4).

Cellular lysis buffer	Nuclear lysis buffer	Dilution buffer
10 mM Tris pH 8.0	50 mM Tris pH 8.0	20 mM Tris pH 8.0
10 mM NaCl	10 mM EDTA	2 mM EDTA
0.2% (v/v) NP-40	1% (w/v) SDS	150 mM NaCl
Roche Complete proteinase inhibitor	Roche Complete proteinase inhibitor	1% (w/v) Triton X-100 Roche Complete proteinase inhibitor

Wash buffer I
20 mM Tris pH 8.0
2 mM EDTA
50 mM NaCl
1% (w/v) Triton X-100
0.1% (w/v) SDS
Roche Complete
proteinase inhibitor

Wash buffer II
10 mM Tris pH 8.0
1 mM EDTA
0.25 mM LiCl
1% (v/v) NP-40
1% (w/v) Deoxycholic acid

Wash buffer III
20 mM Tris pH 7.6
50 mM NaCl

Elution buffer
10 mM $NaHCO_3$
1% (w/v) SDS

Table 4: Oligonucleotide sequences for ChIP

Description	Sequence 5'-3'	Position	Ref. Accession #
HIVEP1 ChIP -307 to -469 SS	GCTAAACGTGCCCTACTCTGC	-307	NC_000006.11
HIVEP1 ChIP -307 to -469 AS	GAGCCACGGCATGATCGC	-469	NC_000006.11
HIVEP1 ChIP -916 to -1097 SS	ACTACGGCCCCGCCCGTC	-916	NC_000006.11
HIVEP1 ChIP -916 to -1097 AS	GAGGGGCGGGGTTAGGGA	-1097	NC_000006.11

3.1.12 siRNA

To knockdown *HIVEP1*, EA.hy926 cells were transfected with a siRNA duplex targeting *HIVEP1* exon 8 using Oligofectamine (Invitrogen) according to manufacturers' protocol. Knockdown efficiency was monitored by semiquantitative PCR. After analyzing the existence of *HIVEP1* transcripts in EA.hy926 cells, *HIVEP1* exon 8 was chosen as target for siRNA. The siRNA was designed using the siRNA selection program "siRNA at WHITEHEAD" (http://sirna.wi.mit.edu/; format: AA(N19)TT) as described by Pei and Tuschl (Pei and Tuschl, 2006). Off-target effects were additionally checked using the net-based program "ParAlign" (http://www.paralign.org/). The most specific siRNA sequence targeting exon 8 (sense 5'-CGACACAAUUCCGUCUGUAUU-3'; antisense 5'-UACAGACGGAAUUGUGUCGUU-3') was elected and synthesized by Ambion (Carlsbad, USA). For control of sequence-independent effects of siRNA transfection, a commercial control siRNA duplex (low GC, Invitrogen) was transfected, harbouring a low sequence homology to any known vertebrate transcript.

A total of 4 x 10^5 cells/well were plated in 6-well plates one day prior transfection. The transfection reagent Oligofectamine (4 µL), 10 µL or 15 µL of HIVEP1 (20 µM) and control siRNA duplexes were diluted in DMEM. After incubation for 10 min at RT, diluted siRNA duplexes were mixed with diluted Oligofectamine and incubated for 20 min at RT. Cells were washed with DMEM and transfection complexes added dropwise to cells in DMEM. After 4h, 5% FCS containing DMEM was added and knockdown was analyzed after 48h. Cells were harvested, RNA isolated (cf. chapter 3.1.1.2), cDNA generated (cf. chapter 3.1.4) and semiquantitative PCR performed (oligonucleotide sequences cf. appendix, Table A1), whereby RP27-PCR served as gel loading control.

3.2 Protein biochemical methods

3.2.1 Extraction of proteins

3.2.1.1 Preparation of cellular protein extracts

Cells were harvested by scraping in lysis buffer to prepare crude proteins. To remove cellular debris, samples were centrifuged (12000 x g, 5 min, 4°C). Supernatants were mixed with pre-heated 4 x SDS-PAGE sample buffer and heated to 95°C for 5 min. Protein samples were aliquoted and stored at -70°C.

Lysis buffer	4 x SDS sample buffer
150 mM sodium chloride	200 mM Tris-HCl, pH 6.8
1% Triton X-100	8% (w/v) SDS
0.5% sodium deoxycholate	0.4% (w/v) bromphenol blue
0.1% SDS	40% (v/v) glycerol
50 mM Tris, pH 8.0	

3.2.1.2 Preparation of nuclear proteins

Nuclear protein extracts were prepared by a modified protocol by Schreiber et al. (Schreiber at al., 1989). A total of 10^7 cells were washed twice with ice-cold PBS, scraped and centrifuged (5000 x g, 2 min, 4°C). Pellets were resuspended in a low salt buffer (500-800 µL) and allowed to swell for 15 min on ice. After addition of 25-75 µL NP-40 (10% solution) and incubation for 5 min at RT, lysed cells were centrifuged (5000 x g, 5 min, 4°C). The supernatant containing the cytosolic protein was removed and stored at -80°C, while pellets were resuspended in a high salt buffer (50-150 µL). After 3h of

incubation, cellular debris was spun down twice (24000 x g, 1h, 4°C) and the nuclear protein extracts were aliquoted on ice, snap frozen in liquid nitrogen and stored at -80°C.

Low salt buffer	High salt buffer
10 mM HEPES, pH 7.9	20 mM HEPES, pH 7.9
10 mM KCl	0.2 mM EDTA pH 8.0
1 mM DTT	1 mM DTT
1.5 mM $MgCl_2$	420 mM NaCl
Roche Complete proteinase inhibitor	1.5 mM $MgCl_2$
	0.5 mM PMSF
	25% (v/v) glycerol
	Roche Complete proteinase inhibitor

3.2.2 Protein quantification

Quantification of the protein content was measured by usage of the BCA Protein Assays Kit (Thermo Fischer). The measurement of a series of dilutions with known concentrations of BSA served as standard curve. Concentrations of proteins were determined photometrically and calculated with reference to the standard curve.

3.2.3 SDS-Polyacrylamide Gel Electrophoresis (PAGE)

A 10% SDS gel was used for separation of protein samples as described by Rittenhouse and Marcus (Rittenhouse and Marcus, 1984). The anionic detergent SDS leads to the negative charge of the protein in relation to its mass, thus the migration distance of the protein in the gel is assumed to be directly proportional the protein size. Denaturation of proteins was achieved by incubation of protein samples in SDS sample buffer at 95°C for 10 min. After incubation on ice for 5 min, samples ran on a stacking gel (4% polyacrylamide) at 80 V and were separated in the following 10% gel at 100 V. Running time depended on protein size and running of the gel was controlled using a prestained marker.

Stacking gel (4%)
560 µL AA/BA, 30%
675 µL 0.5 M Tris-HCl, pH 6.8
675 µL 0.5 M imidazole, pH 6.8
75 µL SDS, 10%
40 µL APS, 10%
5 µL TEMED
add dH_2O to 4.2 mL

Running gel (10%)
2.5 mL AA/BA, 30%
1.9 mL 1.5 M Tris-HCl, pH 8.8
75 µL SDS, 10%
25 µL APS, 10%
5 µL TEMED
add dH_2O to 7.5 mL

1 x SDS running buffer
25 mM Tris base
102 mM glycine
1% (w/v) SDS

3.2.4 Coomassie blue staining

Visualization of protein bands was performed by incubation (1h) of the gel in Coomassie blue staining solution, followed by destaining.

Coomassie staining solution
0.25% (w/v) Coomassie Brilliant Blue R-250
45% (v/v) methanol
10% (v/v) acetic acid
add dH_2O

Destaining solution
45% methanol
10% acetic acid
add dH_2O

3.2.5 Western blot (tank blot)

Proteins were blotted onto a PVDF membrane following the Towbin tank blot protocol (Towbin et al., 1979). After separation of proteins on a SDS gel (cf. chapter 3.2.3). A PVDF membrane was activated for 5 min in methanol and equilibrated in blotting buffer. The membrane was placed onto the gel and covered with two sheets of whatman-paper on each site. Blots were run for 1h at 100 V using cooling units. After blotting, membranes were saturated in blocking buffer at 4°C over night. Detection of proteins of interest was performed by immunodetection using a specific primary antibody for 1h at RT with following dilutions: anti-HIVEP1 (Abcam; mouse) 1:15000 and anti-β-actin (Cell Signaling; rabbit) 1:1000. Horseradish-peroxidase-coupled secondary antibodies (GE Healthcare UK Ltd) were given for 45 min (RT) at following dilutions: anti-mouse 1:100000 and anti-rabbit

of 1:5000. After extensive washing, membranes were incubated for 5 min in SuperSignal West Chemiluminescent Substrate (Pico or Femto, Thermo Scientific) and exposed to CL-X Posure Film (Thermo Fischer). β-actin served as gel loading control.

1 x Blotting buffer	Blocking solution	Washing solution (1 x TBS-T)
25 mM Tris base	4% (w/v) casein	100 mM Tris base
192 mM glycine	in 1 x TBS-T	1.5 mM NaCl
10% methanol		0.03% (v/v) Tween-20

3.3 Cell biological and microbiological methods

3.3.1 Procaryotic cells

3.3.1.1 Procaryotic cell culture and storage

Bacteria were used for the generation and amplification of plasmid DNA. Cultivation of bacteria was performed at 37°C either in liquid medium (lysogeny broth [LB]) or on LB Agar plates. Antibiotics were applied for specific selection of transformed bacteria. Pellets of overnight cultures were resuspended in LB Medium with 15% glycerol and snap frozen in liquid nitrogen and stored at -70°C.

LB Medium	LB Agar
10 g Bactotryptone	15 g Bacto Agar in 1000 mL LB Medium
10 g NaCl	add appropriate antibiotics
5 g Yeast extract	after cool down to 56°C
add dH_2O to 1000 mL, pH 7.0	
Autoclave at 121°C for 120 min	

3.3.1.2 Generation of chemically competent cells

Competent bacterial cells were generated according to a modified protocol by Hanahan (Hanahan, 1983) for preparation and transformation of *E. coli* cells. The transformation efficiency of generated competent cells was routinely controlled by transformation of the pUC19 vector. LB-Medium (200 mL) was inoculated with *E. coli* cells and grown at 37°C to an OD_{600} of 0.5. Cells were incubated for 20 min in an ice bath and harvested by centrifugation (4000 x g, 15 min, 4°C). The pellet was resuspended in $MnCl_2$-transform buffer (10 mL) and incubated on ice for 10 min. After centrifugation (3000 x g, 10 min,

4°C), the pellet was resuspended in $MnCl_2$-transform buffer (7.4 mL) and mixed gently, followed by dropwise addition of 560 µL DMSO. Aliquots of 100 µL were snap frozen in liquid nitrogen and stored at -80°C.

$MnCl_2$-transform buffer
10 mM HEPES, pH 6.8
15 mM $CaCl_2$
20 mM KCl
55 mM $MnCl_2$

3.3.1.3 Transformation

An aliquot of competent cells (100 µL) was thawed on ice, incubated with 50 ng of transforming DNA for 25 min on ice, heat-shocked at 42°C for 30 sec and briefly cooled down on ice for 1 min. After addition of pre-warmed LB-Medium (250 µL), cells were shook at 37°C for 45 min. Cells (100-150 µL) were plated onto antibiotic agar plates and incubated at 37°C over night.

3.3.2 Eukaryotic cells

3.3.2.1 Eukaryotic cell culture

The human vascular endothelial cell line EA.hy926 and the human embryonic kidney cell line HEK293T were maintained in DMEM (Sigma) containing 10% (v/v) FBS (PAA), 100 U/mL penicillin (PAA), 100 µg/mL streptomycin (PAA) and 2 mM/mL L-Glutamine (PAA). For cultivation of HEK293T iron-supplemented FCS was used (Cell Concepts). The human cervix carcinoma cell line HeLa, the human hepatocellular carcinoma cell line HEPG2 and the monocytic cell lines THP1 and U937 were maintained in RPMI 1640 medium containing 10% (v/v) FBS, 100 U/ml penicillin, 100 µg/ml streptomycin and 2 mM/mL L-Glutamine. For cultivation of THP1 and U937 monocytes 1 x modified Eagle's medium amino acid solution (Sigma) was added. Differentiation of monocytes into macrophages was performed by stimulation with 10^{-8} PMA for 72h. The human umbilical vein endothelial cells HUVEC were maintained in DMEM containing 10% (v/v) FBS (PAA), 1000 U/mL penicillin (PAA), 1000 µg/mL streptomycin (PAA), 1% sodium heparin (Sigma) and basic fibroblast growth factor (Invitrogen). For stimulation, cells were treated with TNFα (10 ng/mL, 6h or 24h; Cell Signaling), IL-1β (10 ng/mL, 24h; Calbiochem) or PMA (10^{-8} M, 24h or 72h; Sigma). Statins were applied in following concentrations for 24-30h: 1.2 or 2.4 µM simvastatin (Sigma), 3, 9 or 18 µM atorvastatin (Biomol), 2, 5, 10, or 20 µM rosuvastatin (Biomol) and 1, 5, 10, or 15 µM pravastatin (Sigma). Incubation of cells with

aspirin, used as control experiment for statin-specificity, was performed using 10, 250, 500, 1000 µM acetylsalicylic acid (Sigma) for 24h. THP1 and U937 cells were kept at a concentration of 0.5 to 1 x 10^6/mL. When state of confluence was reached, cells were detached from surface by trypsination and splitted at appropriate ratios for further cultivation. Cells were cultivated at least for 2 passages before used for experiments. The number of passages did not exceed 40 in any case.

3.3.2.2 Storage

For long term storage cells were washed twice with PBS, trypsinated, and transferred to fresh medium. After centrifugation, cells were placed on ice and resuspended in fetal calf serum mixed with DMSO 10% (v/v). Cells were stored at -80°C and transferred to liquid nitrogen the next day. Thawing of cells was performed as quickly as possible, in a waterbath at 37°C. Cells were washed with PBS to remove DMSO from the freezing medium and transferred into pre-warmed medium after centrifugation.

3.3.2.3 Transient transfection

EA.hy926 and THP1 cells were transfected using Nanofectin (PAA). Nanofectin consists of a positively charged polymer with DNA-binding capacity, which is embedded into a porous nanoparticle. In case of EA.hy926, 10^5 cells/well were plated in 24-well plates an transfected the next day. Two hours prior transfection medium was changed. THP1 cells (1.5 x 10^5 cells/well) were plated in 24-well plates immediately prior addition of transfection complexes. For both, EA.hy926 and THP1 cells, 1 µg DNA and 3.2 µl Nanofectin solution was used and diluted in 50 µL NaCl solution (150 mM) and incubated for 10 min at RT. The diluted Nanofectin particles were dropwisly added to the diluted DNA and gently vortexed. After incubation for 30 min at RT, the transfection complexes were dropwisly added to the cell medium. In case of EA.hy926, transfection medium was replaced by fresh medium after 3h. After 24h post transfection, cells were harvested with 100 µL Passive Lysis buffer (Promega) and luciferase activity was determined using a Sirius single-tube luminometer (Berthold detection system). The cell lysate/luciferase substrate ratio was routinely 20 µl/75 µl. The pGL3-Control vector, in which transcription is driven by the competent SV40 viral promoter and additional enhancer, served as positive control. Promotor-less pGL3-Basic vector served as empty shuttle vector control. Transfection experiments were repeated at least three times, in triplicates for each plasmid.

3.3.2.4 Cotransfection

For cotransfection experiments, overexpression of certain proteins, in this study of TFs SP1, EGR1 and WT1, were performed to analyze the possible effect on transcription of the cotransfected reporter gene. The expression vector and reporter gene plasmids were transfected in a 3:1 ratio.

3.3.2.5 Immunofluorescence

For the determination of the cellular localization of HIVEP1, immunofluorescence was performed. Eight chambers of a chamber slide were covered with 1% gelatin and 5 x 10^4 EA.hy926 cells plated in each chamber two days prior antibody incubation. After two washing steps with PBS (+ 1% BSA), cells were fixed using PFA (4%) for 15 min at RT. Cells were washed three times (PBS + 1% BSA) and blocking was performed for 30 min at 37°C by addition of blocking buffer (PBS + 5% FBS), containing 0.1% saponin. Saponin was added to permeabilize the cell membrane. First antibody (HIVEP1, Abcam) was diluted in blocking buffer and applied at a final concentration of 5 µg/mL for 3h at RT. As a control, cells were incubated with the first antibody diluted in blocking buffer without saponin. Unspecific binding of the secondary antibody was controlled in a chamber, which was not incubated with the first antibody. After three washing steps with blocking solution, the secondary Cy3-conjugated anti-mouse antibody (Millipore) was diluted 1:100 and added for 1h at RT in the dark. Cell nuclei staining was performed using 0.25 µg/mL DAPI (Sigma) for 5 min at RT. Cells were washed three times with blocking buffer and covered with cover slides. Analysis of immunfluorescence was performed by microscopy (UV-light, blue and red channel).

3.4 Study population

The current investigation was based on the Münster Molecular Functional Profiling for Mechanism Detection (MolProMD) study. The Münster MolProMD Study is a prospective study of patients with CVD (myocardial infarction, essential hypertension, etc.) and families, aimed at studying molecular genetic mechanism of CVD. The study was approved by the ethics committee of the Medical Faculty, Westfälische Wilhelms-University of Münster and written informed consent was obtained from all study subjects. Genomic DNA from patients of this study was used for the detection of existing genetic variants by sequencing as well as for subcloning and generating gene promoter reporter vectors (Dördelmann et al., 2008).

3.5 Computational analyses of putative TFBS

Prediction of TFBS was performed by *in silico* analysis using PROMO (http://alggen.lsi.upc.es/cgi-bin/promo_v3/promo/promoinit.cgi?dirDB=TF_8.3) and AliBaba2.1 (http://www.generegulation.com/pub/programs/alibaba2/index.html) (Grabe, 2002; Messeguer et al., 2002). Settings of the used algorithms are available upon request. Both programs use information on binding sites of the eukaryotic TRANSFAC database (PROMO, TRANSFAC 8.3; AliBaba2.1, TRANSFAC 7.0)

3.6 Statistical methods

P-values were calculated using the scientific analysis and presentation computer program “Graph Pad Prism 4.0/5.0”. Significance was calculated by unpaired, two-tailed student’s t-test (C.I.95%). The significance levels were set at ***$p<0.001$, **$p<0.01$, and *$p<0.05$.

4 RESULTS

4.1 Endogenous expression of HIVEP1

Determination of cell lines that endogenously express the gene of interest, e.g. *HIVEP1*, is the first important step in promoter studies, since each cell line harbours a distinct composition of TFs to promote stimuli- and tissue-specific gene expression (cf. chapter 1.3). HIVEP1 mRNA expression has been studied in several cell lines, including human cervix carcinoma cells (HeLa), human B and T cells and fibroblasts, using northern blots (Baldwin et al., 1990) (cf. chapter 1.4.2). In the current work, endogenous expression of *HIVEP1* was analyzed using semiquantitative PCR in THP1 and U937 monocytes, vascular endothelial cells (EA.hy926), human embryonic kidney cells (HEK293T), HeLa and human osteosarcoma cells (Saos-2). The constitutively expressed human house-keeping gene *ribosomal protein 27 (RP27)* served as gel loading control. All analyzed cell lines showed moderate endogenous *HIVEP1* expression under basic conditions pointing to an ubiquitous *HIVEP1* expression (Figure 9).

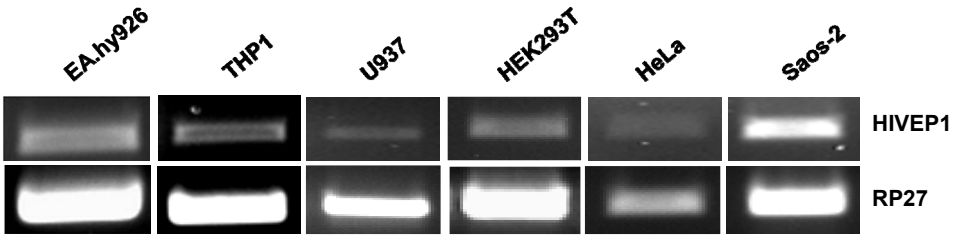

Figure 9: Endogenous expression of *HIVEP1* All analyzed cells, including vascular endothelial cells (EA.hy926), THP1 and U937 monocytes, human embryonic kidney cells (HEK293T), human cervix carcinoma cells (HeLa) and human osteosarcoma cells (Saos-2), revealed endogenous *HIVEP1* expression under basic conditions. Semiquantitative PCR based on generated cDNA and was performed using primers positioned in *HIVEP1* exon 1 and 4. RP27 served as gel loading control.

4.1.1 Influence of proinflammatory stimuli on HIVEP1 mRNA expresssion

Since HIVEP1 is suggested to bind to NF-κB consensus sites (cf. chapter 1.4.2), we studied the potential involvement of HIVEP1 in inflammatory signaling pathways by microarray database research. The effect of proinflammatory stimuli on HIVEP1 mRNA expression was subsequently analyzed in monocytes and endothelial cells, since recruitment of monocytes is a crucial step in the inflammatory response and endothelial "dysfunction" is involved in early stages of VD (cf. chapter 1.2).

4.1.1.1 Microarray database search

We investigated available microarray data (http://www.ncbi.nlm.nih.gov/geo/info/linking.html) with respect to altered HIVEP1 mRNA expression under treatment with pro- and antiinflammatory effectors. We included datasets, which indicated a ≥30% change in HIVEP1 mRNA expression.

Table 5: Involvement of HIVEP1 in inflammatory pathways

Cell type	Effector	HIVEP1 mRNA expression	Reference
HUVEC	IL-1	++ ↑	Mayer et al., 2004
HUVEC	TNFα	++ ↑	Viemann et al., 2006
Monocytes	NF-κB- and PI3K-inhibitor	- ↓	Chan et al., 2008
RASF	IκB	-- ↓	Zhang et al., 2004

Microarray databases indicated HIVEP1 mRNA expression to be affected by inflammatory stimuli. In primary human umbilical vein endothelial cells (HUVEC), treatment with interleukin-1 (IL-1) and tumor necrosis factor α (TNFα) was shown to elicit increased HIVEP1 mRNA expression (++ ↑). Inhibition of the NF-κB and phosphoinositide 3-kinase (PI3K) pathway in monocytes decreased *HIVEP1* expression (- ↓), as did inhibitor kappa B (IκB) in rheumatoid synovial fibroblasts (RASF) (-- ↓), harbouring high TNFα levels. ++: ≥40% positive change, --: ≥40% negative change, -: ≥30% negative change.

Incubation of primary human endothelial cells with IL-1 or TNFα was shown to increase *HIVEP1* expression (Table 5; Mayer et al., 2004; Viemann et al., 2006), while *HIVEP1* expression was downregulated by NF-κB- or phosphoinositide 3-kinase (PI3K)-inhibitors in monocytes (Chan et al., 2008). In addition, inhibition of NF-κB signaling by IκB in inflammatory rheumatoid synovial fibroblasts (RASF), which constitutively yield high TNFα levels, was shown to decrease *HIVEP1* expression (Zhang et al., 2004).

4.1.1.2 Impact of TNFα, IL-1β and PMA on HIVEP1 mRNA expression

To evaluate the potential contribution of HIVEP1 as a mediator of inflammatory processes in onset and progression of VD, we examined the impact of cytokines TNFα and IL-1β on *HIVEP1* expression in the well characterized vascular endothelial cells EA.hy926 and THP1 monocytes. THP1 monocytes were differentiated into macrophages by PMA.
Incubation with TNFα resulted in increased *HIVEP1* expression of both cell lines. IL-1β was a potent activator of endogenous *HIVEP1* expression in EA.hy926 cells (Figure 10). Differentiation of THP1 monocytes to macrophages using PMA led to an increased *HIVEP1* expression.

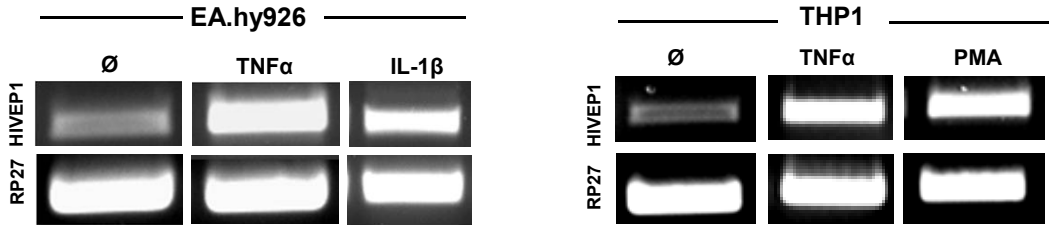

Figure 10: Proinflammatory cytokines increased *HIVEP1* expression in endothelial cells and monocytes Stimulation of EA.hy926 cells with TNFα or IL-1β led to an increase of HIVEP1 expression. TNFα-incubated THP1 cells as well as differentiated macrophages displayed an increase of *HIVEP1* expression. Cells were stimulated with TNFα (10 ng/mL, 24h), IL-1β (10 ng/mL, 24h) or PMA (10^{-8} M, 72h) and total RNA was isolated for cDNA synthesis. RP27 served as loading control. Ø: basic conditions.

4.1.2 Effect of statins on HIVEP1 mRNA expression

One of the major pleiotropic effects of statins is the antiinflammatory property (cf. chapter 1.2.5). In this respect, Dichtl et al. (Dichtl et al., 2003) demonstrated that statins are able to reduce the binding affinity of NF-κB to its consensus site in endothelial cells with subsequently altered NF-κB target gene expression. To analyze a potential effect of statins on *HIVEP1* expression, we examined the impact of clinically used statins on *HIVEP1* expression in endothelial cells.

Treatment of EA.hy926 cells with simvastatin led to a dose-dependent reduction of *HIVEP1* expression. Endogenous *HIVEP1* expression was abrogated by incubation with 2.4 µM simvastatin (Figure 11A). Simvastatin was able to compensate the counterregulating TNFα-effect resulting in decreased *HIVEP1* expression in TNFα-treated EA.hy926 cells (Figure 11A). Equal amounts of atorvastatin (3 µM) did not alter *HIVEP1* expression, while atorvastatin doses of up to 18 µM led to a decrease of *HIVEP1* expression below the basal expression level (mock) (Figure 11B). In TNFα-treated EA.hy926 cells, 9 µM atorvastatin resulted in decreased *HIVEP1* expression, while we observed a paradoxic TNFα/statin effect resulting in increased *HIVEP1* expression, when high-dose atorvastatin (18 µM) was used (Figure 11B). In addition the two lipophilic statins, simvastatin and atorvastatin, we incubated EA.hy926 cells with the hydrophilic statins rosuvastatin and pravastatin. Treatment of rosuvastatin with up to 20 µM led to a dose-dependent reduction of *HIVEP1* expression (Figure 11C). Compensation of the TNFα-effect appeared at rosuvastatin doses of 10 and 20 µM, again dose-dependently (Figure 11C). Pravastatin instead was not able to alter *HIVEP1* expression at any concentration in EA.hy926 cells (Figure 11D). The COX-1 inhibitor aspirin served as treatment control and did not influence *HIVEP1* expression at all (Figure 11E), although we have shown that EA.hy926 cells express the TXA2 receptor, which is necessary for aspirin action (appendix, Figure A1).

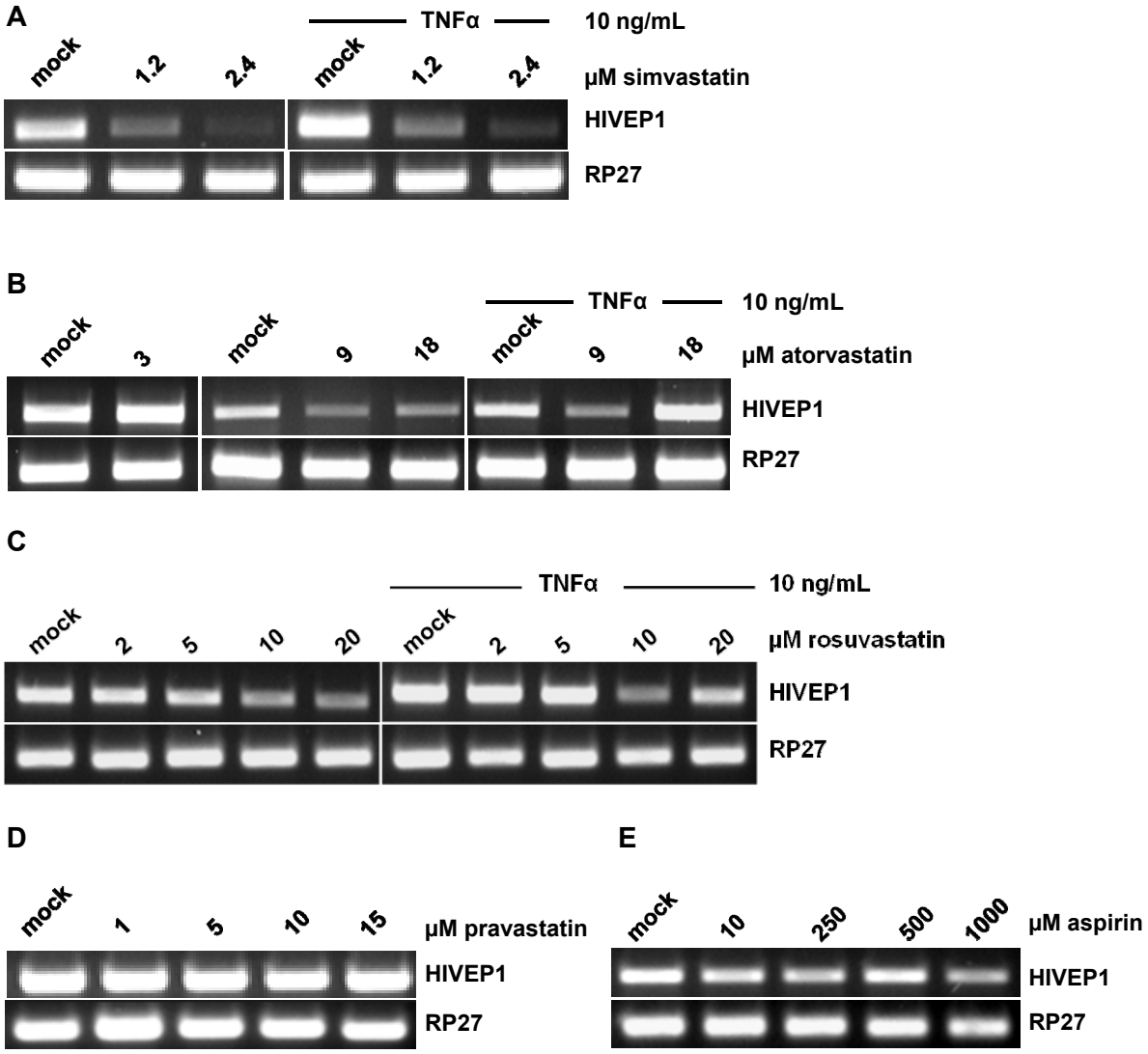

Figure 11: Influence of statins on *HIVEP1* expression in EA.hy926 cells A) Treatment of EA.hy926 cells with simvastatin (1.2 and 2.4 µM) resulted in a dose-dependent decrease of *HIVEP1* expression. In TNFα-treated cells (10 ng/mL, 6h), simvastatin compensated the TNFα-effect, since *HIVEP1* expression abrogated at a simvastatin concentration of 2.4 µM. B) Atrovastatin at a concentration of up to 18 µM led to decreased *HIVEP1* expression. In the presence of TNFα, low-dose atrovastatin (9 µM) still downregulated *HIVEP1* expression, while high-dose atorvastatin (18 µM) increased *HIVEP1* expression. Atorvastatin at a concentration of 3 µM had no effect on *HIVEP1* expression. C) Application of rosuvastatin (2, 5, 10 and 20 µM) dose-dependently decreased *HIVEP1* expression. In TNFα-treated cells, high-dose rosuvastatin (10 µM) was able to compensate the TNFα-effect resulting in a reduction of *HIVEP1* expression. D/E) Neither concentration of pravastatin nor aspirin altered *HIVEP1* expression. EA.hy926 cells were incubated with statins for 24h, subsequently RNA was isolated and cDNA generated. RP27 served as loading control.

4.1.3 Influence of proinflammatory stimuli and statins on HIVEP1 protein expression

To confirm that proinflammatory cytokines such as TNFα and statins affect HIVEP1 expression also at the protein level, we performed western blot analysis using an antibody generated against the C-terminal residue of HIVEP1. In addition, we analyzed the increased *HIVEP1* gene expression in macrophages compared to monocytes at the protein level.

We identified a ~55 kDa HIVEP1 isoform in the nuclear fractions of THP1 monocytes and EA.hy926 cells, as well as in U937 monocytes, HUVEC, HEK293T, human hepatocellular carcinoma (HEPG2) and HeLa cells. By contrast, we could not detect HIVEP1 in the cytoplasm of any above mentioned cells (Figure 12). While we identified a strong signal for HIVEP1 in nuclear extracts of EA.hy926, HeLa and HEK293T cells, the signal was relatively low in THP1 nuclear extracts under basic conditions (Figure 12).

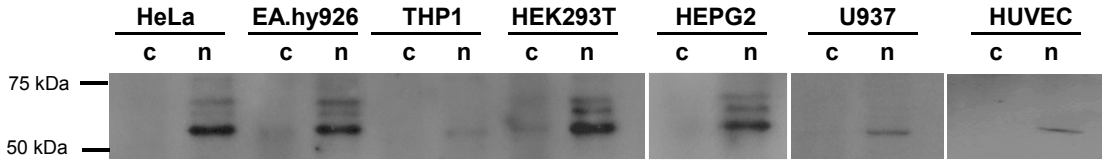

Figure 12: Nuclear localization of HIVEP1 in different cell lines Western blot analysis revealed HIVEP1 protein expression in nuclear extracts. HIVEP1 was absent in the cytoplasm of THP1 and U937 monocytes, as well as in human cervix carcinoma (HeLa), vascular endothelial (EA.hy926), human embryonic kidney (HEK293T), human hepatocellular carcinoma (HEPG2) and human umbilical vein endothelial (HUVEC) cells. HIVEP1 was weakly expressed in THP1 monocytes and we observed elevated amounts of HIVEP1 in EA.hy926, HeLa and HEK293T nuclear extracts. c: cytoplasmic, n: nuclear.

In our western blot analysis, β-actin served as loading control for comparison of the effects of proinflammatory stimuli or statins on HIVEP1 protein expression. All of the analyzed signals in nuclear extracts were comparable, since similar amounts of β-actin were detected in nuclear extracts (Figure 13A/B).

Incubation of THP1 cells with TNFα led to increased HIVEP1 protein expression as well as differentiation of monocytes to macrophages by PMA (Figure 13A), which validate the results obtained at the mRNA level. By contrast, HIVEP1 protein expression was not affected by TNFα incubation or treatment with different statins in nuclear extracts of EA.hy926 cells (Figure 13B). Treatment of TNFα-stimulated cells with different statins had no effect on HIVEP1 protein expression in EA.hy926 nuclear extracts neither (Figure 13B).

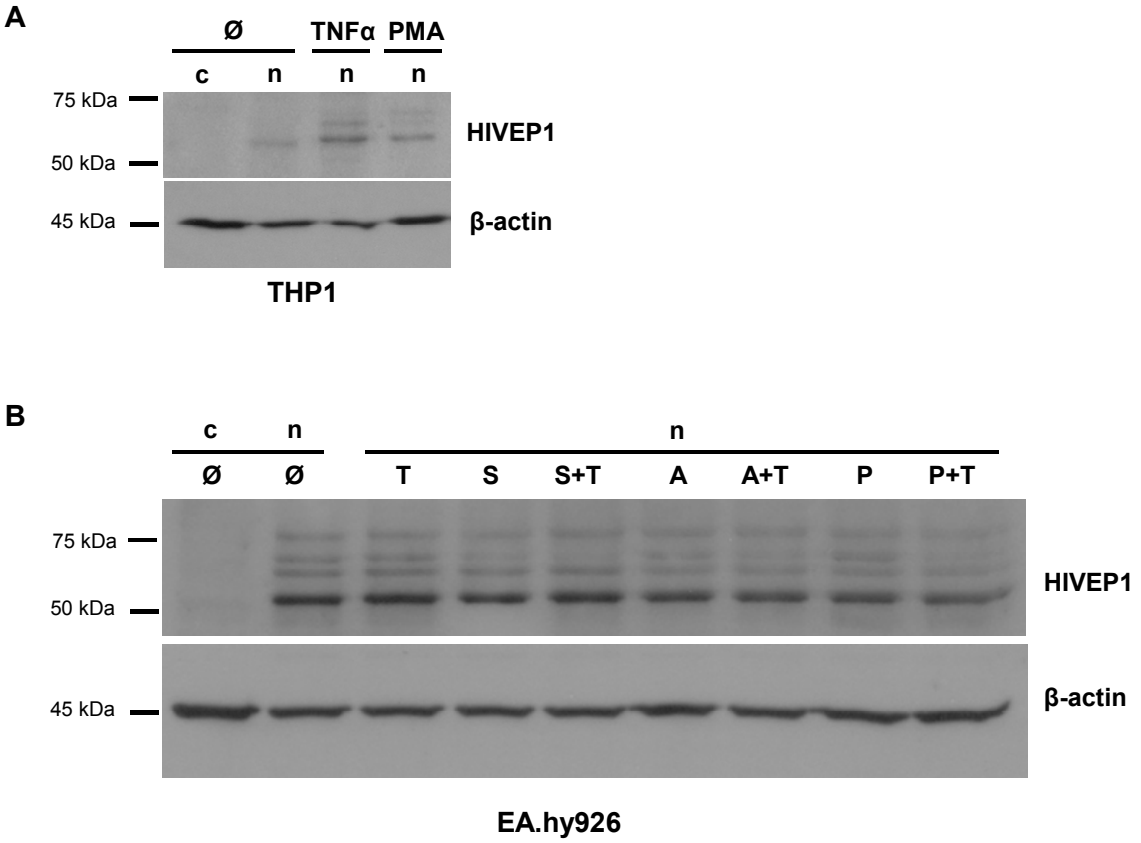

Figure 13: Effect of TNFα stimulation and statins at the HIVEP1 protein level A) TNFα (10 ng/mL, 24h) and PMA (10^{-8} M, 72h) stimulation increased HIVEP1 protein expression in nuclear extracts of THP1 monocytes. B) Incubation of EA.hy926 cells with TNFα (T; 10 ng/mL, 24h) did not alter HIVEP1 protein expression as did treatment with statins in the presence or absence of TNFα. Before preparation of EA.hy926 nuclear extracts, the cells were incubated with statins (simvastatin, S, 2.4 µM; atorvastatin, A, 18 µM; pravastatin, P, 15 µM) for 30h and TNFα (10 ng/mL) was added after 24h for 6h. β-actin served as loading control. c: cytoplasmic, n: nuclear, Ø: basic conditions.

4.1.4 Determination of the cellular localization of endogenous HIVEP1 by immunofluorescence

The HIVEP1 isoform GAAP1 was found in both, the cytoplasm and nucleus of HuH-7 cells, while exclusive nuclear localization of recombinant GAAP1 was demonstrated after deletion of a PEST-like sequence (Lallemand et al., 2002). Using an antibody against the C-terminal HIVEP1 residue, Fan and Maniatis (Fan and Maniatis, 1990) detected nuclear localization of recombinant HIVEP1 in MG63 cells. In that respect, we analyzed the cellular localization of endogenous HIVEP1 in EA.hy926 cells using immunofluorescence. Cells were fixed and incubated with an unlabeled first antibody against the C-terminal HIVEP1 residue and a Cy3-labeled (red channel) secondary antibody. Cell nuclei were labeled with DAPI (blue channel). Antibodies were diluted in PBS, containing 0.1% (w/v) saponin to permeabilize the cell membrane allowing detection of proteins in the nucleus. Antibodies diluted in PBS without saponin served as negative control 2, while negative control 1 was performed by incubation of cells with the secondary antibody without prior incubation with the primary antibody.

Immunofluorescence of HIVEP1 revealed that endogenous HIVEP1 was located within the nuclei of EA.hy926 cells, while absent in the cytoplasm (Figure 14, merge). Negative controls 1 and 2 revealed that the secondary antibody did not bind unspecific and the primary antibody needed the detergent saponin to get into the nucleus of intact cells, respectively (Figure 14).

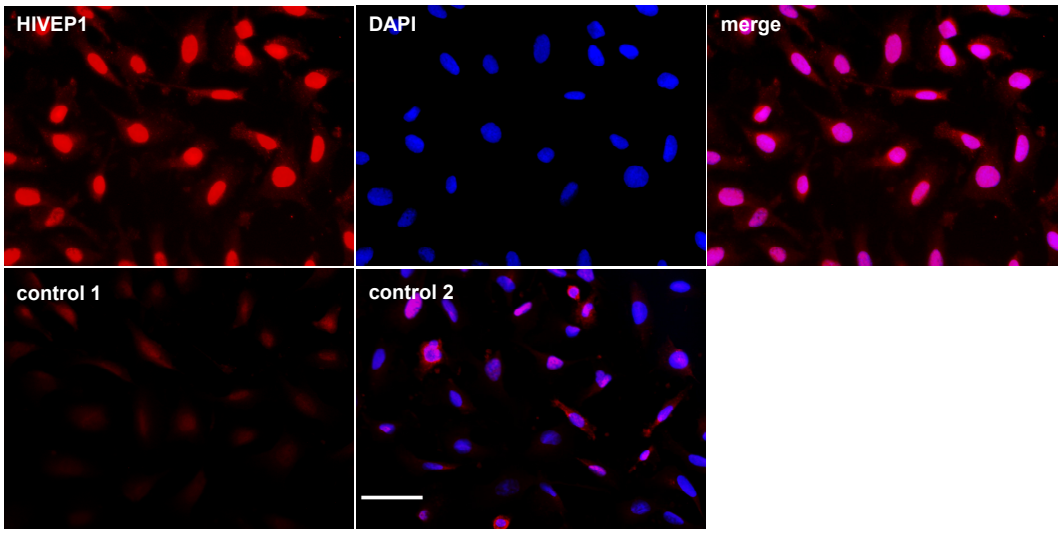

Figure 14: Nuclear localization of HIVEP1 in EA.hy926 cells Immunofluorescence of HIVEP1 in EA.hy926 cells revealed localization of HIVEP1 in the nuclei of EA.hy926 cells. HIVEP1 was visualized with a specific primary antibody and a Cy3-conjugated secondary antibody (red channel). Nuclear staining was performed using DAPI (blue channel). Negative control 1 revealed no unspecific binding of the secondary antibody, while negative control 2 demonstrated the need of saponin to get the primary anti-HIVEP1 antibody into the nucleus of intact cells. Scale bar 50 µm.

4.2 Identification and functional analysis of genetic variants in the *HIVEP1* 5'-flanking region

Since we recently identified a tagging SNP (rs169713T>C) positioned 90 kb upstream of the *HIVEP1* gene to be replicatively associated with VT (Morange et al., 2010), we performed reporter gene assays to analyze the potential enhancer capacity of the region flanking rs169713 (cf. chapter 4.2.1). Dördelmann et al. as well as Hagedorn et al. (Dördelmann et al., 2008; Hagedorn et al., 2009) demonstrated the potential impact of SNPs and molecular haplotypes on gene expression regulation, therefore we screened the region 5 kb upstream of *HIVEP1* with respect to genetic variants in CVD patients. Subsequently, we analyzed the impact of molecular haplotypes on *HIVEP1* gene expression regulation in EA.hy926 and THP1 cells.

4.2.1 Potential enhancer capacity of the rs169713 polymorphic site

The analysis of the putative enhancer site was conducted by cloning a 319 bp fragment comprising either rs169713 C or T allele into the pGL3-Promoter vector upstream of the *luciferase* gene. The pGL3-Promoter vector contains the SV40 promoter for PIC assembly, but lacks an active enhancer. Transient transfection assays were performed in EA.hy926 and THP1 cells and transcriptional activities of reporter constructs were assessed as relative light units (RLU).

In EA.hy926 cells, the construct containing the C allele displayed transcriptional activity at the level of the pGL3-Promoter shuttle vector (Figure 15A). Insertion of the T allele significantly increased transcriptional activity compared to the construct harbouring the C allele and the pGL3-Promoter vector (Figure 15A, both $p<0.001$), indicating a potential enhancer function for the rs169713 T allel-carrying portion. We observed similar results in THP1 cells but with smaller effects. The construct comprising the T allele displayed the strongest transcriptional activity compared to the C allele and the pGL3-Promoter vector (Figure 15B).

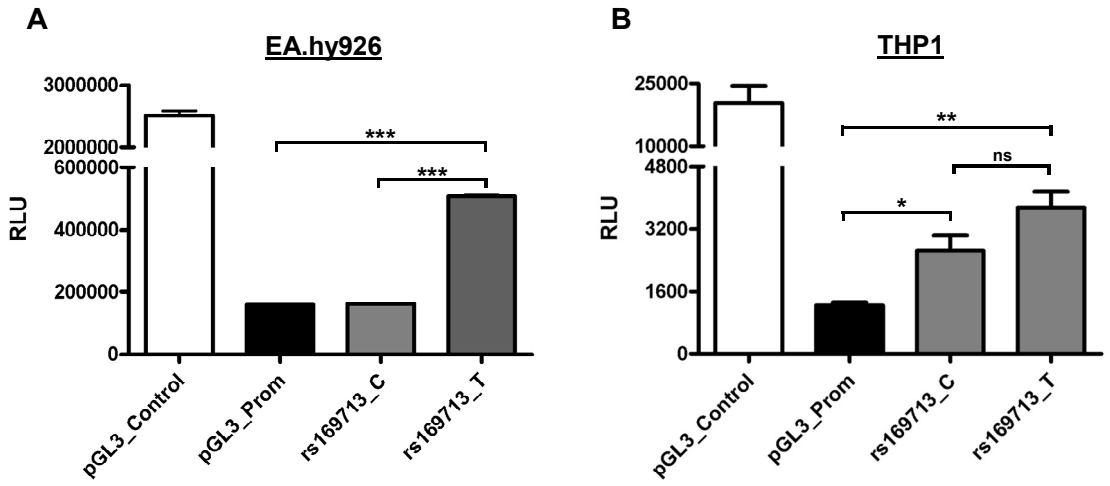

Figure 15: Enhancer capacity of a 90 kb upstream region harbouring the rs169713 T allele A) The construct containing the T allele had a significant higher transcriptional activity compared to the C allele-carrying construct and the pGL3-Promoter vector in EA.hy926 cells (both p<0.001). B) In THP1 cells, we observed the strongest transcriptional activity for the construct harbouring rs169713 T allele. White bars indicate transcriptional activity of the pGL3-Control, black bars of the pGL3-Promoter (Prom) vector. Transcriptional activity was assessed as relative light units (RLU). ***p<0.001, **p<0.01, *p<0.05, ns = not significant.

4.2.2 Identification of additional *HIVEP1* promoter variants

Screening of 5 kb of the HIVEP1 5'-flanking region in 57 patients with CVD (MolProMD study) revealed ten genetic variants (Figure 16, red and blue lines), while two of them were newly identified (blue lines). Positions of tagging SNPs rs169713 and rs2282220 as well as the *HIVEP1* gene architecture are schematically shown in Figure 16.

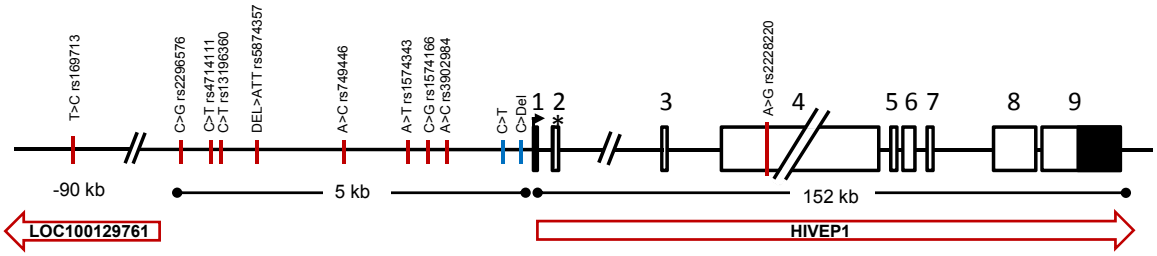

Figure 16: Genetic architecture of the *HIVEP1* gene and positions of identified genetic variants The *HIVEP1* gene maps to chromosome 6, spans 152 kb and consists of 9 exons (boxes). Black boxes represent the 5'- and 3'-untranslated regions. The TSS is indicated by an arrow and the translation start in exon 2 by an asterisk. Ten genetic variants (red and blue lines), two of which were novel (blue lines), were identified in 57 individuals of the MolProMD study. Tagging SNP rs169713 maps to the pseudogene LOC100129671 90 kb upstream of *HIVEP1* and rs2282220 to *HIVEP1* exon 4.

4.2.3 MolHap analysis

We subsequently analyzed the identified genetic variants in the *HIVEP1* 5'-flanking region with respect to MolHaps formation. Three adjacent SNPs (rs1574343_A>T, rs1574166_C>G, rs3902984_A>C), located between positions -1060 to -953 relative to the TSS of *HIVEP1*, were identified by individual subcloning to constitute four MolHaps (MolHaps 1-4, Figure 17A). MolHap1 (A^{-1060}-C^{-1037}-A^{-953}) represents the most frequent MolHap. We generated *HIVEP1* MolHap promoter constructs by cloning a *HIVEP1* promoter fragment, comprising positions -1650 to +79, harbouring either one of the MolHap sequences into the pGL3-Basic vector. Transient transfection assays in EA.hy926 cells revealed a moderate stepwise decrease of transcriptional activity by introducing allele combinations of MolHap2-4 (Figure 17B). Transcriptional activity of MolHap4 was significantly decreased to 50% of transcriptional activity of MolHap1 ($p<0.001$). By contrast, transcriptional activity of MolHap1-4 did not differ in THP1 monocytes (Figure 17C), indicating a cell type-specific effect of the identified MolHaps on *HIVEP1* promoter activity.

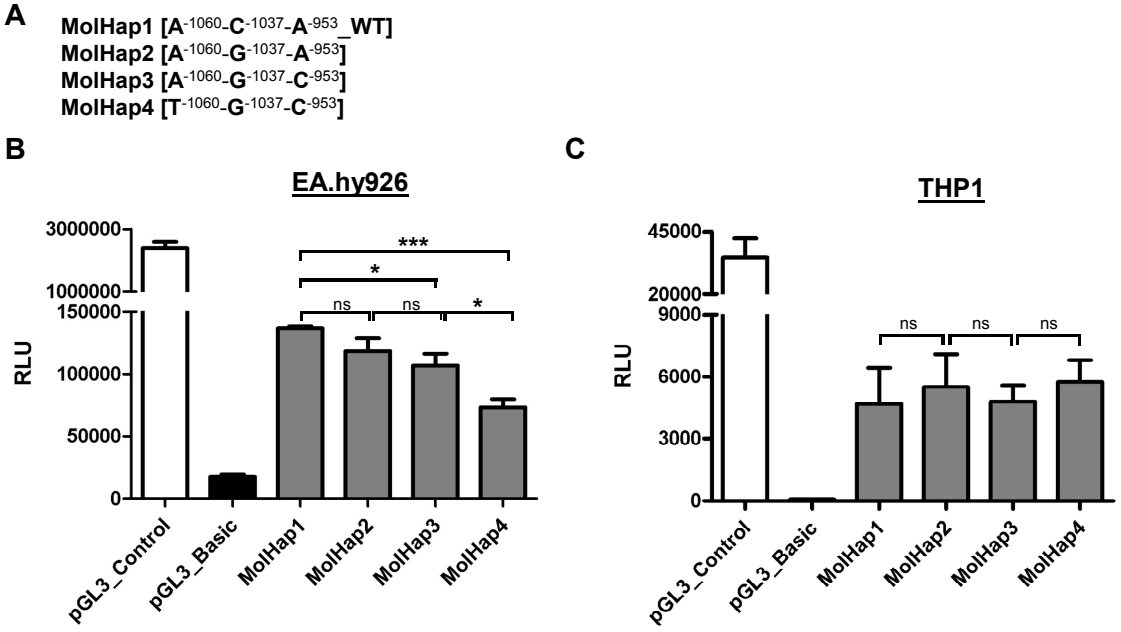

Figure 17: Transient transfection of MolHaps1-4 in EA.hy926 and THP1 cells A) We identified four MolHaps, generated by three SNPs located between positions -1060 to -953, which we introduced into a *HIVEP1* promoter construct comprising positions -1650 to +79. B) Introduction of alleles representing MolHap2 and 3 led to a stepwise decrease of transcriptional activity, transcriptional activity of MolHap4 revealed ~50% of the transcriptional activity of MolHap1 in EA.hy926 cells. C) We observed no difference in transcriptional activity between MolHap1-4 in THP1 cells. White bars indicate transcriptional activity of the pGL3-Control, black bars of the pGL3-Basic vector. Transcriptional activity was assessed as relative light units (RLU). WT: wild type. ***$p<0.001$, *$p<0.05$, ns = not significant.

4.3 Identification of *cis*-active elements affecting HIVEP1 mRNA expression

Since we aimed at investigating how inflammatory factors affect the *HIVEP1* expression regulation, we functionally characterized the 5'-flanking region of *HIVEP1* and determined the location of *cis*-active elements. Therefore, serial promoter deletion constructs comprising up to 4.8 kb of the 5'-flanking region of *HIVEP1* were designed (Figure 18A). Promoter fragments were cloned into the pGL3-Basic vector. Transcriptional activity of transiently transfected deletion constructs thereby depended on the ability of inserted promoter portions to drive the expression of the firefly *luciferase (LUC)* gene. The pGL3-Control vector, which harbours a SV40 promoter and enhancer leading to a strong *LUC* gene expression, served as positive control for transfection efficiency.

4.3.1 Characterization of the 5'-flanking *HIVEP1* structure

Transient transfection of promoter deletion constructs in EA.hy926 cells revealed basal transcriptional activity residing between proximal positions -1097 and -469, since deletion constructs -469/+79, -740/+79 and -1097/+79 exhibited moderate transcriptional activity (Figure 18B). A significant increase in transcriptional activity was observed for the distal deletion construct -1241/+79 compared to construct -1097/+79 ($p<0.001$), while deletion construct -1650/+79 contained the highest transcriptional activity ($p<0.01$ compared to -1241/+79). Transfection of deletion constructs -2288/+79 and -4790/+79, harbouring further upstream portions of the 5'-flanking region, resulted in a significant decrease of transcriptional activity compared to deletion construct -1650/+79 (both $p<0.001$). In conclusion, the strongest transcriptional activity resided between positions -1650 and -1241. Transient transfection of *HIVEP1* promoter constructs in THP1 cells demonstrated a similar activity pattern as observed in EA.hy926 cells (Figure 18C).

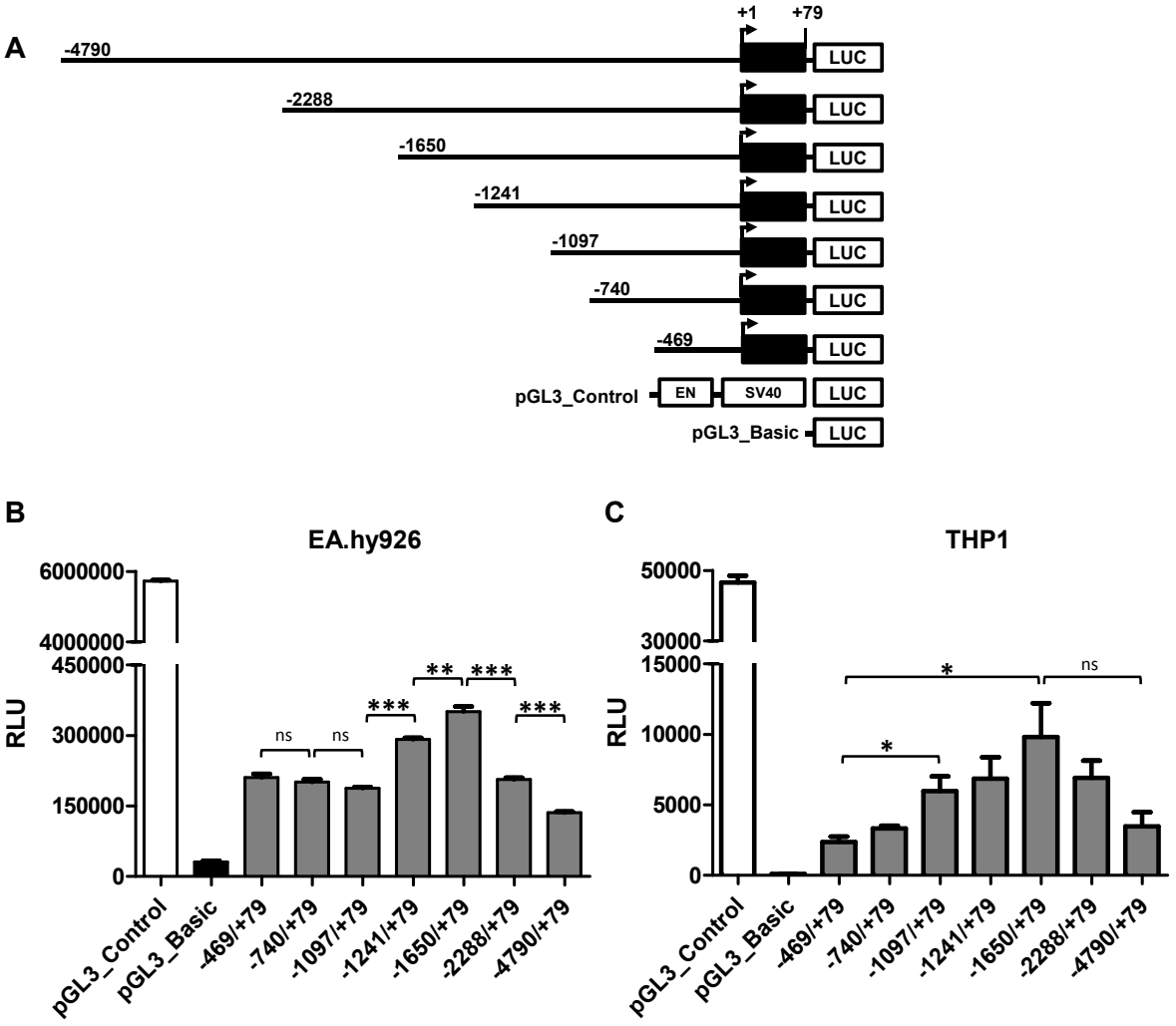

Figure 18: Characterization of the *HIVEP1* promoter A) Serial *HIVEP1* promoter deletion constructs were cloned into the pGL3-vector system and transiently transfected into EA.hy926 and THP1 cells. B) Moderate transcriptional activity was observed for proximal *HIVEP1* promoter deletion constructs -469/+79, -740/+79 and -1097/+79 in EA.hy926 cells, suggesting basal promoter activity between positions -1097 and -469. Transcriptional activity significantly increased for deletion construct -1241/+79 ($p<0.001$), peaked in construct -1650/+79 ($p<0.01$), and significantly decreased for deletion constructs -2288/+79 and -4790/+79 (both $p<0.001$) compared to deletion construct -1650/+79, indicating strongest promoter activity between distal positions -1650 and -1241. C) In THP1 cells, strongest transcriptional activity was identified for deletion construct -1650/+79, resulting in a similar promoter architecture as observed in EA.hy926 cells. White bars indicate transcriptional activity of pGL3-Control vector driven by a powerful SV40 promoter and enhancer (EN) (white box), serving as control for transfection efficiency. Black bars indicate transcriptional activity of promoter-less pGL3-Basic vector, serving as vector shuttle control. Transcriptional activity was assessed as relative light units (RLU). ***$p<0.001$, **$p<0.01$, *$p<0.05$, ns = not significant. LUC indicates *luciferase* gene; black boxes exon 1 5'-UTR; arrow indicates TSS.

4.3.2 Influence of TNFα and PMA on *HIVEP1* promoter constructs' transcriptional activities

Since *HIVEP1* expression was affected by TNFα and PMA treatment (cf. chapter 4.1.1.2), we analyzed the effect of these stimuli on *HIVEP1* promoter constructs. The impact of each stimulus on the transcriptional activity of the deletion constructs is calculated in fold induction (FI) values, i.e. promoter constructs' relative transcriptional activitiy over the pGL3-Basic shuttle vector.

In EA.hy926 cells, stimulation with TNFα did not alter transcriptional activity of deletion constructs, since the mean FI was 0.84 (Figure 19).

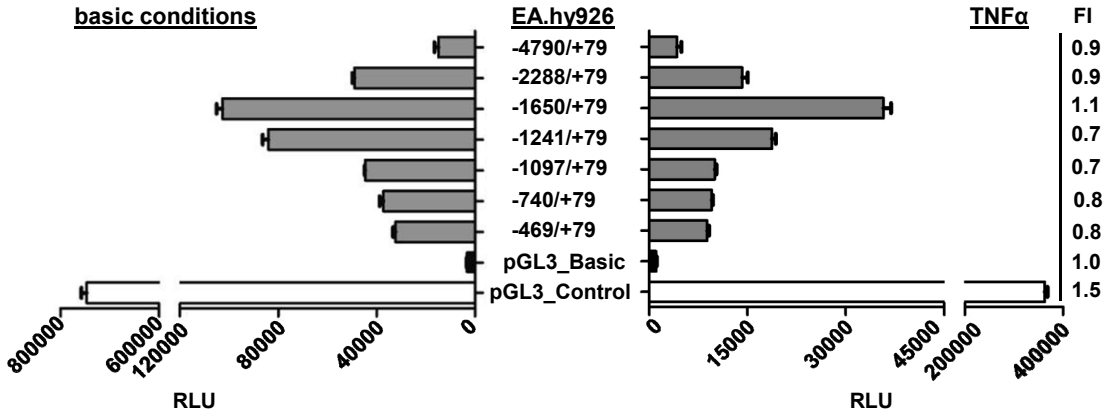

Figure 19: TNFα had no effect on transcriptional activity of *HIVEP1* promoter deletion constructs Stimulation of EA.hy926 cells with TNFα (10 ng/mL, 24h) did not influence transcriptional activity of *HIVEP1* promoter deletion constructs (mean fold induction [FI]=0.84). We obtained similar results in THP1 cells. FI was calculated as promoter constructs' relative transcriptional activity over the promoter-less pGL3-Basic vector. Transcriptional activity was assessed as relative light units (RLU).

Treatment of EA.hy926 cells with PMA resulted in a decrease in transcriptional activity of *HIVEP1* promoter deletion constructs (mean FI=0.54) (Figure 20A), while constructs' transcriptional activity was stimulated by PMA leading to a mean FI of 6.75 in THP1 cells (Figure 20B). Of note, the strongest effect of PMA was observed for transcriptional activity of distal deletion constructs starting with construct -1241/+79.

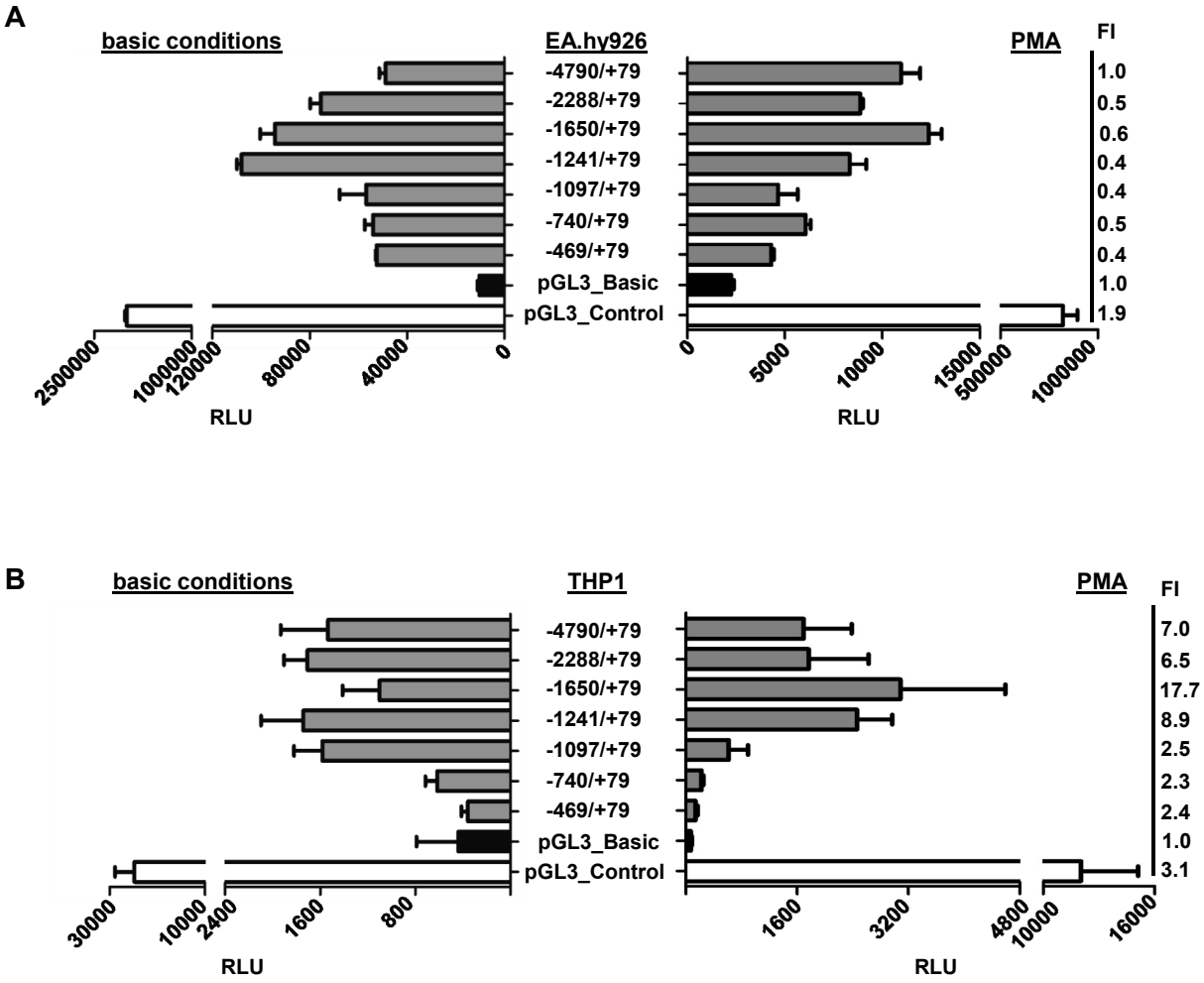

Figure 20: Cell type-specific effect of PMA on transcriptional activity of *HIVEP1* promoter deletion constructs A) In PMA-stimulated EA.hy926 cells transcriptional activity of *HIVEP1* promoter deletion constructs was decreased compared to basic conditions (mean fold induction [FI]=0.54). B) In THP1 cells, stimulation with PMA led to an increase of transcriptional activity of deletion constructs (mean FI=6.75). Cells were incubated with PMA (10^{-8} M) for 24h. FI was calculated as promoter constructs' relative transcriptional activity over the promoter-less pGL3-Basic vector. Transcriptional activity was assessed as relative light units (RLU).

4.3.3 Regulatory effect of an intronic modulator on *HIVEP1* expression

Apart from the localization of *cis*-regulatory elements within the 5'-flanking regions, modulators of gene expression can be found within intronic regions in vicinity of TSS (Seshasayee et al., 2000; Kim et al., 2005). Therefore, we analyzed the impact of a defined region in intron 1 on the transcriptional *HIVEP1* promoter activity. To determine the part of intron 1, which may possess a regulatory property on *HIVEP1* expression, we performed *in silico* analysis using AliBaba2.1 based on the database of eukaryotic TFs (TRANSFAC 7.0). Clustered binding of specificity protein 1 (SP1) and conserved binding sites for Wilms' tumor protein 1 (WT1) were indicated within the first ~350 bp of intron 1 (Figure 21). Predictions of TF binding were validated using another web-based tool PROMO 3.0.2 accessing TRANSFAC 8.3. Subsequently, we added this intronic region to *HIVEP1* deletion constructs and used it as biotinylated probe in EMSA analysis (cf. chapter 4.4.2.2).

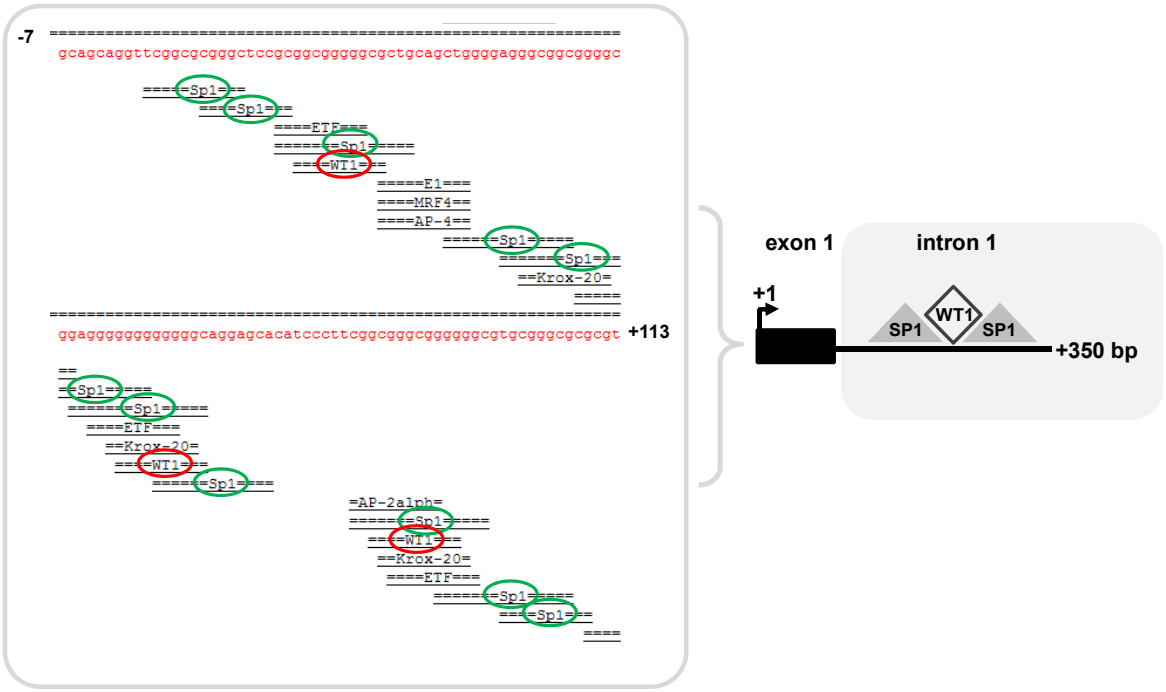

Figure 21: Schematic representation of predicted TFs SP1 and WT1 binding in intron 1 of the *HIVEP1* gene *In silico* analysis using AliBaba2.1 (TRANSFAC 7.0) indicated binding sites for TFs specificity protein 1 (SP1, green circles) and Wilms' tumor protein 1 (WT1, red circles) in the first about 350 bp of intron 1 in the *HIVEP1* gene. Binding of a proposed TF module comprising SP1 (triangle) and WT1 (diamond) to intron 1 of the *HIVEP1* gene is schematically shown.

In EA.hy926 cells, addition of the intronic region, i.e. the first 345 bp of intron 1, to *HIVEP1* deletion constructs, resulted in a significant decrease of transcriptional activity of all analyzed deletion constructs (all p-values <0.001, Figure 22A). The constructs (-469/+421, -740/+421, -1097/+421, -1650/+421) displayed 50% of the activity (FI values ≤0.5) of deletion constructs lacking intron 1 (-469/+79, -740/+79, 1097/+79, -1650/+79) (Figure 22B). These results demonstrate a strong influence of the intronic modulator on *HIVEP1* promoter activity in endothelial cells.

In THP1 cells, addition of the intronic modulator to deletion construct -1650/+79 led to a significant ~3-fold increase in transcriptional activity (p<0.01) (Figure 22C/D). Activities of deletion constructs -740/+421 and -1097/+421 were instead not affected by the intronic region in monocytes, while addition of intron 1 to deletion construct -469/+79, comprising the proximal promoter, led to abrogation of transcriptional activity (p<0.01, FI=0.05, Figure 22C/D). In both cell lines, deletion construct +10/+421, harbouring the isolated intronic modulator and exon 1 alone, did not exhibit individual transcriptional activity. This indicates that an intronic modulator interacts with distinct 5'-flanking promoter regions in both cell lines, altering transcriptional activity in a cell type-specific manner.

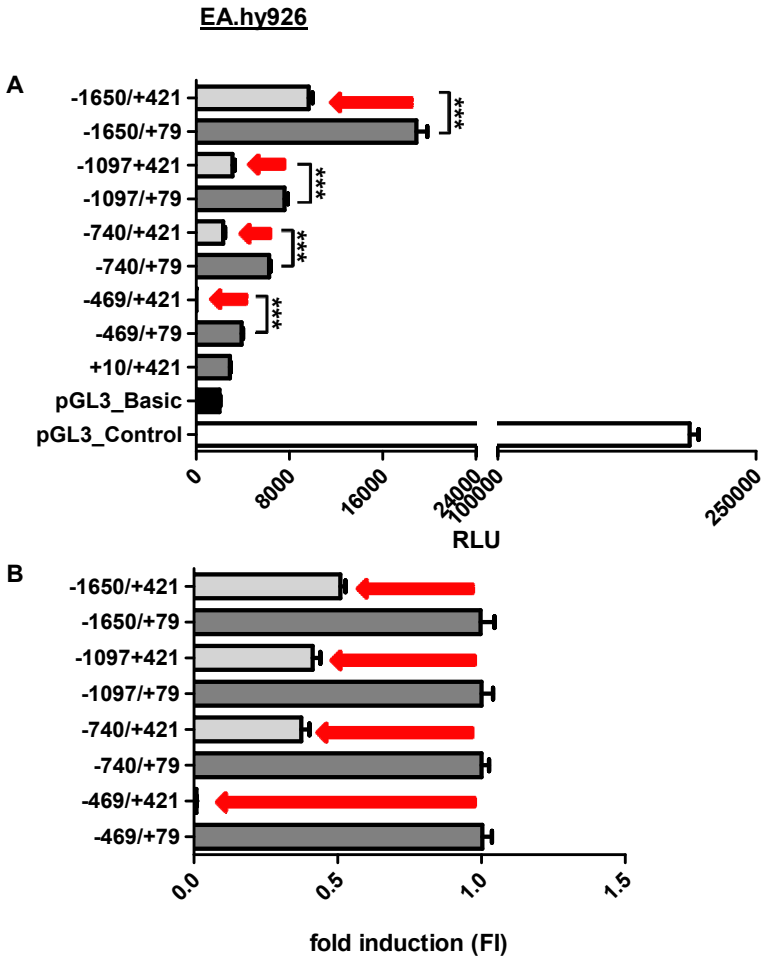

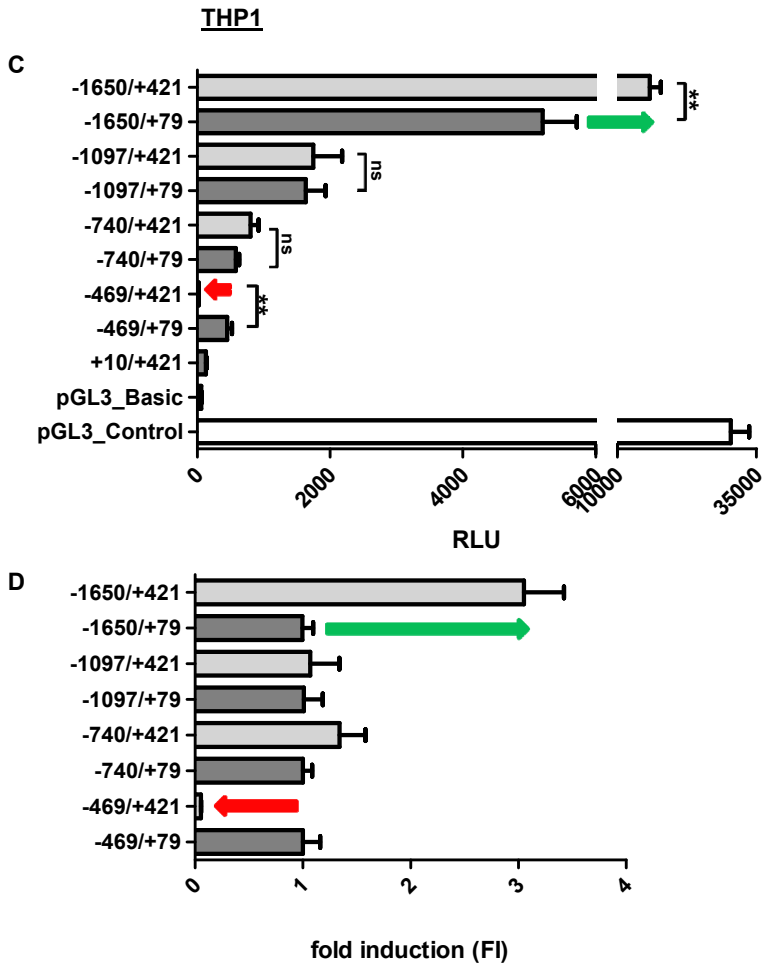

Figure 22: An intronic modulator regulates cell type-specific *HIVEP1* promoter activity A) In EA.hy926 cells, addition of a 345 bp portion of intron 1 resulted in significantly decreased transcriptional activities of *HIVEP1* promoter constructs (all p-values <0.001). B) Effect of the intronic modulator displayed as fold induction (FI) demonstrates a ≥0.5-fold reduction of activity of constructs harbouring the defined part of intron 1. C/D) Transcriptional activity of deletion construct -1650/+79 was significantly increased by addition of intron 1 ($p<0.01$; FI=3) in THP1 cells, while constructs -1097/+79 and -740/+79 remained unaffected. A significant decrease of transcriptional activity ($p<0.01$; FI=0.05) was observed for deletion construct -469/+79 by adding the intronic region. FI was calculated as relative transcriptional activity of each construct harbouring the intronic region compared to the deletion construct lacking intron 1 (FI=1). Transcriptional activity was assessed as relative light units (RLU). ***$p<0.001$, **$p<0.01$, ns = not significant.

4.4 Analysis of candidate *trans*-acting factors modulating *HIVEP1* expression regulation

Since our investigation of the *HIVEP1* promoter structure (cf. chapter 4.3.1) indicated that the 5 kb of the 5'-flanking region harbour activating regulatory *cis*-elements, we analyzed the interaction of *trans*-acting factors with the identified promoter region of *HIVEP1*. Therefore, we performed *in silico* analyses for the prediction of TFBS in the promoter region of *HIVEP1* using net-based programs AliBaba 2.1 and PROMO 3.0.2. Subsequently, we analyzed the impact of predicted TFs on the *HIVEP1* promoter *in vitro* using overexpression and EMSA experiments, while *in vivo* confirmation of TF binding to the promoter region was conducted by ChIP analysis.

4.4.1 *In silico* analyses of putative TFBS in the *HIVEP1* promoter

The first 1500 bp of the 5'-flanking region display a high GC content (74%) and computational analysis based on the TRANSFAC 7.0 database suggested binding of Zn finger proteins SP1, early growth response factor 1 (EGR1) and WT1, which recognize GC-rich sequences (Figure 23). Clusters of SP1 were proposed between positions -1000 and -1 (relative to the TSS) of the *HIVEP1* 5'-flanking region. Four conserved EGR1 and three WT1 binding sites were predicted between positions -700 to -500. In addition, two NF-κB binding sites were indicated in the distal *HIVEP1* promoter structure flanking position -1200.

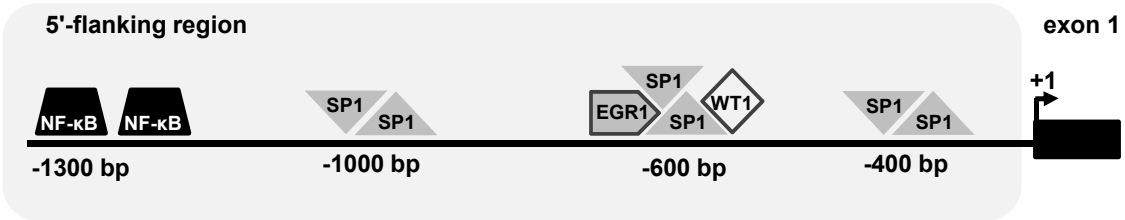

Figure 23: Schematic representation of predicted TFBS for SP1, EGR1, WT1 and NF-κB in the 5'-flanking region of *HIVEP1* Clusters of SP1 binding sites were predicted in the first 1000 bp of the 5'-flanking region and two κB-sites, surrounding position -1200 relative to the TSS (arrow). Three WT1 and four EGR1 binding sites were predicted at positions -700 to -500.

4.4.2 Zn finger proteins SP1, EGR1 and WT1 affect *HIVEP1* expression

To determine the influence of proposed Zn finger containing TFs on *HIVEP1* expression regulation *in vitro*, we performed overexpression experiments with SP1, EGR1 or WT1 in EA.hy926 cells (cf. chapter 4.4.2.1). EMSA experiments with subsequent antibody treatment were conducted to analyze the DNA/protein interactions, i.e. the interaction of predicted Zn finger proteins with certain *HIVEP1* promoter fragments, in EA.hy926 and THP1 cells *in vitro* (cf. chapter 4.4.2.2). We analyzed *in vivo* binding of predicted TFs with specific antibodies against the Zn finger proteins by ChIP assays (cf. chapter 4.4.2.3) in EA.hy926 cells.

4.4.2.1 Cotransfection assays

We analyzed the impact of TF overexpression on transcriptional activity in all *HIVEP1* deletion constructs, here exemplary shown for deletion constructs -740/+79, -740/+421, -1097/+79 and -1097/+421 in EA.hy926 cells. The effect of TF overexpression on transcriptional activity was expressed as relative activity of the deletion construct compared to the pGL3-Basic shuttle vector (FI=1). Overexpression of SP1 resulted in a significant 2.9 to 4.9-fold increase of transcriptional activity of *HIVEP1* deletion constructs (Figure 24A). The effect was independent of the intronic modulator (all p-values <0.001). Similar results were obtained, when EGR1 was overexpressed in EA.hy926 cells. EGR1 cotransfection led to a significant increase of the transcriptional activity of all *HIVEP1* constructs (all p-values <0.001; 3.8 to 4.8-fold, Figure 24B). By contrast, overexpression of WT1 led to a 2.85-fold increase of transcriptional activity of constructs, comprising the intronic modulator (both p<0.001; -1097/+421, -740/+421), while a decrease in deletion constructs' activities was observed for constructs lacking intron 1 (both FI=0.5, Figure 24C). In these cotransfection experiments, we overexpressed the WT1(-KTS) isoform, lacking the KTS-motif, i.e. the insertion of the three amino acids lysine-threonine-serine, since WT1(-KTS) is described to act as a TF, while WT1(+KTS) rather interacts with splicing factors (Roberts, 2005).

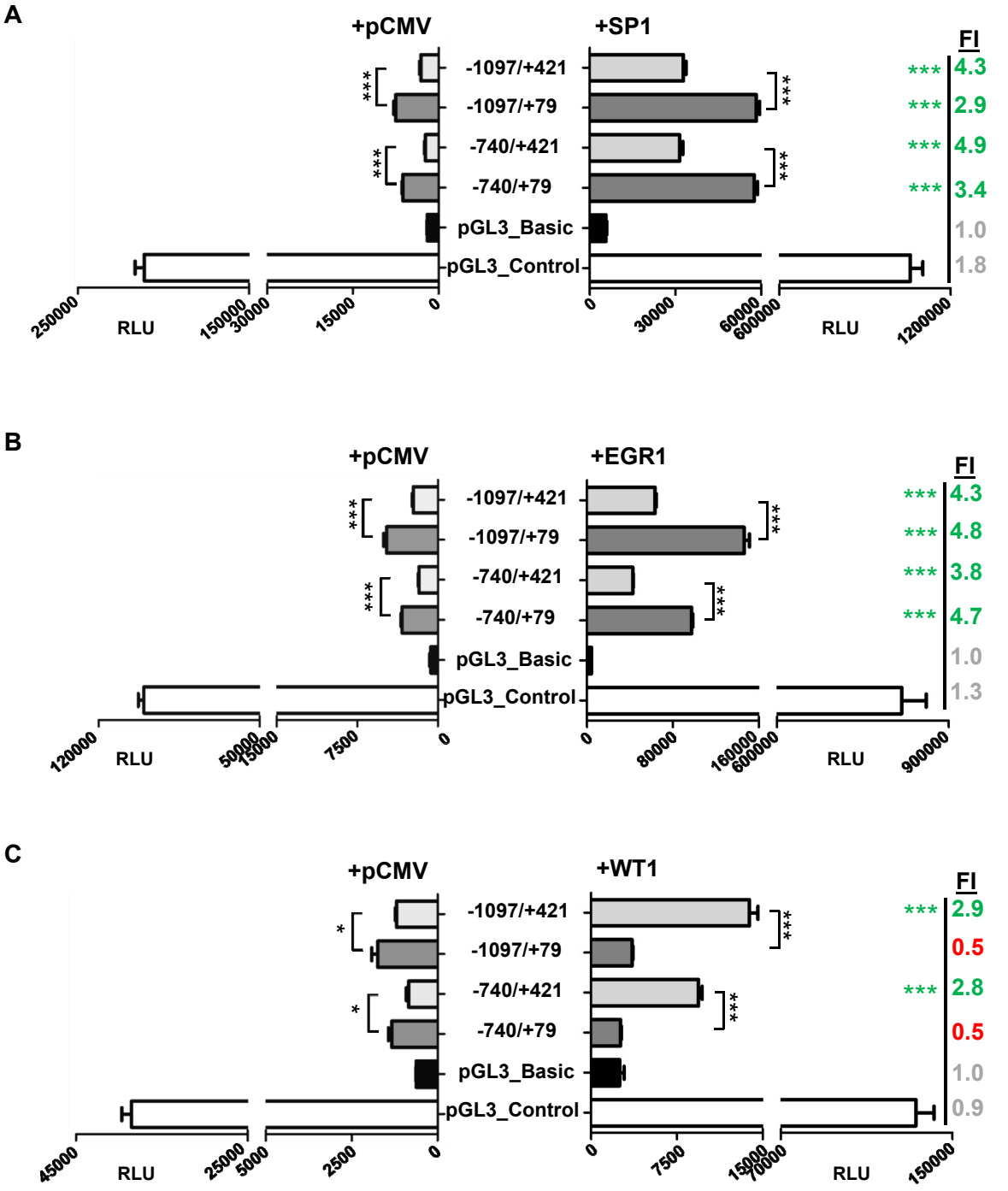

Figure 24: Cotransfection of SP1, EGR1 and WT1 in EA.hy926 cells SP1 (A) and EGR1 (B) overexpression led to a mean ~3.9 (SP1) and ~4.4 (EGR1)-fold increase of transcriptional activity of all deletion constructs compared to deletion constructs cotransfected with pCMV shuttle vector. C) WT1 overexpression resulted in a mean ~2.85-fold increased transcriptional activity of constructs harbouring intron 1 compared to shuttle vector activity, whereas a decrease in activity was shown for constructs lacking intron 1. FI was calculated as relative transcriptional activity of each construct compared to promoter-less pGL3-Basic (+pCMV) (FI=1). Transcriptional activity was assessed as relative light units (RLU). ***p<0.001, *p<0.05.

4.4.2.2 EMSAs

To analyze binding of the predicted TFs to the identified *HIVEP1* regulatory elements, we performed EMSAs using EA.hy926 and THP1 nuclear extracts. Nuclear extracts were isolated from unstimulated or TNFα-stimulated cells to compare interactions of TFs with the *HIVEP1* promoter regions under basic and inflammatory conditions. THP1 monocytes were treated with PMA to analyze differential binding patterns in monocytes compared to macrophages. Biotinylated PCR products, harbouring part of intron 1 or the proximal *HIVEP1* promoter, served as EMSA probes. Sequence-specific binding was visualized using the unlabeled PCR fragment (competitor) in a 200-fold molar excess for signal competition.

To analyze the interaction of SP1 and WT1 with the intronic modulator region, we designed an EMSA probe (138 bp) according to predicted SP1 and WT1 binding sites in intron 1 at position -14 to +124 (Figure 25A). Detection with an anti-biotin antibody revealed two specific band shifts (arrows), indicating interaction of EA.hy926 nuclear proteins with SP1 and WT1 binding sites, whereas THP1 nuclear proteins showed no sequence-specific interaction with the EMSA probe (Figure 25B). To identify the proteins, which mediated the specific band shifts by binding to the applied EMSA probe, EMSA blots were incubated with a SP1- or WT1-specific antibody to detect binding of the two predicted TFs at intron 1. Interaction of SP1 but not WT1 with intron 1 (black arrow) was observed for EMSAs performed with EA.hy926 nuclear extracts, while no binding of WT1 or SP1 was detected in THP1 cells.

Besides the investigation of TF binding to the intronic modulator, we analyzed the interaction of the predicted TF modul comprising SP1, EGR1 and WT1 with the 5'-flanking promoter region of *HIVEP1*. A fragment spanning positions -728 to -462 was used as biotinylated probe in EMSA (Figure 26A). Under basic conditions, no specific band shift was observed using THP1 or EA.hy926 nuclear extracts (Figure 26B). Differentiation of THP1 monocytes into macrophages led to sequence-specific interaction of nuclear proteins with the probe (black arrow), while we observed no band shift in PMA-stimulated EA.hy926 cells. Another specific band shift was observed when THP1 cells were stimulated with TNFα (open arrow). These band shift assays indicated that the region between -728 and -462 harbours *cis*-regulatory elements, differentially recognized by nuclear proteins under distinct inflammatory conditions.

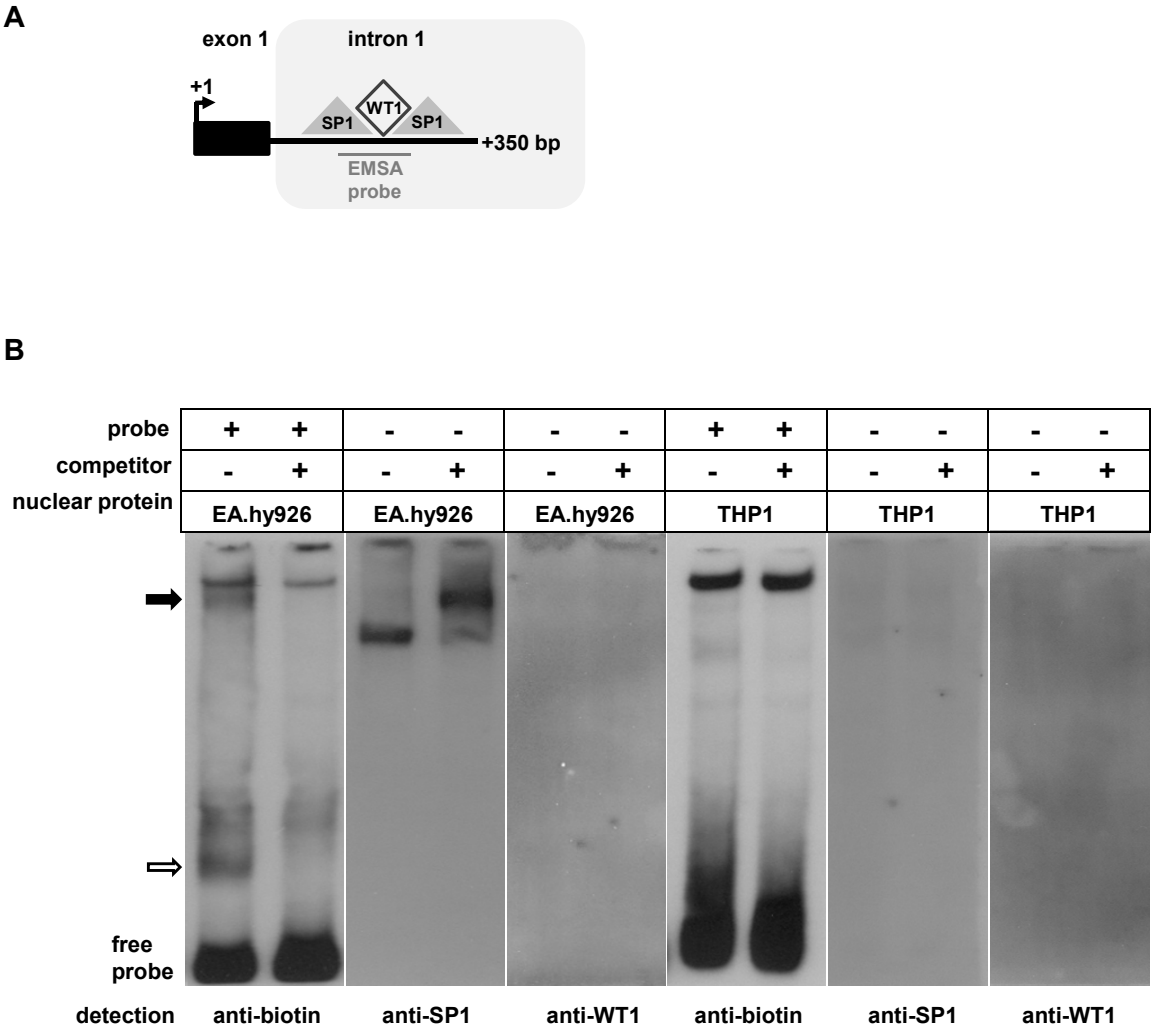

Figure 25: Interaction of SP1 with the intronic modulator in EA.hy926 cells A) Schematic representation of the EMSA probe harbouring SP1 and WT1 binding sites in intron 1. B) EMSA analysis, using an anti-biotin antibody, revealed two band shifts (arrows), demonstrating sequence-specific interaction of nuclear EA.hy926 proteins with the intron 1 probe (138 bp), comprising SP1 and WT1 binding sites. Detection of EMSA blots with a specific SP1 or WT1 antibody resulted in a defined signal for SP1 but not for WT1, in case of the competed upper band (black arrow). No specific band shift was observed for this position using THP1 nuclear extracts and no signal was observed by detection with a specific SP1 or WT1 antibody. Sequence-specific competitor was applied in a 200-fold excess (8 pmol). Free probe: Unbound oligonucleotides.

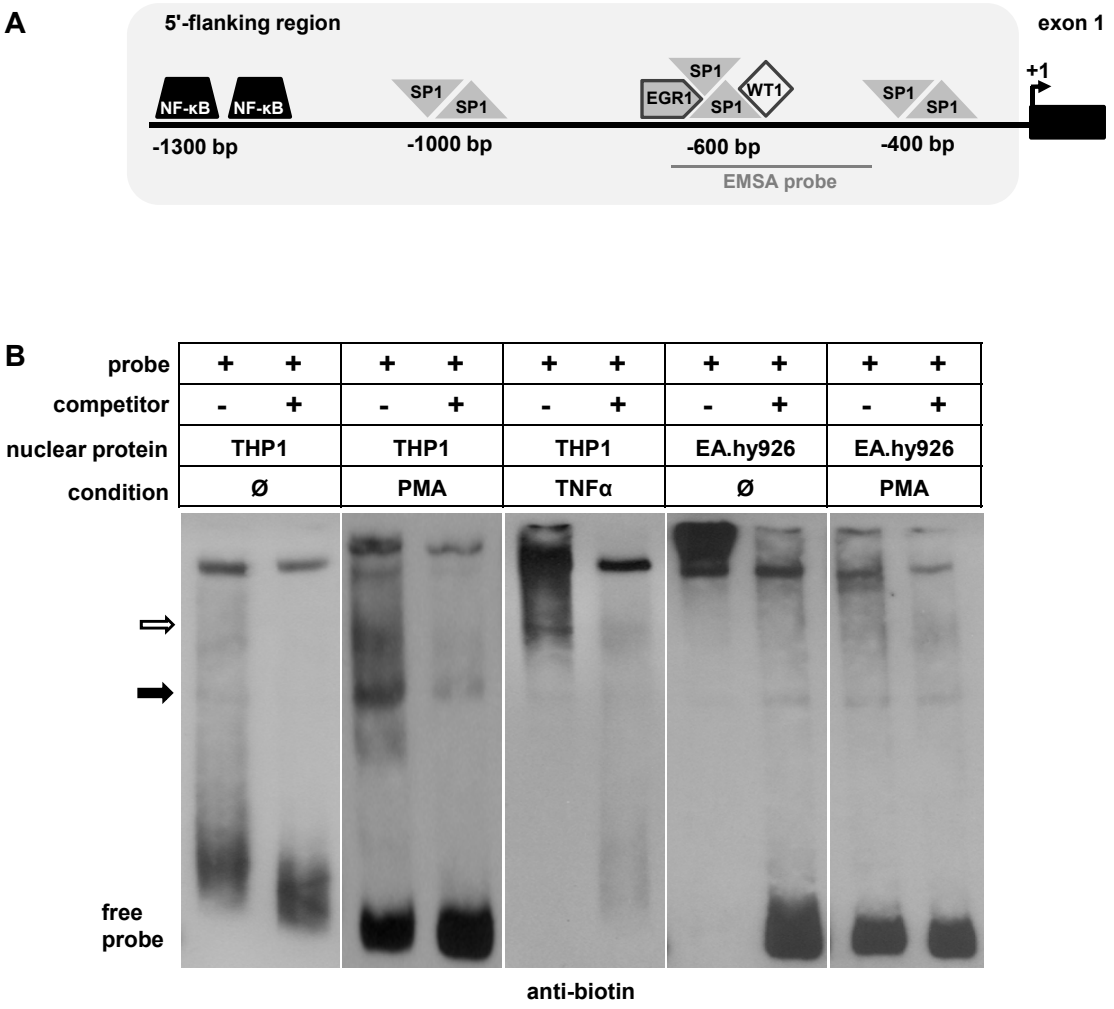

Figure 26: Stimuli-specific interaction of nuclear proteins with the proximal promoter of *HIVEP1* A) Schematic representation of the EMSA probe harbouring promoter portion -728 to -462. B) Stimulation of THP1 cells with PMA (10^{-8} M, 72h) or TNFα (10 ng/mL, 24h) resulted in two specific band shifts (black and open arrow). No specific band shift was observed in THP1 cells under basic conditions. When untreated or with PMA stimulated EA.hy926 nuclear extracts were employed, no competable band shift was observed. Sequence-specific competitor was applied in a 200-fold excess (8 pmol). Free probe: Unbound oligonucleotides. Ø: basic conditions.

4.4.2.3 ChIP analysis

To confirm the binding of potential *trans*-acting factors in the 5'-flanking region of *HIVEP1 in vivo*, we performed ChIP assays using EA.hy926 cells. Interactions of proteins with the chromatin were fixed and DNA was sonificated. Subsequently, specific antibodies against SP1, EGR1 and WT1 were applied for precipitation of bound *cis*-regulatory elements. Chromatin incubated with magnetic beads alone or with serum, but without antibodies, served as negative controls 1 and 2, respectively (Figure 27). PCR was performed to amplify specific *HIVEP1* promoter elements, for which binding of TFs SP1, EGR1 or WT1 was suggested (cf. chapter 4.4.1). Positive PCR control was conducted using 10% of extracted chromatin (Input) as template.

The ChIP analysis revealed a specific interaction of SP1 with *HIVEP1* promoter portions flanking positions -1000 and -400 under basic conditions, while no interaction of EGR1 and WT1 with the *HIVEP1* promoter was detectable *in vivo*.

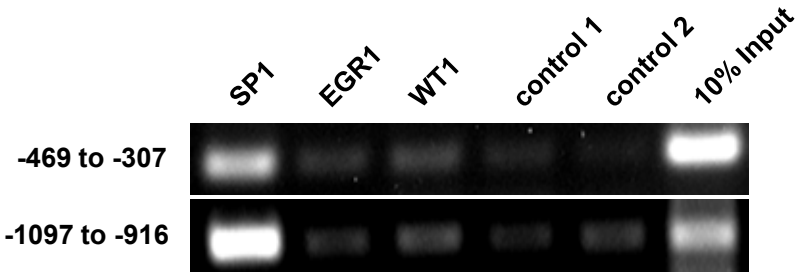

Figure 27: The *HIVEP1* promoter is bound by SP1 *in vivo* ChIP analysis in EA.hy926 cells demonstrated *in vivo* binding of SP1 to *HIVEP1* promoter portions -469 to -307 and -1097 to -916. Chromatin treated with magnetic beads or with beads and serum served as negative control (control 1 and 2, respectively). Input: Extracted chromatin served as positive control for PCR.

4.4.3 Interaction of nuclear proteins with NF-κB binding sites in the *HIVEP1* promoter

Since HIVEP1 has been proposed to be involved in NF-κB signaling and HIVEP1 expression was altered during inflammatory conditions (cf. chapter 4.1.1), we analyzed the *HIVEP1* promoter region with respect to NF-κB binding motifs. Two conserved NF-κB binding sites were predicted (TRANSFAC 7.0) at positions -1236 to -1227 and -1268 to -1259, both located in deletion construct -1650/+79, harbouring the major *HIVEP1* promoter activity. To determine if nuclear proteins of EA.hy926 cells interact with these predicted NF-κB binding sites in the *HIVEP1* promoter region, we designed different EMSA probes (Figure 28A), comprising one of the two (probe A or B) or both (probe AB) NF-κB binding motifs.

Application of EMSA probe AB revealed three band shifts (arrows) that were competed with the unlabeled probe AB in EA.hy926 cells under basic conditions (Figure 28B). The unlabeled EMSA probe A competed each of the three specific band shifts and the unlabeled EMSA probe B was able to compete the two lower band shifts (black arrows), leaving the residual band shift unaffected (open arrow, Figure 28B). Two different specific band shifts (black arrows) were observed when probe A was employed, harbouring the predicted NF-κB recognition site at positions -1268 to -1259 (Figure 28B). EMSA probe B revealed a specific band shift, comprising the isolated NF-κB binding site at positions -1236 to -1227 (Figure 28B). These results indicate specific interactions of nuclear proteins in EA.hy926 cells with both predicted NF-κB binding sites in the *HIVEP1* promoter.

In addition, two of the three specific band shifts (black arrows) observed for EMSA probe AB were also competed using a commercial NF-κB consensus site (c) as competitor (Lenardo and Baltimore, 1989), substantiating the interaction of NF-κB family members with the *HIVEP1* promoter portion (Figure 28C). These interactions were not altered when EA.hy926 cells were incubated with TNFα (10 ng/mL, 24h), since the three specific band shifts were still detectable with identical intensity compared to basic conditions (Figure 28C/D). Interestingly, the intensity of the three band shifts were reduced to ~50% upon incubation of EA.hy926 cells with simvastatin (2.4 µM, 24h), applied alone or in combination with TNFα (10 ng/mL, 6h) compared to basic conditions (Figure 28C/D), indicating that simvastatin reduces the affinity of nuclear proteins to NF-κB binding sites in the *HIVEP1* promoter.

Subsequent detection of EMSA blots with specific antibodies against NF-κB family members (RelA, RelB, c-Rel, p105/50, p100/p52) could not demonstrate binding of any of the NF-κB factors to predicted NF-κB sites in these EMSA experiments (data not shown).

A


EMSA probes
NFκB
NFκB
-1275 TTCACAATGACTTTCCCCTTCCTTCTACGCGTTGCTGAGGAAACCCCCTTG -1224
AB
A
B

B

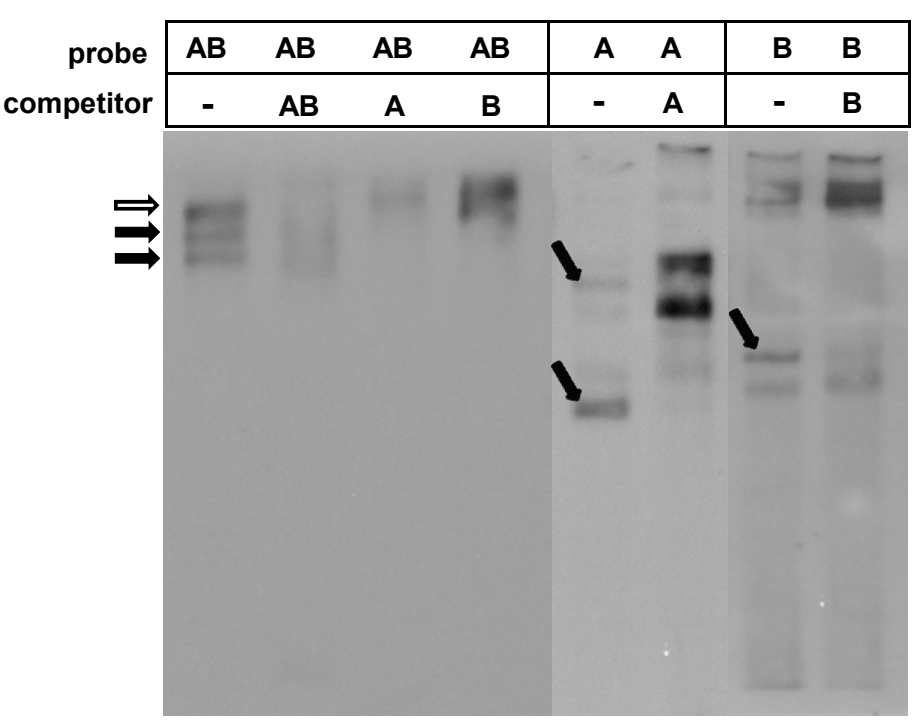
probe AB AB AB AB A A B B
competitor - AB A B - A - B

EA.hy926 Ø

C

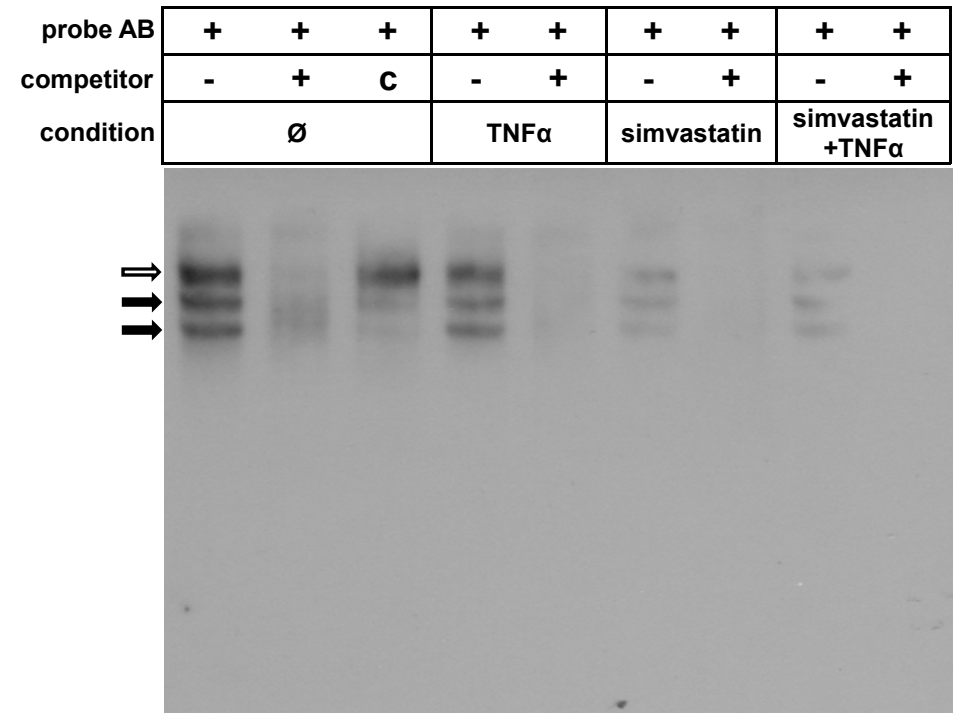
probe AB + + + + + + + + +
competitor - + c - + - + - +
condition Ø TNFα simvastatin simvastatin +TNFα

EA.hy926

D

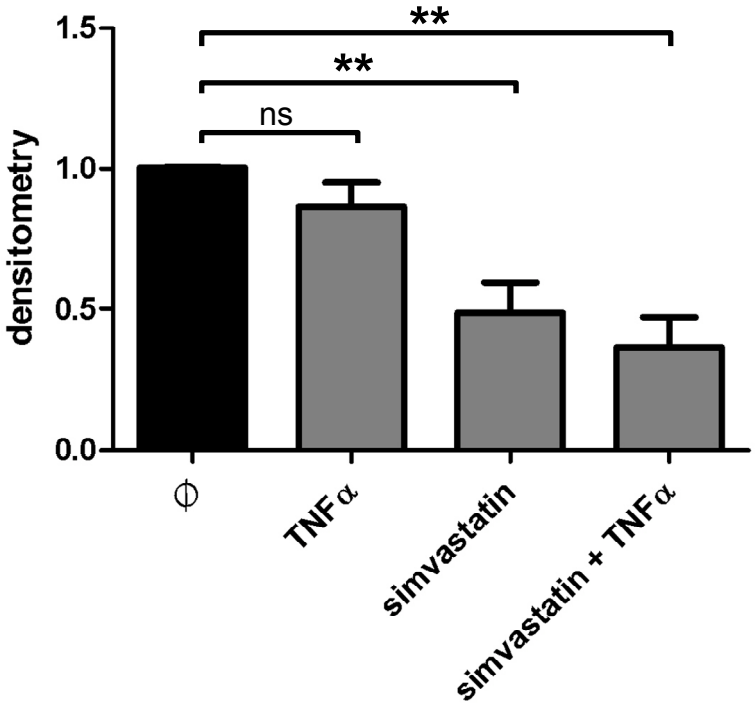
densitometry
1.5
1.0
0.5
0.0
**
**
ns
ϕ
TNFα
simvastatin
simvastatin + TNFα

Figure 28: Interaction of nuclear proteins with NF-κB binding sites in the *HIVEP1* promoter is altered by simvastatin A) EMSA probes were designed harbouring one of the two (probe A or B) or both (probe AB) predicted NF-κB binding sites at positions -1236 to -1227 and -1268 to -1259 in the *HIVEP1* 5'-flanking region. B) We detected three specific band shifts under basic conditions using EMSA probe AB (black and open arrows). The unlabeled EMSA probe A competed all three band shifts, while EMSA probe B competed the two lower band shifts (black arrows). Using EMSA probe A revealed two and application of EMSA probe B one specific band shift (black arrows) under basic conditions in EA.hy926 cells. C) Two of the three band shifts detected (black arrows), using EMSA probe AB were also competed using the NF-κB consensus site (c) as competitor (Lenardo and Baltimore, 1989). After treatment of EA.hy926 cells with simvastatin (2.4 µM, 24h) with or without inflammatory TNFα (10 ng/mL, 6h) background, the intensity of the three band shifts was reduced, while TNFα alone (10 ng/mL, 24h) had no influence on the interaction of nuclear proteins with EMSA probe AB. D) Densitometric analysis revealed a significant reduction of the three band shifts to ~50% upon simvastatin treatment compared to basic conditions or treatment of cells with TNFα alone. Densitometric analysis involved three EMSA blots. Basic conditions were used as reference and set 1. **p<0.01, ns = not significant. Ø: basic conditions.

4.5 Knockdown of *HIVEP1* by siRNA

Since there is scare information and data on HIVEP1 signaling, we planned a siRNA approach to identify *HIVEP1* target genes. Knockdown efficiency was monitored at the HIVEP1 mRNA level by semiquantitative PCR. The first step was to analyze the existence of HIVEP1 transcripts predicted by ENSEMBLE database in EA.hy926 and THP1 cells. For this purpose, we conducted PCRs using cDNA as template and different primer pairs (appendix, Figure A2, Table A1). The results of the sequential analysis of HIVEP1 transcripts supposed existence of the full length HIVEP1 transcript, comprising exon 1c to 9, coding for full length HIVEP1 in EA.hy926 and THP1 cells (appendix, Figure A2). In addition, a transcript harbouring the alternative exon 5 and exons 6 to 9, and another transcript containing two alternative exons, termed 1a and 1b, were detected. We choose exon 8 as target for the siRNA to knockdown the detected *HIVEP1* transcripts, which code for full length HIVEP1 and a putative isoform, harbouring the C-terminal HIVEP1 residue (exon 5 to 9). The sequence of the siRNA duplex was designed using the siRNA selection program “siRNA at WHITEHEAD” (format: AA(N19)TT) as described by Pei and Tuschl (Pei and Tuschl, 2006). Since many off-target effects (i.e. down-regulation of unintended targets) of siRNAs exist (Jackson and Linsley, 2010), off-target effects were additionally checked using the net-based program “ParAlign”. The siRNA duplex was elected, for whom only two putative off-targets were predicted: the pseudogene teratocarcinoma-derived growth factor 6 (TDGF6) and the Ras protein-specific guanine

nucleotide-releasing factor 2 (RASGRF2). A commercial control siRNA duplex (low GC, Invitrogen), which displays a minimized sequence homology to any known vertebrate transcript, served as control for sequence-independent effects of siRNA transfection. When PCR was conducted using primers located in exon 1(c) and at the start of exon 4, transient transfection of EA.hy926 cells with the HIVEP1 siRNA duplex targeting exon 8 for 48h resulted in a ~50% knockdown of HIVEP1 mRNA expression compared to the transfected siRNA control duplex (Ctrl) (Figure 29A). For the PCR product comprising exon 8, a ~75% knockdown of *HIVEP1* was achieved compared to control, independent of siRNA concentrations applied (200 and 300 nM; Figure 29B). Thus, the designed siRNA duplex targeting exon 8 is able to knockdown HIVEP1 transcripts by transient transfection of 200 -300 nM siRNA using oligofectamine for 48h.

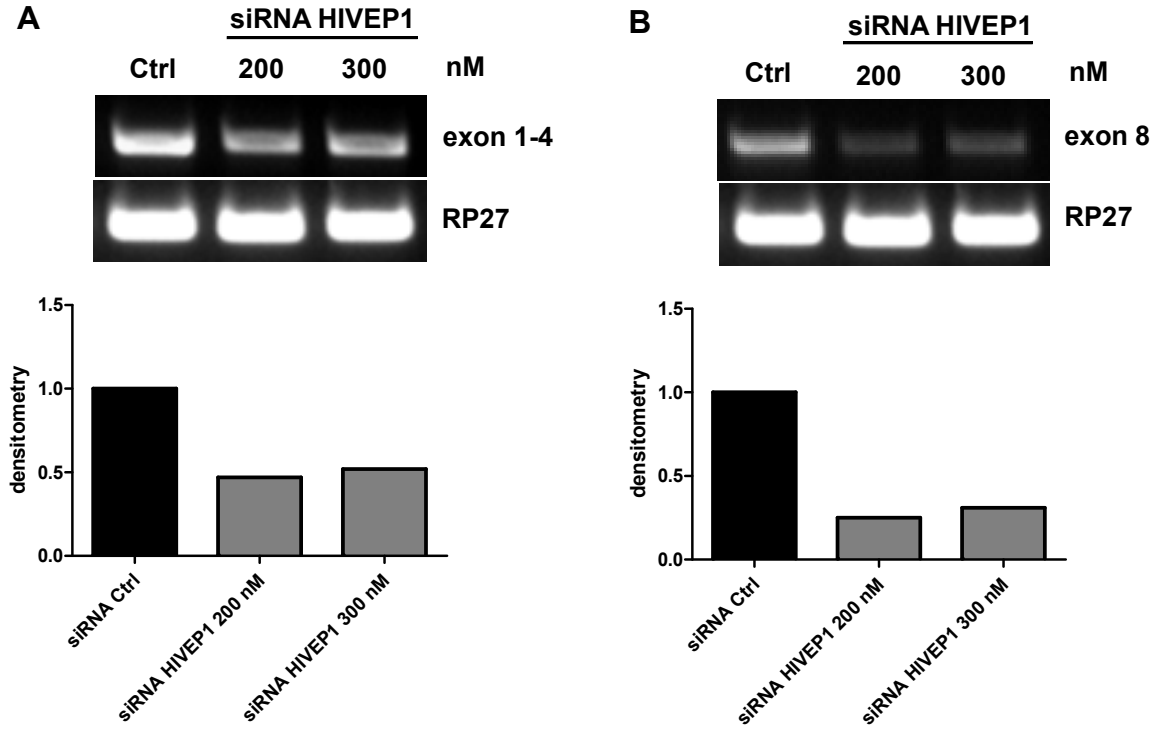

Figure 29: Knockdown of *HIVEP1* by siRNA in EA.hy926 cells A siRNA duplex (200 or 300 nM) targeting *HIVEP1* exon 8 was transiently transfected into EA.hy926 cells. We observed a ~50% (A) and a ~75% (B) knockdown of *HIVEP1* compared to the control siRNA (Ctrl) after 48h, for the PCR product comprising exon 1(c) to 4 and exon 8, respectively. RNA was isolated and used for cDNA synthesis. RP27-PCR served as loading control. Ctrl, siRNA control duplex.

5 DISCUSSION

5.1 Proximal and distal regulatory elements for *HIVEP1* expression

The transcriptional control of active genes is mediated by interaction of *trans*-acting factors at specific *cis*-active elements in the promoter region to mediate precise spatial and temporal gene expression (Maston et al., 2006). As described in chapter 1.3, the promoter region can be subdivided into a core promoter region, harbouring recognition sequences necessary for PIC assembly, and proximal promoter regions, possessing binding sites for cofactors. In addition, further distant regulatory elements may take part in gene expression regulation by silencing or enhancing specific gene expression (Maston et al., 2006).

By a multistage approach following GWA, including individuals from the MARTHA, FARIVE and MEGA study, a SNP (rs169713) located 90 kb upstream of the *HIVEP1* gene has been associated with VT (Morange et al., 2010). It has been suggested, that this SNP is a marker of a chromosomal region susceptible for VT, thereby indicating that functional, yet identified, SNPs may be located within the *HIVEP1* gene. In a further GWA, using more genetic markers (dense fine map) in formerly proposed phenotype-associated loci, the *HIVEP1* gene was confirmed to be highly associated (*HIVEP1* exon 4) with VT (Germain et al., 2011). The region encompassing the tagging SNP rs169713 was analyzed in this study with regard to its potential enhancer or silencer capacity for the *HIVEP1* gene, since enhancers may be located even hundreds of kbp away from their target gene (Maston et al., 2006). One regulatory element, for example, controls the expression of three different genes, IL-4, IL-13 and IL-5, spread over 120 kb at human 5q31 (Loots et al., 2000) and the *α-globulin* gene expression is under the control of elements positioned 60 kb upstream (Higgs et al., 1990; Higgs et al., 2008). In our analysis, a 319 bp region harbouring the rs169713 T allele was found to enhance the pGL3-Promoter activity using reporter gene assays in EA.hy926 and THP1 cells. Thus, the region 90 kb upstream of *HIVEP1* may harbour allele-dependent enhancer capacity for *HIVEP1.* Cloning of the potential enhancer element in a vector, comprising the identified *HIVEP1* proximal promoter region in front of the *luciferase* gene instead of the minimal SV40 promoter, would demonstrate the interplay of the enhancer with the *HIVEP1* promoter and support this hypothesis.

Besides the analysis of the potential enhancer, reporter gene asssays revealed a core promoter region sufficient to guide basal *HIVEP1* expression between positions -1099 and

-469, whereas the strongest transcriptional activity was observed between positions -1650 and -1241 in both, endothelial and monocytic cells. An intronic modulator affected *HIVEP1* expression in a cell type-specific manner. In THP1 cells, the intronic modulator exclusively increased transcriptional activity of deletion construct -1650/+79, harbouring the most considerable promoter activity, and decreased transcriptional activity of the very proximal construct -469/+79. This result indicates that the intronic modulator differentially interacts with the core and proximal promoter region of *HIVEP1* in monocytic cells. In endothelial cells, the intronic modulator strongly influenced the core and proximal promoter activity by decreasing *HIVEP1* 5'-flanking deletion constructs' transcriptional activities, indicating that crucial *cis*-active regulatory elements for endothelial *HIVEP1* expression are positioned in intron 1. That intronic regions may possess cell type-specifc promoter activity has also been demonstrated for the *kidney brain* (*KIBRA)* gene promoter (K. Guske, PhD thesis), the *SM α-actin (SMαA)* promoter (Kawada et al., 1999) or the erythroid-specific *GATA-1* gene expression regulation (Seshasayee et al., 2000).

5.2 Involvement of Zn finger proteins and NF-κB in *HIVEP1* expression regulation

In silico analyses in general predict the binding of distinct TFs to the analyzed DNA sequence, e.g. the promoter sequence of the gene of interest. These predictions of TFs and TF families, which might be involved in the expression regulation of the analyzed gene, e.g. HIVEP1, are limited, since they are exclusively based on DNA sequence. However, different physiological conditions may alter the affinity of TFs to their consensus sequences, which are not considered in computational analyses. On the one hand, the relative respective abundance of distinct TFs is altered upon different stimulations, as shown for EGR1, which expression is increased upon PMA stimulation (Silverman and Collins, 1999), leading to synergistic interactions or to competition at consensus sites, as described for Zn finger proteins SP1, EGR1 and WT1 at their overlapping binding sites in the *TXA2* promoter (Gannon et al., 2009). On the other hand, distinct physiological states of cells may mediate posttranslational modifications that could be necessary for TF activation or TF translocation into the nucleus, as shown for NF-kB family members (Zhong et al., 2002). Since *in silico* analyses predicted binding sites for Zn finger proteins SP1, WT1 and EGR1 in the *HIVEP1* promoter region, the impact of these factors on *HIVEP1* expression regulation was analyzed under basic and stimulatory conditions.

Overexpression, EMSA and ChIP experiments revealed that SP1 is involved in basal *HIVEP1* expression regulation in endothelial cells by binding to the repressive intronic

modulator region as well as to positions -1000 and -400 in the 5'-flanking region of *HIVEP1* in EA.hy926 cells. The ubiquitously expressed SP1 binds with high affinity to GC-boxes and its activity is altered by posttranslational modifications, such as phosphorylation (Chu and Ferro, 2005), or by interaction with other proteins, such as tumor suppressors and oncogenes (Black et al., 2001). Binding of SP1 molecules to two or more consensus sites has a synergistically activating effect and SP1 binding to another SP1 molecule leads to the so-called superactivator capacity of SP1 (Pascal and Tjian, 1991). As SP1 recruits TBP/TFIID and the chromatin remodeling complex SWI/SNF, it is known to initiate the gene transcription of TATA-less genes (Wierstra, 2008). No TATA motif (TATA-A/T-AA-A/G) was found in the first 50 bp of the *HIVEP1* 5'-flanking region, indicating that the *HIVEP1* promoter lacks a TATA box. Instead, the first 1500 bp of the *HIVEP1* 5'-flanking region harbour a GC content of 74% and a CpG island is predicted between positions -180 to +570 (UCSC Genome Browser, http://genome.ucsc.edu/), including the intronic modulator. GC-rich promoters are typically lacking a TATA-box (Carninci et al., 2006), suggesting *HIVEP1* to be transcriptionally controlled by a CpG island promoter.

In THP1 cells, the intronic modulator exclusively increased transcriptional activity of deletion construct -1650/+79 harbouring the most considerable promoter activity. Our EMSAs did not reveal any binding of SP1 to the intronic modulator under basic conditions, while SP1 overexpression increased transcriptional activity of *HIVEP1* promoter deletion constructs in monocytes (data not shown). This suggests an interaction of TFs that bind between positions -1650 and -1097 in the *HIVEP1* 5'-flanking region with the intronic modulator in THP1 monocytes.

Since SP1 increased the promoter activity in cotransfection assays in THP1 cells, SP1 is suggested to be involved in basal *HIVEP1* expression by binding to the 5'-flanking region in THP1 and to both, the 5'-flanking and intronic region as shown in EMSA, ChIP and cotransfection assays, in EA.hy926 cells.

In addition to SP1, EGR1 and WT1 were able to significantly alter *HIVEP1* expression. While overexpression of EGR1 increased transcriptional activity of all promoter deletion constructs, WT1 exclusively increased transcriptional activities of constructs comprising the intronic region in EA.hy926 cells, demonstrating the modulating impact of intron 1 on *HIVEP1* expression. The tumor suppressor WT1 plays a pivotal role during development. It is predominantly expressed in the kidney and genital organs (Rauscher, 1993), while we observed endogenous expression of *WT1* in endothelial EA.hy926 and monocytic THP1 cells using RT-PCR. WT1 acts both, as a transcriptional repressor and activator, depending on the presence of associated proteins, which modulate the regulatory potential of WT1 (Rauscher, 1993). Upon association with p53, WT1 has been described

as a potent transcriptional activator for the growth arrest and DNA damage-inducible protein GADD45 (Zhan et al., 1998). Since the HIVEP1 isoform GAAP1 increases the expression of tumor suppressor gene *p53* (Lallemand et al., 2002), the observed activating effect of WT1 overexpression on *HIVEP1* promoter constructs comprising the intronic modulator could be a positive feedback mechanism for *HIVEP1* expression. Thereby, binding of the p53-WT1 complex to the regulatory intronic region of *HIVEP1* leads to upregulation of *HIVEP1* expression, in turn increasing *p53* expression by GAAP1. Since our EMSA experiments revealed binding of SP1, and not WT1 to the intronic modulator under basic conditions, certain physiological states could be crucial for the interaction of the p53-WT1 complex with the *HVEP1* intronic modulator. GAAP1 and not full length HIVEP1 is involved in this hypothesized feedback mechanism. Since WT1 has been found to colocalize and interact with spliceosomal components (Larsson et al., 1995; Davies et al., 1998) and GAAP1 arises from alternative splicing, binding of WT1 to the intronic modulator could result in alternative splicing of HIVEP1 pre-mRNA, generating GAAP1. Additionally, *p53* expression is upregulated by EGR1 (Nair et al., 1997) and was shown to form a complex with EGR1 (Liu et al., 2001). Thus, EGR1 may be involved in the p53-HIVEP1-feedback mechanism, since EGR1 overexpression significantly increased *HIVEP1* promoter activity. EGR1 belongs to the group of “immediate-early response genes”, indicating that it is rapidly and transiently induced in response to certain stimuli. Those stimuli include shear stress, mechanical injury, hypoxia, ROS and the plateled-derived growth factor (PDGF), which are implicated in the development of VD (Silverman and Collins, 1999). Therefore, EGR1 target genes, such as TNFα, IL-2, ICAM-1 and tissue factor (Yao et al., 1997; Skerka et al., 1995; Maltzman et al., 1996; Cui et al., 1996), are involved in the pathogenesis of VD. In this respect, the *HIVEP1* gene, which was shown in this work to be induced by inflammatory stimuli and whose locus is associated with VT, could be another EGR1 target gene involved in the development of VD.

EGR1, SP1 and WT1 recognize similar GC-rich consensus sequences and overlapping binding sites are often found in promoters (Silverman and Collins, 1999). An identical situation for the *HIVEP1* promoter is described in this work. The interplay between SP1, EGR1 and WT1 in gene expression regulation has already been reported for several genes, such as the *human copper-zinc superoxide dismutase* gene (Minc et al., 1999) or the *TXA2* gene (Gannon et al., 2009). SP1 occupies the consensus sites under basic conditions, providing basal gene expression, while stimulation, for example with PMA, induces *EGR1* expression (Silverman and Collins, 1999). Subsequently, EGR1 competes with SP1 and is able to displace SP1 at their overlapping consensus sites (Kubosaki et al., 2009) leading to enhanced gene expression, as shown for *TXA2* (Gannon et al., 2009)

and *PDGF A-chain* gene expression (Khachigian et al., 1995). Notably, we only observed EGR1 protein expression in EA.hy926 cells and activated monocytes after stimulation with PMA (data not shown). Thus, altered *HIVEP1* expression, at least during the differentiation of monocytes to macrophages may be mediated in part by increased EGR1 protein expression. WT1 in turn is able to compete with EGR1 at its binding sites (Rauscher et al., 1990). Detection of EMSA blots with a SP1- or WT1-specific antibody demonstrated binding of SP1 and not WT1 to the intronic modulator under basic conditions. In addition, ChIP analyses under basic conditions revealed binding of SP1 and not of EGR1 or WT1 to their overlapping consensus sites in the *HIVEP1* promoter, indicating that SP1 is involved in basal *HIVEP1* expression. Stimulation of cells with PMA instead could lead to binding of EGR1 to the GC-rich elements displacing SP1 and increasing *HIVEP1* expression. However, the distinct physiological conditions, in which EGR1 and WT1 act on *HIVEP1* expression regulation, remain to be investigated in detail.

Since binding of recombinant HIVEP1 to NF-κB sites in enhancer and promoter regions has been shown in several studies (cf. chapter 1.4.2) and two NF-κB binding sites were predicted by computational analysis in the 5'-flanking of *HIVEP1*, we performed EMSAs to analyze the interaction of nuclear proteins with *HIVEP1* NF-κB consensus sites at positions -1268 to -1227. EMSA demonstrated binding of EA.hy926 nuclear proteins to NF-κB sites in the *HIVEP1* promoter, which confirms that TFs binding to NF-κB consensus sites are involved in *HIVEP1* expression regulation. Notably, EMSA probes harbouring one of the two NF-κB sites were able to compete those band shifts emerged by interaction of nuclear proteins with the EMSA probe containing both NF-κB sites, indicating that the binding of TFs to one of the two NF-κB consensus sequences influences interaction of TFs with the other NF-κB site in the *HIVEP1* promoter. However, no signal at competed band shifts was observed, when EMSA blots were detected with antibodies against NF-κB family members. On the one hand, binding of a protein to a DNA sequence leads to changes in protein conformation, which in turn could mask the epitope recognized by the used antibody. On the other hand, antibodies that are useful in western blots do not necessarily fit in EMSA, since denatured proteins are applied in western blots and native proteins in EMSA experiments. Indeed, a commercial NF-κB consensus sequence (Lenardo and Baltimore, 1989) was an effective competitor in these EMSA experiments, confirming the hypothesis that, besides Zn finger proteins, NF-κB family members are involved in *HIVEP1* expression regulation by binding to the *HIVEP1* promoter.

5.3 Impact of genetic variants on *HIVEP1* promoter activity

Genetic variants residing within or in close proximity to TFBS may influence the interaction of *trans*-acting factors with their consensus sequences leading to altered gene expression. Each nucleotide change in the consensus sequence may alter the TF binding, i.e. weakening TF binding affinity to this consensus site or completely disrupting the interaction (Telgmann et al., 2009). Alterations of TF binding patterns due to the existence of different alleles at the locus have already been demonstrated for different promoter regions (Dördelmann et al., 2008; Hagedorn et al., 2009). In this respect, we analyzed the impact of HIVEP1 MolHap1-4, generated by three adjacent SNPs (rs1574343_A>C, rs1574166_C>G, rs3902984_A>C) at positions -1060 to -953, on *HIVEP1* promoter activity in the context of deletion construct -1650/+79, harbouring the major promoter activity. Step wise alteration of the wt sequence revealed a step wise decrease of transcriptional activity. This observation indicates a change in TF affinities or binding patterns at consensus sites, harbouring the analyzed SNPs. *In silico* analysis predicted a change for binding patterns generated by rs1574166_C>G and rs3902984_A>C. A substitution of the rs1574166 C allele with the minor G allele predicted to lead to the deletion of the consensus site for TF Yin-Yang (YY-1), which binds to the Inr element (Lee et al., 1993), and to the addition of two SP1 binding sites. Addition of a binding site for the TF family activator protein-2α (AP-2α) was supposed for the site including the rs3902984 minor C allele. MolHap4 comprises both, the rs1574166 and rs3902984 minor alleles, and displayed a transcriptional activity reduced to 50% compared to that of wt (MolHap1). Thus, the change of TF binding patterns, especially the gain of an AP-2α consensus site, could lead to the decreased *HIVEP1* promoter activity observed for MolHap4, since AP-2α TFs act also as a repressor and compete with SP1 at its binding sites (Mitchell and DiMario, 2010), which has been shown in here to be crucial for basal *HIVEP1* expression.

5.4 Pro- and antiinflammatory stimuli regulate *HIVEP1* expression

5.4.1 Modulation of *HIVEP1* expression by cytokines

As HIVEP1 binds to the NF-κB consensus sequence (Muchardt et al., 1992) and has been shown to be expressed in human atherosclerotic plaques (Morange et al., 2010), HIVEP1 has been suggested to be involved in inflammatory signaling cascades. Our analysis from available microarray datasets suggested an influence of inflammatory stimuli on *HIVEP1* expression. In this work, incubation of EA.hy926 cells and monocytes with the cytokines TNFα and IL-1β increased HIVEP1 mRNA expression, while relatively high HIVEP1 mRNA expression was detected in macrophages without stimulation in this study. The

increase of *HIVEP1* expression by PMA and TNFα was also detected at the protein level in THP1 cells, suggesting HIVEP1 mRNA level as an indicator for HIVEP1 protein amounts in untreated and stimulated monocytes. By contrast, in EA.hy926 cells, lower HIVEP1 mRNA expression translated into increased HIVEP1 protein concentrations under basic conditions. In EA.hy926 cells, TNFα stimulation did not result in higher HIVEP1 protein expression. In addition, TNFα had no effect on *HIVEP1* promoter activity in neither cell line, whereas EMSA analyses revealed differential binding of THP1 nuclear proteins after stimulation with TNFα and PMA to the *HIVEP1* promoter, indicating that the region between -728 and -462 harbours *cis*-regulatory elements, differentially recognized by nuclear proteins under distinct inflammatory conditions. Compared to TNFα, PMA altered transcriptional activity of deletion constructs in THP1 and EA.hy926 cells.

Taken together, these results indicate that changes in TF/promoter interaction do not necessarily result in altered HIVEP1 expression but may affect mRNA stability, dependent on distinct inflammatory signals and cell types. mRNA stability is estimated to control the translation efficiency of ~10% of human genes. While housekeeping-genes provide mRNAs with long and invariant half-lives, short mRNA half-lives are characteristic for immediate-early response genes, such as oncogenes and cytokines (Bolognani and Perrone-Bizzozero, 2008). In that respect, TNFα has been reported to influence mRNA stability by affecting the 3'-UTR of a given gene (Matsumiya et al., 2010). Usually, the 3’-UTR harbours the sequences that affect mRNA in/stability, such as the adenylate-uridylate rich element (ARE) AUUUA (Shaw and Kamen, 1986), which can lead to mRNA stabilization, e.g. by Hu proteins, or degradation, e.g. by tristetraprolin (TTP), depending on the binding protein (Jaksik and Rzeszowska-Wolny, 2012). The 3'-UTR of *HIVEP1* possesses AU-stretches, of which one is similar to the ARE (Fan and Maniatis, 1990), indicating that *HIVEP1* expression may be influenced by mRNA de/stabilization processes. Thus, in TNFα-stimulated EA.hy926 cells, increased HIVEP1 mRNA levels may result from increased HIVEP1 mRNA stability by recruitment of TNFα-induced RNA-binding proteins, which protect HIVEP1 mRNA from degradation, delivering a stabile mRNA depot that can be rapidly used for protein synthesis. Since the detected HIVEP1 protein expression does not alter upon TNFα stimulation compared to basic conditions, the HIVEP1 protein turn over may be increased by TNFα challenge, in contrast to the HIVEP1 mRNA expression. Combination of distinct inflammatory cytokines (TNFα, IL1-β, IL-4) may result in an increased HIVEP1 protein expression. In THP1 cells, TNFα may alter TF binding patterns, which leads to an increased HIVEP1 mRNA stability that is translated in increased HIVEP1 protein amount compared to basic HIVEP1 expression level in monocytes.

5.4.2 Impact of statins on *HIVEP1* expression

Since the antiinflammatory, so-called pleiotropic actions of statins have been suggested to also depend on altered protein interaction at NF-κB consensus motifs (Dichtl et al., 2003), we analyzed the impact of commonly clinically used statins on *HIVEP1* expression *in vitro*. While HMG-CoA reductase inhibitors simvastatin, atorvastatin and rosuvastatin led to a significantly decreased *HIVEP1* expression, pravastatin and the antiinflammatory COX inhibitor aspirin (Yin et al., 1998), as a control, did not affect *HIVEP1* expression, suggesting a substance-specific effect of statins on *HIVEP1* expression. More importantly, in TNFα-stimulated endothelial cells, high-dose atorvastatin challenge led to a paradoxically increased *HIVEP1* expression. Dose-dependent opposed effects of atorvastatin on endothelial cell migration and proliferation as well as on angiogenesis have been reported. Thereby, low-dose atorvastatin enhanced angiogenesis in mice as well as migration and proliferation of endothelial cells, while high-dose atorvastatin reversed the effects (Weis et al., 2002). Simvastatin was shown to dose-dependently increase the expression of TNFα type I receptor (TNFαRI) (Tang et al., 2006) and pravastatin as well as fluvastatin were able to induce TNFα production in monocytes under distinct conditions (Takahashi et al., 2005), suggesting that high doses of atorvastatin may also be able to potentiate the TNFα-mediated *HIVEP1* expression by increasing the TNFαRI expression or TNFα production during inflammatory conditions. Otherwise, simvastatin and rosuvastatin were able to compensate the TNFα-induced *HIVEP1* expression below basic HIVEP1 mRNA expression, suggesting that simvastatin and rosuvastatin may be more effective as atorvastatin in inflammatory signaling involving HIVEP1. In addition, simvastatin was able to reduce the interaction of nuclear proteins with NF-κB sites in the *HIVEP1* promoter. This observation confirms the by Dichtl et al. (Dichtl et al., 2003) previously described effect of simvastatin to alter the NF-κB binding affinity to κB consensus sites, here demonstrated at consensus sites in the *HIVEP1* promoter. Statins are able to mediate their antiinflammatory potential by reducing the amount of active Rho resulting in a reduction of NF-kB activation (Sposito and Chapman, 2002). In hypercholesterolemic individuals, simvastatin was shown to decrease TNFα and IL-1β levels (Ferro et al., 2000), indicating that simvastatin is able to mediate its effect on *HIVEP1* expression by decreasing cytokines. Use of rosuvastatin in apparently healthy individuals significantly reduced the occurrence of VTE (Glynn et al., 2009), while a prospective study of pravastatin did not reveal any effect on VTE (Freeman et al., 2011). A recent meta-analysis regarding the effect of statins in the prevention of VTE, revealed a protective effect of statin use on VTE and DVT (Pai et al., 2011). In addition, statin application in patients with atherosclerosis was demonstrated to be associated with a significant reduction in VTE occurrence, thereby a dose-related statin response was

observed (Khemasuwan et al., 2011). A recent prospective cohort study regarding unintended effects of statin use gave a hint that certain statins may have a protective impact on VTE (Hippisley-Cox and Coupland, 2010). In conclusion, the demonstrated effect of certain statins, especially simvastatin and rosuvastatin, on *HIVEP1* expression together with the documented effects of statins on VT in several studies, underline the involvement of HIVEP1 in inflammatory processes and the link of HIVEP1 to VT.

However, it has to be mentioned that our findings have not yet been validated fully at the protein level. A HIVEP1 antibody against the C-terminal residue of HIVEP1, located in exon 9, was used in this work, while the PCRs for documentation of statin effects on *HIVEP1* expression were performed with primers, positioned in the N-terminal HIVEP1 residue, generating a PCR fragment comprising exon 1c, 2, 3 and the start of exon 4. There is evidence that, besides full length HIVEP1, the N- and C-terminal part of HIVEP1 may exist independently and be regulated differently resulting in two separate HIVEP1 proteins. Firstly, both, recombinant N- and C-terminal HIVEP1, each harbouring one set of Zn fingers, had been shown to bind to NF-κB sites independently (Fan and Maniatis, 1990). Secondly, the results regarding HIVEP1 transcripts, obtained by sequential PCRs in combination with the predictions from ENSEMBLE und UCSC database indicated that alternative splice events or different TSS in front of *HIVEP1* exon 4 or 5 would result in a transcript harbouring the C-terminal part, i.e. *HIVEP1* exon 5 to 9. The 70 kDa HIVEP1 isoform GAAP1 lacks exon 4 and recombinant GAAP1 was exclusively found in the nucleus, when the PEST-like domain was depleted (Lallemand et al., 2002). Thus, the 55 kDa isoform detected by western blot analysis in this work might be encoded by exon 5 to 9 and lack the PEST-like domain, explaining its smaller size and exclusive nuclear location. Third, to date there are no studies, which demonstrated the existence of a full length HIVEP1 protein *in vivo*. However, we also observed the decreasing effect of, for example, simvastatin on *HIVEP1* expression in EA.hy926 cells by PCR amplifying a fragment comprising exon 5 to 9, even with smaller effects. This observation suggests that a full length HIVEP1 mRNA transcript is regulated by application of statins or that C- and N-terminal transcripts are both influenced in a similar manner by statin application. In addition, increased HIVEP1 expression upon inflammatory conditions could be detected on both, mRNA (N-terminal) and protein level (C-terminal) in THP1 monocytes. In conclusion, besides the antibody against the C-terminal residue, another HIVEP1 antibody recognizing the N-terminal residue of HIVEP1 could confirm the effect of statins on HIVEP1 expression at the protein level.

5.5 Nuclear localization of endogenous HIVEP1 in endothelial cells

The cellular localization of endogenous HIVEP1 has not yet been studied using a commercial antibody. HIVEP1 was detected within the nuclei of osteosarcoma cells using an antibody against the C-terminal part of HIVEP1 (Fan and Maniatis, 1990), while the HIVEP1 isoform GAAP1, lacking exon 4, was found in both, the cytoplasm and the nucleus of hepatocarcinoma cells (Lallemand et al., 2002). Exclusive nuclear localization was reported, when the PEST-like sequence of recombinant eGFP-tagged GAAP1 had been deleted (Lallemand et al., 2002).

In this study, immunofluorescence of endogenous HIVEP1 in endothelial cells revealed exclusive nuclear localization of HIVEP1 using an antibody against the C-terminal residue of HIVEP1. In accordance to this finding, application of the same HIVEP1 antibody in western blot analysis showed exclusive nuclear localization of the detected ~55 kDa HIVEP1 isoform in several cell lines (cf. chapter 4.1.3). Thus, endogenous HIVEP1 isoforms harbouring the C-terminal residue are localized in the nucleus of endothelial cells EA.hy926. Subsequent immunofluorescence experiments performed with an antibody against the N-terminal part of HIVEP1 would support these findings of exclusive nuclear localization of N- and C-terminal HIVEP1. If HIVEP1 is already localized in the nucleus under basic conditions to permit target gene expression, this would be in contrast to TFs of the NF-κB family, which have to be translocated into the nucleus upon stimulation.

5.6 Conclusion

VT is the third most common VD after ischemic stroke and mycocardial infarction (Reitsma et al., 2012). In addition to mechanical stress due to trauma-derived injury of the vein wall or to chemical stress induced by ROS or sepsis, which all result in endothelial “dysfunction”, the individual balance of pro- and anticoagulants considerably influences the development of thrombus formation at the site of “injury”. The individual level of coagulation factors is determined by “classical” genetic risk factors for VT, such as deficiency of the anticoagulation factor antithrombin or the increase of the procoagulant prothrombin (~50%; Reitsma et al., 2012). Since VT is a complex disease and residual idiopathic VT cannot be explained by the above mentioned “classical” genetic risk factors, it is conceivable that both, rare genetic variants with a strong effect and multiple common SNPs with a more moderate impact, may determine the individual genetic susceptibility for the remaining VT (Morange and Trégouët, 2011). In that respect, GWAs were performed (Trégouët et al., 2009; Morange et al., 2010) to identify new genetic risk factors for VT as

a non-hypothesis driven approach. In addition to the *nuclear factor of activated T-cells cytoplasmic 3 (NFATC3)* and the *protein tyrosine phosphatase receptor type F (PTPRF)* gene, the *HIVEP1* locus on chromosome 6 was identified as a susceptible locus for VT. In a multistage approach following the first GWA performed for VT, including ~6000 VT cases and ~7000 healthy individuals, a tagging SNP located 90 kb upstream of *HIVEP1* (rs169713) was shown to be replicatively associated with VT (Morange et al., 2010). In a subsequent GWA, performed with dense fine mapping, a SNP (rs2228220) in *HIVEP1* exon 4 was found to be associated with VT (Germain et al., 2011). HIVEP1 protein function and gene regulation are poorly understood to date, except that recombinant N- and C-terminal HIVEP1 bind to NF-κB consensus sequences within regulatory elements of genes involved in inflammatory processes *in vitro* (Baldwin et al., 1990; Muchardt et al., 1992; Fan and Maniatis, 1990). In the current study, we were able to demonstrate that I) *HIVEP1* expression is increased under inflammatory conditions in endothelial cells and monocytes/macrophages; II. an intronic modulator is implicated in cell type-specific *HIVEP1* expression regulation; III. NF-κB and Zn finger proteins SP1, EGR1 and WT1 are involved in *HIVEP1* expression regulation; IV. simvastatin decreases the binding affinity of NF-κB to its binding sites in the *HIVEP1* promoter region; V. simvastatin, rosuvastatin and low-dose atorvastatin decrease the *HIVEP1* expression in endothelial cells under inflammatory conditions. Interestingly, a protective impact of statins on VTE was observed by a recent meta-analysis of statin use in the prevention of VTE (Pai et al., 2011) and a recent prospective cohort study regarding unintended effects of statin use suggested a protective impact on VTE by certain statins (Hippisley-Cox and Coupland, 2010). The identification of additional common VT-associated SNPs will require much larger GWAs, including more than 100 000 individuals, as shown for the identification of novel SNPs for CAD by studying 140 000 individuals (Schunkert et al., 2011) or more than 200 000 individuals for blood pressure or hypertension by Ehret et al. (Ehret et al., 2011). Whether HIVEP1 is causally involved in VT development may be further evaluated in appropriate animal and clinical studies. Our results indicate a prominent effect of certain statins (substance-specific) on *HIVEP1* expression and may serve as a link between statin use and prevention of VT and therefore VTE development.

6 OUTLOOK

Since data on HIVEP1 signaling is rather scarce to date, future HIVEP1 knockdown studies using siRNA and subsequent microarray analysis are warranted to identify potential HIVEP1 target genes and to substantiate the role of HIVEP1 as an inflammatory TF during the development of VT. Overexpression of HIVEP1 may be used to confirm the results obtained by knockdown experiments. An up to ~75% *HIVEP1* knockdown was achieved in the current work documented by RT-PCR, but still has to be confirmed at the protein level. To investigate the existence of two separate and independent N- and C-terminal HIVEP1 protein isoforms expressed from alternative TSS, the analysis of a potential TSS upstream of exon 4 or 5 could be performed by 5'-rapid amplification of cDNA ends (5'-RACE). Since CpG island promoters are characterized by broad TSS distribution (Carninci et al., 2006), we suggest the *HIVEP1* gene to be transcribed from different independent TSS, which may be used in a cell type-specific manner.

To underline the involvement of HIVEP1 during inflammatory conditions *in vivo*, future studies should involve animal models with inflammatory background. TNFα-transgenic mice in comparison to wt mice could be used to study the impact of different *HIVEP1* expression levels on vascular phenotypes. The involvement of NF-κB signal transduction in *HIVEP1* expression regulation and the influence of statins on the NF-κB binding affinity to the *HIVEP1* promoter region could be confirmed *in vivo* by ChIP analyses performed with antibodies against different NF-κB family members in untreated or TNFα/statin-treated endothelial cells.

To further determine the causal involvement of HIVEP1 in the pathophysiology of VT, HIVEP1 expression may be analyzed and compared in venous samples from VT patients and non-VT patients, whereby the potential use of statins has to be considered in the interpretation of the observed results. To definitely demonstrate the protective effect of statin therapy on VT and VTE, prospective controlled clinical studies should be conducted in individuals with predisposition (familial [genetic], susceptibility factor [e.g. HIVEP1]) to VT and VTE. The effect of each statin (rosuvastatin, simvastatin, atorvastatin, pravastatin) on VT/VTE and HIVEP1 expression will have to be documented. Patients groups should be divided into low- and high-dose statin users and the level of inflammatory markers should be documented to reveal potential paradoxical effects of statins as proposed in our current analysis. In addition, the effect of statin use in combination with vitamin K antagonists or new anticoagulants on VT/VTE should be studied in prospective clinical trials. An optimized therapeutic prevention of VT/VTE, which comprises certain statins in particular doses in combination with well-known anticoagulants, for individuals, which are characterized by certain biomarkers, e.g. HIVEP1 (predisposition to VT or VTE), could be

deduced from results obtained in prospective clinical studies performed as described above.

7 REFERENCES

Ahlbom A, Lichtenstein P, Malmström H, Feychting M, Hemminki K, Pedersen NL. Cancer in twins: genetic and nongenetic familial risk factors. J Natl Cancer Inst 1997;89:287-93.

Aikawa M, Rabkin E, Sugiyama S, Voglic SJ, Fukumoto Y, Furukawa Y, Shiomi M, Schoen FJ, Libby P. An HMG-CoA reductase inhibitor, cerivastatin, suppresses growth of macrophages expressing matrix metalloproteinases and tissue factor in vivo and in vitro. Circulation 2001;103:276-83.

Amir RE, Haecker H, Karin M, Ciechanover A. Mechanism of processing of the NF-kappa B2 p100 precursor: identification of the specific polyubiquitin chain-anchoring lysine residue and analysis of the role of NEDD8-modification on the SCF(beta-TrCP) ubiquitin ligase. Oncogene 2004;23:2540-7.

Arnett DK, Baird AE, Barkley RA, Basson CT, Boerwinkle E, Ganesh SK, Herrington DM, Hong Y, Jaquish C, McDermott DA, O'Donnell CJ; American Heart Association Council on Epidemiology and Prevention; American Heart Association Stroke Council; Functional Genomics and Translational Biology Interdisciplinary Working Group. Relevance of genetics and genomics for prevention and treatment of cardiovascular disease: a scientific statement from the American Heart Association Council on Epidemiology and Prevention, the Stroke Council, and the Functional Genomics and Translational Biology Interdisciplinary Working Group. Circulation 2007;115:2878-901.

Austin MA, Sandholzer C, Selby JV, Newman B, Krauss RM, Utermann G. Lipoprotein(a) in women twins: heritability and relationship to apolipoprotein(a) phenotypes. Am J Hum Genet 1992;51:829-40.

Baldwin AS Jr, LeClair KP, Singh H, Sharp PA. A large protein containing zinc finger domains binds to related sequence elements in the enhancers of the class I major histocompatibility complex and kappa immunoglobulin genes. Mol Cell Biol 1990;10:1406-14.

Bartel DP. MicroRNAs: genomics, biogenesis, mechanism, and function. Cell 2004;116:281-97.

Black AR, Black JD, Azizkhan-Clifford J. Sp1 and krüppel-like factor family of transcription factors in cell growth regulation and cancer. J Cell Physiol 2001;188:143-60.

Blake MC, Jambou RC, Swick AG, Kahn JW, Azizkhan JC. Transcriptional initiation is controlled by upstream GC-box interactions in a TATAA-less promoter. Mol Cell Biol 1990;10:6632-41.

Bolognani F, Perrone-Bizzozero NI. RNA-protein interactions and control of mRNA stability in neurons. J Neurosci Res 2008;86:481-9.

Boomsma D, Busjahn A, Peltonen L. Classical twin studies and beyond. Nat Rev Genet 2002;3:872-82.

Bourcier T, Libby P. HMG CoA reductase inhibitors reduce plasminogen activator inhibitor-1 expression by human vascular smooth muscle and endothelial cells. Arterioscler Thromb Vasc Biol 2000;20:556-62.

Boyd KE, Wells J, Gutman J, Bartley SM, Farnham PJ. c-Myc target gene specificity is determined by a post-DNAbinding mechanism. Proc Natl Acad Sci U S A 1998;95:13887-92.

Brand K, Page S, Rogler G, Bartsch A, Brandl R, Knuechel R, Page M, Kaltschmidt C, Baeuerle PA, Neumeier D. Activated transcription factor nuclear factor-kappa B is present in the atherosclerotic lesion. J Clin Invest 1996;97:1715-22.

Brand-Herrmann SM. Where do we go for atherothrombotic disease genetics? Stroke 2008;39:1070-5.

Buckland PR. The importance and identification of regulatory polymorphisms and their mechanisms of action. Biochim Biophys Acta 2006;1762:17-28.

Burley SK. The TATA box binding protein. Curr Opin Struct Biol 1996;6:69-75.

Butler JE, Kadonaga JT. Enhancer-promoter specificity mediated by DPE or TATA core promoter motifs. Genes Dev 2001;15:2515-9.

Cambien F, Tiret L. Genetics of cardiovascular diseases: from single mutations to the whole genome. Circulation 2007;116:1714-24.

Carninci P, Sandelin A, Lenhard B, Katayama S, Shimokawa K, Ponjavic J, Semple CA, Taylor MS, Engström PG, Frith MC, Forrest AR, Alkema WB, Tan SL, Plessy C, Kodzius R, Ravasi T, Kasukawa T, Fukuda S, Kanamori-Katayama M, Kitazume Y, Kawaji H, Kai C, Nakamura M, Konno H, Nakano K, Mottagui-Tabar S, Arner P, Chesi A, Gustincich S, Persichetti F, Suzuki H, Grimmond SM, Wells CA, Orlando V, Wahlestedt C, Liu ET, Harbers M, Kawai J, Bajic VB, Hume DA, Hayashizaki Y. Genome-wide analysis of mammalian promoter architecture and evolution. Nat Genet 2006;38:626-35.

Cauley K, Verma IM. Kappa B enhancer-binding complexes that do not contain NF-kappa B are developmentally regulated in mammalian brain. Proc Natl Acad Sci U S A 1994;91:390-4.

Celermajer DS. Endothelial dysfunction: does it matter? Is it reversible? J Am Coll Cardiol 1997;30:325-33.

Chalkley GE, Verrijzer CP. DNA binding site selection by RNA polymerase II TAFs: a TAF(II)250-TAF(II)150 complex recognizes the initiator. EMBO J 1999;18:4835-45.

Chan G, Bivins-Smith ER, Smith MS, Yurochko AD. Transcriptome analysis of NF-kappaB- and phosphatidylinositol 3-kinase-regulated genes in human cytomegalovirus-infected monocytes. J Virol 2008;82:1040-6.

Chen LF, Greene WC. Shaping the nuclear action of NF-kappaB. Nat Rev Mol Cell Biol 2004;5:392-401.

Chen Z, Issa B, Brothman LJ, Hendricksen M, Button D, Brothman AR. Nonrandom rearrangements of 6p in malignant hematological disorders. Cancer Genet Cytogenet 2000;121:22-5.

Chu S, Ferro TJ. Sp1: regulation of gene expression by phosphorylation. Gene 2005;348:1-11.

Colli S, Eligini S, Lalli M, Camera M, Paoletti R, Tremoli E. Vastatins inhibit tissue factor in cultured human macrophages. A novel mechanism of protection against atherothrombosis. Arterioscler Thromb Vasc Biol 1997;17:265-72.

Cui MZ, Parry GC, Oeth P, Larson H, Smith M, Huang RP, Adamson ED, Mackman N. Transcriptional regulation of the tissue factor gene in human epithelial cells is mediated by Sp1 and EGR-1. J Biol Chem 1996;271:2731-9.

Dahlöf B. Cardiovascular disease risk factors: epidemiology and risk assessment. Am J Cardiol 2010;105:3A-9A.

Davies RC, Calvio C, Bratt E, Larsson SH, Lamond AI, Hastie ND. WT1 interacts with the splicing factor U2AF65 in an isoform-dependent manner and can be incorporated into spliceosomes. Genes Dev 1998;12:3217-25.

Deanfield JE, Halcox JP, Rabelink TJ. Endothelial function and dysfunction: testing and clinical relevance. Circulation 2007;115:1285-95.

Deaton AM, Bird A. CpG islands and the regulation of transcription. Genes Dev 2011;25:1010-22.

Deng W, Roberts SG. Core promoter elements recognized by transcription factor IIB. Biochem Soc Trans 2006;34:1051-3.

Devin A, Lin Y, Yamaoka S, Li Z, Karin M, Liu Zg. The alpha and beta subunits of IkappaB kinase (IKK) mediate TRAF2-dependent IKK recruitment to tumor necrosis factor (TNF) receptor 1 in response to TNF. Mol Cell Biol 2001;21:3986-94.

Dichtl W, Dulak J, Frick M, Alber HF, Schwarzacher SP, Ares MP, Nilsson J, Pachinger O, Weidinger F. HMG-CoA reductase inhibitors regulate inflammatory transcription factors in human endothelial and vascular smooth muscle cells. Arterioscler Thromb Vasc Biol 2003;23:58-63.

Dördelmann C, Telgmann R, Brand E, Hagedorn C, Schröer B, Hasenkamp S, Baumgart P, Kleine-Katthöfer P, Paul M, Brand-Herrmann SM. Functional and structural profiling of the human thrombopoietin gene promoter. J Biol Chem 2008;283:24382-91.

Edgell CJ, McDonald CC, Graham JB. Permanent cell line expressing human factor VIII-related antigen established by hybridization. Proc Natl Acad Sci U S A 1983;80:3734-7.

Esmon CT. Basic mechanisms and pathogenesis of venous thrombosis. Blood Rev 2009;23:225-9.

Esteller M. Non-coding RNAs in human disease. Nat Rev Genet 2011;12:861-74.

Fan CM, Maniatis T. A DNA-binding protein containing two widely separated zinc finger motifs that recognize the same DNA sequence. Genes Dev 1990;4:29-42.

Fanghänel J, Pera F, Anderhuber F, Nitsch R. Waldeyer, Anatomie des Menschen. Walter de Gruyter GmbH & Co. KG, Berlin 2003.

Felsenfeld G. Chromatin unfolds. Cell 1996;86:13-9.

Ferro D, Parrotto S, Basili S, Alessandri C, Violi F. Simvastatin inhibits the monocyte expression of proinflammatory cytokines in patients with hypercholesterolemia. J Am Coll Cardiol 2000;36:427-31.

Freeman DJ, Robertson M, Brown EA, Rumley A, Tobias ES, Frölich M, Slagboom PE, Jukema JW, de Craen AJ, Sattar N, Ford I, Gaw A, Greer IA, Lowe GD, Stott DJ. Incident venous thromboembolic events in the Prospective Study of Pravastatin in the Elderly at Risk (PROSPER). BMC Geriatr 2011;11:8.

Fuda NJ, Ardehali MB, Lis JT Defining mechanisms that regulate RNA polymerase II transcription in vivo. Nature 2009;461:186-92.

Galkina E, Ley K. Immune and inflammatory mechanisms of atherosclerosis. Annu Rev Immunol 2009;27:165-97.

Galton F. The history of twins, as a criterion of the relative powers of nature and nuture. Fraser's Magazine 1875;12:566-76.

Gannon AM, Turner EC, Reid HM, Kinsella BT. Regulated expression of the alpha isoform of the human thromboxane A2 receptor during megakaryocyte differentiation: a coordinated role for WT1, Egr1, and Sp1. J Mol Biol 2009;394:29-45.

Germain M, Saut N, Greliche N, Dina C, Lambert JC, Perret C, Cohen W, Oudot-Mellakh T, Antoni G, Alessi MC, Zelenika D, Cambien F, Tiret L, Bertrand M, Dupuy AM, Letenneur L, Lathrop M, Emmerich J, Amouyel P, Trégouët DA, Morange PE. Genetics of venous thrombosis: insights from a new genome wide association study. PLoS One 2011;6:e25581.

Gilmore TD. Introduction to NF-kappaB: players, pathways, perspectives. Oncogene 2006;25:6680-4.

Glynn RJ, Danielson E, Fonseca FA, Genest J, Gotto AM Jr, Kastelein JJ, Koenig W, Libby P, Lorenzatti AJ, MacFadyen JG, Nordestgaard BG, Shepherd J, Willerson JT, Ridker PM. A randomized trial of rosuvastatin in the prevention of venous thromboembolism. N Engl J Med 2009;360:1851-61.

Goldstein JL, Brown MS. Regulation of the mevalonate pathway. Nature 1990;343:425-30.

Grabe N. AliBaba2: context specific identification of transcription factor binding sites. In Silico Biol 2002;2:S1-15.

Grönberg H. Prostate cancer epidemiology. Lancet 2003;361:859-64.

Guijarro C, Blanco-Colio LM, Ortego M, Alonso C, Ortiz A, Plaza JJ, Díaz C, Hernández G, Egido J. 3-Hydroxy-3-methylglutaryl coenzyme a reductase and isoprenylation inhibitors induce apoptosis of vascular smooth muscle cells in culture. Circ Res 1998;83:490-500.

Gusella JF, Wexler NS, Conneally PM, Naylor SL, Anderson MA, Tanzi RE, Watkins PC, Ottina K, Wallace MR, Sakaguchi AY, Young AB, Shoulson I, Bonilla E, Martin JB. A polymorphic DNA marker genetically linked to Huntington's disease. Nature 1983;306:234-8.

Hagedorn C, Telgmann R, Dördelmann C, Schmitz B, Hasenkamp S, Cambien F, Paul M, Brand E, Brand-Herrmann SM. Identification and functional analyses of molecular haplotypes of the human osteoprotegerin gene promoter. Arterioscler Thromb Vasc Biol 2009;29:1638-43.

Hall JM, Lee MK, Newman B, Morrow JE, Anderson LA, Huey B, King MC. Linkage of early-onset familial breast cancer to chromosome 17q21. Science 1990;250:1684-9.

Hanahan D. Studies on transformation of Escherichia coli with plasmids. J Mol Biol 1983;166:557-80.

Hansson GK, Hermansson A. The immune system in atherosclerosis. Nat Immunol 2011;12:204-12.

Hansson GK, Robertson AK, Söderberg-Nauclér C. Inflammation and atherosclerosis. Annu Rev Pathol 2006;1:297-329.

Hansson GK. Inflammation, atherosclerosis, and coronary artery disease. N Engl J Med 2005;352:1685-95.

Harris MB, Mostecki J, Rothman PB. Repression of an interleukin-4-responsive promoter requires cooperative BCL-6 function. J Biol Chem 2005;280:13114-21.

Harrison SC. A structural taxonomy of DNA-binding domains. Nature 1991;353:715-9.

Hayden MS, Ghosh S. Shared principles in NF-kappaB signaling. Cell 2008;132:344-62.

He L, Hannon GJ. MicroRNAs: small RNAs with a big role in gene regulation. Nat Rev Genet 2004;5:522-31.

Heintzman ND, Ren B. Finding distal regulatory elements in the human genome. Curr Opin Genet Dev 2009;19:541-9.

Heintzman ND, Ren B. The gateway to transcription: identifying, characterizing and understanding promoters in the eukaryotic genome. Cell Mol Life Sci 2007;64:386-400.

Hicar MD, Liu Y, Allen CE, Wu LC. Structure of the human zinc finger protein HIVEP3: molecular cloning, expression, exon-intron structure, and comparison with paralogous genes HIVEP1 and HIVEP2. Genomics 2001;71:89-100.

Higgs DR, Vernimmen D, Wood B. Long-range regulation of alpha-globin gene expression. Adv Genet 2008;61:143-73.

Higgs DR, Wood WG, Jarman AP, Sharpe J, Lida J, Pretorius IM, Ayyub H. A major positive regulatory region located far upstream of the human alpha-globin gene locus. Genes Dev 1990;4:1588-601.

Hippisley-Cox J, Coupland C. Unintended effects of statins in men and women in England and Wales: population based cohort study using the QResearch database. BMJ 2010;340:c2197.

Hirschhorn JN, Daly MJ. Genome-wide association studies for common diseases and complex traits. Nat Rev Genet 2005;6:95-108.

Hoffmann A, Natoli G, Ghosh G. Transcriptional regulation via the NF-kappaB signaling module. Oncogene 2006;25:6706-16.

International Consortium for Blood Pressure Genome-Wide Association Studies, Ehret GB, Munroe PB, Rice KM, Bochud M, Johnson AD, Chasman DI, Smith AV, Tobin MD, Verwoert GC, Hwang SJ, Pihur V, Vollenweider P, O'Reilly PF, Amin N, Bragg-Gresham JL, Teumer A, Glazer NL, Launer L, Zhao JH, Aulchenko Y, Heath S, Sõber S, Parsa A, Luan J, Arora P, Dehghan A, Zhang F, Lucas G, Hicks AA, Jackson AU, Peden JF, Tanaka T, Wild SH, Rudan I, Igl W, Milaneschi Y, Parker AN, Fava C, Chambers JC, Fox ER, Kumari M, Go MJ, van der Harst P, Kao WH, Sjögren M, Vinay DG, Alexander M, Tabara Y, Shaw-Hawkins S, Whincup PH, Liu Y, Shi G, Kuusisto J, Tayo B, Seielstad M, Sim X, Nguyen KD, Lehtimäki T, Matullo G, Wu Y, Gaunt TR, Onland-Moret NC, Cooper MN, Platou CG, Org E, Hardy R, Dahgam S, Palmen J, Vitart V, Braund PS, Kuznetsova T, Uiterwaal CS, Adeyemo A, Palmas W, Campbell H, Ludwig B, Tomaszewski M, Tzoulaki I, Palmer ND; CARDIoGRAM consortium; CKDGen Consortium; KidneyGen Consortium; EchoGen consortium; CHARGE-HF consortium, Aspelund T, Garcia M, Chang YP, O'Connell JR, Steinle NI, Grobbee DE, Arking DE, Kardia SL, Morrison AC, Hernandez D, Najjar S, McArdle WL, Hadley D, Brown MJ, Connell JM, Hingorani AD, Day IN, Lawlor DA, Beilby JP, Lawrence RW, Clarke R, Hopewell JC, Ongen H, Dreisbach AW, Li Y, Young JH, Bis JC, Kähönen M, Viikari J, Adair LS, Lee NR, Chen MH, Olden M, Pattaro C, Bolton JA, Köttgen A, Bergmann S, Mooser V, Chaturvedi N, Frayling TM, Islam M, Jafar TH, Erdmann J, Kulkarni SR, Bornstein SR, Grässler J, Groop L, Voight BF, Kettunen J, Howard P, Taylor A, Guarrera S, Ricceri F, Emilsson V, Plump A, Barroso I, Khaw KT, Weder AB, Hunt SC, Sun YV, Bergman RN, Collins FS, Bonnycastle LL, Scott LJ, Stringham HM, Peltonen L, Perola M, Vartiainen E, Brand SM, Staessen JA, Wang TJ, Burton PR, Artigas MS, Dong Y, Snieder H, Wang X, Zhu H, Lohman KK, Rudock ME, Heckbert SR, Smith NL, Wiggins KL, Doumatey A, Shriner D, Veldre G, Viigimaa M, Kinra S, Prabhakaran D, Tripathy V, Langefeld CD, Rosengren A, Thelle DS, Corsi AM, Singleton A, Forrester T, Hilton G, McKenzie CA, Salako T, Iwai N, Kita Y, Ogihara T, Ohkubo T, Okamura T, Ueshima H, Umemura S, Eyheramendy S, Meitinger T, Wichmann HE, Cho YS, Kim HL, Lee JY, Scott J, Sehmi JS, Zhang W, Hedblad B, Nilsson P, Smith GD, Wong A, Narisu N, Stančáková A, Raffel LJ, Yao J, Kathiresan S, O'Donnell CJ, Schwartz SM, Ikram MA, Longstreth WT Jr, Mosley TH, Seshadri S, Shrine NR, Wain LV, Morken MA, Swift AJ, Laitinen J, Prokopenko I, Zitting P, Cooper JA, Humphries SE, Danesh J, Rasheed A, Goel A, Hamsten A, Watkins H, Bakker SJ, van Gilst WH, Janipalli CS, Mani KR, Yajnik CS, Hofman A, Mattace-Raso FU, Oostra BA, Demirkan A, Isaacs A, Rivadeneira F, Lakatta EG, Orru M, Scuteri A, Ala-Korpela M, Kangas AJ, Lyytikäinen LP, Soininen P, Tukiainen T, Würtz P, Ong RT, Dörr M, Kroemer HK, Völker U, Völzke H, Galan P, Hercberg S, Lathrop M, Zelenika D, Deloukas P, Mangino M, Spector TD, Zhai G, Meschia JF, Nalls MA, Sharma P, Terzic J, Kumar MV, Denniff M, Zukowska-Szczechowska E, Wagenknecht LE, Fowkes FG, Charchar FJ, Schwarz PE, Hayward C, Guo X, Rotimi C, Bots ML, Brand E, Samani NJ, Polasek O, Talmud PJ, Nyberg F, Kuh D, Laan M, Hveem K, Palmer LJ, van der Schouw YT, Casas JP, Mohlke KL, Vineis P, Raitakari O, Ganesh SK, Wong TY, Tai ES, Cooper RS, Laakso M, Rao DC, Harris TB, Morris RW, Dominiczak AF, Kivimaki M, Marmot MG, Miki T, Saleheen D, Chandak GR, Coresh J, Navis G, Salomaa V, Han BG, Zhu X, Kooner JS, Melander O, Ridker PM, Bandinelli S, Gyllensten UB, Wright AF, Wilson JF, Ferrucci L, Farrall M, Tuomilehto J, Pramstaller PP, Elosua R, Soranzo N, Sijbrands EJ, Altshuler D, Loos RJ, Shuldiner AR, Gieger C, Meneton P, Uitterlinden AG, Wareham NJ, Gudnason V, Rotter JI, Rettig R, Uda M, Strachan DP, Witteman JC, Hartikainen AL, Beckmann JS, Boerwinkle E, Vasan RS, Boehnke M, Larson MG, Järvelin MR, Psaty BM, Abecasis GR, Chakravarti A, Elliott P, van Duijn CM, Newton-Cheh C, Levy D, Caulfield MJ, Johnson T. Genetic variants in novel pathways influence blood pressure and cardiovascular disease risk. Nature 2011;478:103-9.

Istvan ES, Deisenhofer J. Structural mechanism for statin inhibition of HMG-CoA reductase. Science 2001;292:1160-4.

Ito K, Barnes PJ, Adcock IM. Glucocorticoid receptor recruitment of histone deacetylase 2 inhibits interleukin-1beta-induced histone H4 acetylation on lysines 8 and 12. Mol Cell Biol 2000;20:6891-903.

Iuchi S. Three classes of C2H2 zinc finger proteins. Cell Mol Life Sci 2001;58:625-35.

Jackson AL, Linsley PS. Recognizing and avoiding siRNA off-target effects for target identification and therapeutic application. Nat Rev Drug Discov 2010;9:57-67.

Jaksik R, Rzeszowska-Wolny J. The distribution of GC nucleotides and regulatory sequence motifs in genes and their adjacent sequences. Gene 2012;492:375-81.

Kawada N, Moriyama T, Ando A, Koyama T, Hori M, Miwa T, Imai E. Role of intron 1 in smooth muscle alpha-actin transcriptional regulation in activated mesangial cells in vivo. Kidney Int. 1999 Jun;55(6):2338-48.

Kerem B, Rommens JM, Buchanan JA, Markiewicz D, Cox TK, Chakravarti A, Buchwald M, Tsui LC. Identification of the cystic fibrosis gene: genetic analysis. Science 1989;245:1073-80.

Khachigian LM, Williams AJ, Collins T. Interplay of Sp1 and Egr-1 in the proximal platelet-derived growth factor A-chain promoter in cultured vascular endothelial cells. J Biol Chem 1995;270:27679-86.

Khemasuwan D, Chae YK, Gupta S, Carpio A, Yun JH, Neagu S, Lucca AB, Valsecchi ME, Mora JI. Dose-related effect of statins in venous thrombosis risk reduction. Am J Med 2011;124:852-9.

Kim TH, Barrera LO, Zheng M, Qu C, Singer MA, Richmond TA, Wu Y, Green RD, Ren B. A high-resolution map of active promoters in the human genome. Nature 2005;436:876-80.

Kingston RE, Narlikar GJ. ATP-dependent remodeling and acetylation as regulators of chromatin fluidity. Genes Dev 1999;13:2339-52.

Klag MJ, Ford DE, Mead LA, He J, Whelton PK, Liang KY, Levine DM. Serum cholesterol in young men and subsequent cardiovascular disease. N Engl J Med 1993;328:313-8.

Klug A, Rhodes D. Zinc fingers: a novel protein fold for nucleic acid recognition. Cold Spring Harb Symp Quant Biol 1987;52:473-82.

Korner M, Rattner A, Mauxion F, Sen R, Citri Y. A brain-specific transcription activator. Neuron 1989;3:563-72.

Krappmann D, Hatada EN, Tegethoff S, Li J, Klippel A, Giese K, Baeuerle PA, Scheidereit C. The I kappa B kinase (IKK) complex is tripartite and contains IKK gamma but not IKAP as a regular component. J Biol Chem 2000;275:29779-87.

Krishna SS, Majumdar I, Grishin NV. Structural classification of zinc fingers: survey and summary. Nucleic Acids Res 2003;31:532-50.

Kubosaki A, Tomaru Y, Tagami M, Arner E, Miura H, Suzuki T, Suzuki M, Suzuki H, Hayashizaki Y. Genome-wide investigation of in vivo EGR-1 binding sites in monocytic differentiation. Genome Biol 2009;10:R41.

Lagrange T, Kapanidis AN, Tang H, Reinberg D, Ebright RH. New core promoter element in RNA polymerase II-dependent transcription: sequence-specific DNA binding by transcription factor IIB. Genes Dev 1998;12:34-44.

Lallemand C, Palmieri M, Blanchard B, Meritet JF, Tovey MG. GAAP-1: a transcriptional activator of p53 and IRF-1 possesses pro-apoptotic activity. EMBO Rep 2002;3:153-8.

Lander ES, Linton LM, Birren B, Nusbaum C, Zody MC, Baldwin J, Devon K, Dewar K, Doyle M, FitzHugh W, Funke R, Gage D, Harris K, Heaford A, Howland J, Kann L, Lehoczky J, LeVine R, McEwan P, McKernan K, Meldrim J, Mesirov JP, Miranda C, Morris W, Naylor J, Raymond C, Rosetti M, Santos R, Sheridan A, Sougnez C, Stange-Thomann N, Stojanovic N, Subramanian A, Wyman D, Rogers J, Sulston J, Ainscough R, Beck S, Bentley D, Burton J, Clee C, Carter N, Coulson A, Deadman R, Deloukas P, Dunham A, Dunham I, Durbin R, French L, Grafham D, Gregory S, Hubbard T, Humphray S, Hunt A, Jones M, Lloyd C, McMurray A, Matthews L, Mercer S, Milne S, Mullikin JC, Mungall A, Plumb R, Ross M, Shownkeen R, Sims S, Waterston RH, Wilson RK, Hillier LW, McPherson JD, Marra MA, Mardis ER, Fulton LA, Chinwalla AT, Pepin KH, Gish WR, Chissoe SL, Wendl MC, Delehaunty KD, Miner TL, Delehaunty A, Kramer JB, Cook LL, Fulton RS, Johnson DL, Minx PJ, Clifton SW, Hawkins T, Branscomb E, Predki P, Richardson P, Wenning S, Slezak T, Doggett N, Cheng JF, Olsen A, Lucas S, Elkin C, Uberbacher E, Frazier M, Gibbs RA, Muzny DM, Scherer SE, Bouck JB, Sodergren EJ, Worley KC, Rives CM, Gorrell JH, Metzker ML, Naylor SL, Kucherlapati RS, Nelson DL, Weinstock GM, Sakaki Y, Fujiyama A, Hattori M, Yada T, Toyoda A, Itoh T, Kawagoe C, Watanabe H, Totoki Y, Taylor T, Weissenbach J, Heilig R, Saurin W, Artiguenave F, Brottier P, Bruls T, Pelletier E, Robert C, Wincker P, Smith DR, Doucette-Stamm L, Rubenfield M, Weinstock K, Lee HM, Dubois J, Rosenthal A, Platzer M, Nyakatura G, Taudien S, Rump A, Yang H, Yu J, Wang J, Huang G, Gu J, Hood L, Rowen L, Madan A, Qin S, Davis RW, Federspiel NA, Abola AP, Proctor MJ, Myers RM, Schmutz J, Dickson M, Grimwood J, Cox DR, Olson MV, Kaul R, Raymond C, Shimizu N, Kawasaki K, Minoshima S, Evans GA, Athanasiou M, Schultz R, Roe BA, Chen F, Pan H, Ramser J, Lehrach H, Reinhardt R, McCombie WR, de la Bastide M, Dedhia N, Blöcker H, Hornischer K, Nordsiek G, Agarwala R, Aravind L, Bailey JA, Bateman A, Batzoglou S, Birney E, Bork P, Brown DG, Burge CB, Cerutti L, Chen HC, Church D, Clamp M, Copley RR, Doerks T, Eddy SR, Eichler EE, Furey TS, Galagan J, Gilbert JG, Harmon C, Hayashizaki Y, Haussler D, Hermjakob H, Hokamp K, Jang W, Johnson LS, Jones TA, Kasif S, Kaspryzk A, Kennedy S, Kent WJ, Kitts P, Koonin EV, Korf I, Kulp D, Lancet D, Lowe TM, McLysaght A, Mikkelsen T, Moran JV, Mulder N, Pollara VJ, Ponting CP, Schuler G, Schultz J, Slater G, Smit AF, Stupka E, Szustakowski J, Thierry-Mieg D, Thierry-Mieg J, Wagner L, Wallis J, Wheeler R, Williams A, Wolf YI, Wolfe KH, Yang SP, Yeh RF, Collins F, Guyer MS, Peterson J, Felsenfeld A, Wetterstrand KA, Patrinos A, Morgan MJ, de Jong P, Catanese JJ, Osoegawa K, Shizuya H, Choi S, Chen YJ; International Human Genome Sequencing Consortium. Initial sequencing and analysis of the human genome. Nature 2001;409:860-921.

Landy A. Dynamic, structural, and regulatory aspects of lambda site-specific recombination. Annu Rev Biochem 1989;58:913-49.

Larsson SH, Charlieu JP, Miyagawa K, Engelkamp D, Rassoulzadegan M, Ross A, Cuzin F, van Heyningen V, Hastie ND. Subnuclear localization of WT1 in splicing or transcription factor domains is regulated by alternative splicing. Cell 1995;81:391-401.

Latchman DS. Transcription factors: an overview. Int J Biochem Cell Biol 1997;29:1305-12.

Laufs U, Liao JK. Post-transcriptional regulation of endothelial nitric oxide synthase mRNA stability by Rho GTPase. J Biol Chem 1998;273:24266-71.

Lee CK, Shibata Y, Rao B, Strahl BD, Lieb JD. Evidence for nucleosome depletion at active regulatory regions genome-wide. Nat Genet 2004;36:900-5.

Lee JS, Galvin KM, Shi Y. Evidence for physical interaction between the zinc-finger transcription factors YY1 and Sp1. Proc Natl Acad Sci U S A 1993;90:6145-9.

Lefer AM, Campbell B, Shin YK, Scalia R, Hayward R, Lefer DJ. Simvastatin preserves the ischemic-reperfused myocardium in normocholesterolemic rat hearts. Circulation 1999;100:178-84.

Lenardo MJ, Baltimore D. NF-kappa B: a pleiotropic mediator of inducible and tissue-specific gene control. Cell 1989;58:227-9.

Levy D, Ehret GB, Rice K, Verwoert GC, Launer LJ, Dehghan A, Glazer NL, Morrison AC, Johnson AD, Aspelund T, Aulchenko Y, Lumley T, Köttgen A, Vasan RS, Rivadeneira F, Eiriksdottir G, Guo X, Arking DE, Mitchell GF, Mattace-Raso FU, Smith AV, Taylor K, Scharpf RB, Hwang SJ, Sijbrands EJ, Bis J, Harris TB, Ganesh SK, O'Donnell CJ, Hofman A, Rotter JI, Coresh J, Benjamin EJ, Uitterlinden AG, Heiss G, Fox CS, Witteman JC, Boerwinkle E, Wang TJ, Gudnason V, Larson MG, Chakravarti A, Psaty BM, van Duijn CM. Genome-wide association study of blood pressure and hypertension. Nat Genet 2009;41:677-87.

Li L, He S, Sun JM, Davie JR. Gene regulation by Sp1 and Sp3. Biochem Cell Biol 2004;82:460-71.

Li Q, Verma IM. NF-kappaB regulation in the immune system. Nat Rev Immunol 2002;2:725-34.

Liao JK, Laufs U. Pleiotropic effects of statins. Annu Rev Pharmacol Toxicol 2005;45:89-118.

Lim CY, Santoso B, Boulay T, Dong E, Ohler U, Kadonaga JT. The MTE, a new core promoter element for transcription by RNA polymerase II. Genes Dev 2004;18:1606-17.

Liu J, Grogan L, Nau MM, Allegra CJ, Chu E, Wright JJ. Physical interaction between p53 and primary response gene Egr-1. Int J Oncol 2001;4:863-70.

Liu S, Spinner DS, Schmidt MM, Danielsson JA, Wang S, Schmidt J. Interaction of MyoD family proteins with enhancers of acetylcholine receptor subunit genes in vivo. J Biol Chem 2000;275:41364-8.

Loots GG, Locksley RM, Blankespoor CM, Wang ZE, Miller W, Rubin EM, Frazer KA. Identification of a coordinate regulator of interleukins 4, 13, and 5 by cross-species sequence comparisons. Science 2000;288:136-40.

Lopez JA, Kearon C, Lee AY. Deep venous thrombosis. Hematology Am Soc Hematol Educ Program 2004:439-56.

Luger K, Mäder AW, Richmond RK, Sargent DF, Richmond TJ. Crystal structure of the nucleosome core particle at 2.8 A resolution. Nature 1997;389:251-60.

Lusis AJ. Atherosclerosis. Nature 2000;407:233-41.

Maltzman JS, Carmen JA, Monroe JG. Transcriptional regulation of the Icam-1 gene in antigen receptor- and phorbolester-stimulated B lymphocytes: role for transcription factor EGR1. J Exp Med 1996;183:1747-59.

Marenberg ME, Risch N, Berkman LF, Floderus B, de Faire U. Genetic susceptibility to death from coronary heart disease in a study of twins. N Engl J Med 1994;330:1041-6.

Matsumiya T, Ota K, Imaizumi T, Yoshida H, Kimura H, Satoh K. Characterization of synergistic induction of CX3CL1/fractalkine by TNF-alpha and IFN-gamma in vascular endothelial cells: an essential role for TNF-alpha in post-transcriptional regulation of CX3CL1. J Immunol 2010;184:4205-14.

Maston GA, Evans SK, Green MR. Transcriptional regulatory elements in the human genome. Annu Rev Genomics Hum Genet 2006;7:29-59.

Mayer H, Bilban M, Kurtev V, Gruber F, Wagner O, Binder BR, de Martin R. Deciphering regulatory patterns of inflammatory gene expression from interleukin-1-stimulated human endothelial cells. Arterioscler Thromb Vasc Biol 2004;24:1192-8.

Medzhitov R. Origin and physiological roles of inflammation. Nature 2008;454:428-35.

Mellor J. The dynamics of chromatin remodeling at promoters. Mol Cell 2005;19:147-57.

Messeguer X, Escudero R, Farré D, Núñez O, Martínez J, Albà MM. PROMO: detection of known transcription regulatory elements using species-tailored searches. Bioinformatics 2002;18:333-4.

Miller J, McLachlan AD, Klug A. Repetitive zinc-binding domains in the protein transcription factor IIIA from Xenopus oocytes. EMBO J 1985;4:1609-14.

Minc E, de Coppet P, Masson P, Thiery L, Dutertre S, Amor-Guéret M, Jaulin C. The human copper-zinc superoxide dismutase gene (SOD1) proximal promoter is regulated by Sp1, Egr-1, and WT1 via non-canonical binding sites. J Biol Chem 1999;274:503-9.

Mitchell DL, DiMario JX. AP-2 alpha suppresses skeletal myoblast proliferation and represses fibroblast growth factor receptor 1 promoter activity. Exp Cell Res 2010;316:194-202

Mizuno Y, Jacob RF, Mason RP. Inflammation and the development of atherosclerosis. J Atheroscler Thromb 2011;18:351-8.

Moerman AM, Mao X, Lucas MM, Barger SW. Characterization of a neuronal kappaB-binding factor distinct from NF-kappaB. Brain Res Mol Brain Res 1999;67:303-15.

Morange PE, Bezemer I, Saut N, Bare L, Burgos G, Brocheton J, Durand H, Biron-Andreani C, Schved JF, Pernod G, Galan P, Drouet L, Zelenika D, Germain M, Nicaud V, Heath S, Ninio E, Delluc A, Münzel T, Zeller T, Brand-Herrmann SM, Alessi MC, Tiret L, Lathrop M, Cambien F, Blankenberg S, Emmerich J, Trégouët DA, Rosendaal FR. A follow-up study of a genome-wide association scan identifies a susceptibility locus for venous thrombosis on chromosome 6p24.1. Am J Hum Genet 2010;86:592-5.

Morange PE, Trégouët DA. Lessons from genome-wide association studies in venous thrombosis. J Thromb Haemost 2011;9 Suppl 1:258-64.

Muchardt C, Seeler JS, Nirula A, Shurland DL, Gaynor RB. Regulation of human immunodeficiency virus enhancer function by PRDII-BF1 and c-rel gene products. J Virol 1992;66:244-50.

Mullis K, Faloona F, Scharf S, Saiki R, Horn G, Erlich H. Specific enzymatic amplification of DNA in vitro: the polymerase chain reaction. Cold Spring Harb Symp Quant Biol 1986;51:263-73.

Myers DD, Hawley AE, Farris DM, Wrobleski SK, Thanaporn P, Schaub RG, Wagner DD, Kumar A, Wakefield TW. P-selectin and leukocyte microparticles are associated with venous thrombogenesis. J Vasc Surg 2003;38:1075-89.

Myers LC, Kornberg RD. Mediator of transcriptional regulation. Annu Rev Biochem 2000;69:729-49.

Myocardial Infarction Genetics Consortium, Kathiresan S, Voight BF, Purcell S, Musunuru K, Ardissino D, Mannucci PM, Anand S, Engert JC, Samani NJ, Schunkert H, Erdmann J, Reilly MP, Rader DJ, Morgan T, Spertus JA, Stoll M, Girelli D, McKeown PP, Patterson CC, Siscovick DS, O'Donnell CJ, Elosua R, Peltonen L, Salomaa V, Schwartz SM, Melander O, Altshuler D, Ardissino D, Merlini PA, Berzuini C, Bernardinelli L, Peyvandi F, Tubaro M, Celli P, Ferrario M, Fetiveau R, Marziliano N, Casari G, Galli M, Ribichini F, Rossi M, Bernardi F, Zonzin P, Piazza A, Mannucci PM, Schwartz SM, Siscovick DS, Yee J, Friedlander Y, Elosua R, Marrugat J, Lucas G, Subirana I, Sala J, Ramos R, Kathiresan S, Meigs JB, Williams G, Nathan DM, MacRae CA, O'Donnell CJ, Salomaa V, Havulinna AS, Peltonen L, Melander O, Berglund G, Voight BF, Kathiresan S, Hirschhorn JN, Asselta R, Duga S, Spreafico M, Musunuru K, Daly MJ, Purcell S, Voight BF, Purcell S, Nemesh J, Korn JM, McCarroll SA, Schwartz SM, Yee J, Kathiresan S, Lucas G, Subirana I, Elosua R, Surti A, Guiducci C, Gianniny L, Mirel D, Parkin M, Burtt N, Gabriel SB, Samani NJ, Thompson JR, Braund PS, Wright BJ, Balmforth AJ, Ball SG, Hall AS; Wellcome Trust Case Control Consortium, Schunkert H, Erdmann J, Linsel-Nitschke P, Lieb W, Ziegler A, König I, Hengstenberg C, Fischer M, Stark K, Grosshennig A, Preuss M, Wichmann HE, Schreiber S, Schunkert H, Samani NJ, Erdmann J, Ouwehand W, Hengstenberg C, Deloukas P, Scholz M, Cambien F, Reilly MP, Li M, Chen Z, Wilensky R, Matthai W, Qasim A, Hakonarson HH, Devaney J, Burnett MS, Pichard AD, Kent KM, Satler L, Lindsay JM, Waksman R, Knouff CW, Waterworth DM, Walker MC, Mooser V, Epstein SE, Rader DJ, Scheffold T, Berger K, Stoll M, Huge A, Girelli D, Martinelli N, Olivieri O, Corrocher R, Morgan T, Spertus JA, McKeown P, Patterson CC, Schunkert H, Erdmann E, Linsel-Nitschke P, Lieb W, Ziegler A, König IR, Hengstenberg C, Fischer M, Stark K, Grosshennig A, Preuss M, Wichmann HE, Schreiber S, Hólm H, Thorleifsson G, Thorsteinsdottir U, Stefansson K, Engert JC, Do R, Xie C, Anand S, Kathiresan S, Ardissino D, Mannucci PM, Siscovick D, O'Donnell CJ, Samani NJ, Melander O, Elosua R, Peltonen L, Salomaa V, Schwartz SM, Altshuler D. Genome-wide association of early-onset myocardial infarction with single nucleotide polymorphisms and copy number variants. Nat Genet 2009;41:334-41.

Naess IA, Christiansen SC, Romundstad P, Cannegieter SC, Rosendaal FR, Hammerstrøm J. Incidence and mortality of venous thrombosis: a population-based study. J Thromb Haemost 2007;5:692-9.

Nair P, Muthukkumar S, Sells SF, Han SS, Sukhatme VP, Rangnekar VM. Early growth response-1-dependent apoptosis is mediated by p53. J Biol Chem 1997;272:20131-8.

Nakano S, Fujimoto M, Hara H, Sugimoto N. Nucleic acid duplex stability: influence of base composition on cation effects. Nucleic Acids Res 1999;27:2957-65.

Nathan C, Ding A. Nonresolving inflammation. Cell 2010;140:871-82.

Natoli G, Saccani S, Bosisio D, Marazzi I. Interactions of NF-kappaB with chromatin: the art of being at the right place at the right time. Nat Immunol 2005;6:439-45.

Newton-Cheh C, Johnson T, Gateva V, Tobin MD, Bochud M, Coin L, Najjar SS, Zhao JH, Heath SC, Eyheramendy S, Papadakis K, Voight BF, Scott LJ, Zhang F, Farrall M, Tanaka T, Wallace C, Chambers JC, Khaw KT, Nilsson P, van der Harst P, Polidoro S, Grobbee DE, Onland-Moret NC, Bots ML, Wain LV, Elliott KS, Teumer A, Luan J, Lucas G, Kuusisto J, Burton PR, Hadley D, McArdle WL; Wellcome Trust Case Control Consortium, Brown M, Dominiczak A, Newhouse SJ, Samani NJ, Webster J, Zeggini E, Beckmann JS, Bergmann S, Lim N, Song K, Vollenweider P, Waeber G, Waterworth DM, Yuan X, Groop L, Orho-Melander M, Allione A, Di Gregorio A, Guarrera S, Panico S, Ricceri F, Romanazzi V, Sacerdote C, Vineis P, Barroso I, Sandhu MS, Luben RN, Crawford GJ, Jousilahti P, Perola M, Boehnke M, Bonnycastle LL, Collins FS, Jackson AU, Mohlke KL, Stringham HM, Valle TT, Willer CJ, Bergman RN, Morken MA, Döring A, Gieger C, Illig T, Meitinger T, Org E, Pfeufer A, Wichmann HE, Kathiresan S, Marrugat J, O'Donnell CJ, Schwartz SM, Siscovick DS, Subirana I, Freimer NB, Hartikainen AL, McCarthy MI, O'Reilly PF, Peltonen L, Pouta A, de Jong PE, Snieder H, van Gilst WH, Clarke R, Goel A, Hamsten A, Peden JF, Seedorf U, Syvänen AC, Tognoni G, Lakatta EG, Sanna S, Scheet P, Schlessinger D, Scuteri A, Dörr M, Ernst F, Felix SB, Homuth G, Lorbeer R, Reffelmann T, Rettig R, Völker U, Galan P, Gut IG, Hercberg S, Lathrop GM, Zelenika D, Deloukas P, Soranzo N, Williams FM, Zhai G, Salomaa V, Laakso M, Elosua R, Forouhi NG, Völzke H, Uiterwaal CS, van der Schouw YT, Numans ME, Matullo G, Navis G, Berglund G, Bingham SA, Kooner JS, Connell JM, Bandinelli S, Ferrucci L, Watkins H, Spector TD, Tuomilehto J, Altshuler D, Strachan DP, Laan M, Meneton P, Wareham NJ, Uda M, Jarvelin MR, Mooser V, Melander O, Loos RJ, Elliott P, Abecasis GR, Caulfield M, Munroe PB. Genome-wide association study identifies eight loci associated with blood pressure. Nat Genet 2009;41:666-76.

Ogbourne S, Antalis TM. Transcriptional control and the role of silencers in transcriptional regulation in eukaryotes. Biochem J 1998;331:1-14.

Ohler U, Wassarman DA. Promoting developmental transcription. Development 2010;137:15-26.

Olavesen MG, Bentley E, Mason RV, Stephens RJ, Ragoussis J. Fine mapping of 39 ESTs on human chromosome 6p23-p25. Genomics 1997;46:303-6.

Pabo CO, Sauer RT. Transcription factors: structural families and principles of DNA recognition. Annu Rev Biochem 1992;61:1053-95.

Pai M, Evans NS, Shah SJ, Green D, Cook D, Crowther MA. Statins in the prevention of venous thromboembolism: a meta-analysis of observational studies. Thromb Res 2011;128:422-30.

Pascal E, Tjian R. Different activation domains of Sp1 govern formation of multimers and mediate transcriptional synergism. Genes Dev 1991;5:1646-56.

Pavletich NP, Pabo CO. Zinc finger-DNA recognition: crystal structure of a Zif268-DNA complex at 2.1 A. Science 1991;252:809-17.

Pei Y, Tuschl T. On the art of identifying effective and specific siRNAs. Nat Methods 2006;3:670-6.

Pericak-Vance MA, Bebout JL, Gaskell PC Jr, Yamaoka LH, Hung WY, Alberts MJ, Walker AP, Bartlett RJ, Haynes CA, Welsh KA, Earl NL, Heyman A, Clark CM, Roses AD. Linkage studies in familial Alzheimer disease: evidence for chromosome 19 linkage. Am J Hum Genet 1991;48:1034-50.

Plutzky J. The vascular biology of atherosclerosis. Am J Med 2003;115:55S-61S.

Pober JS, Min W, Bradley JR. Mechanisms of endothelial dysfunction, injury, and death. Annu Rev Pathol 2009;4:71-95.

Pokholok DK, Harbison CT, Levine S, Cole M, Hannett NM, Lee TI, Bell GW, Walker K, Rolfe PA, Herbolsheimer E, Zeitlinger J, Lewitter F, Gifford DK, Young RA. Genome-wide map of nucleosome acetylation and methylation in yeast. Cell 2005;122:517-27.

Polgar J, Matuskova J, Wagner DD. The P-selectin, tissue factor, coagulation triad. J Thromb Haemost 2005;3:1590-6.

Rahman I, Gilmour PS, Jimenez LA, MacNee W. Oxidative stress and TNF-alpha induce histone acetylation and NF-kappaB/AP-1 activation in alveolar epithelial cells: potential mechanism in gene transcription in lung inflammation. Mol Cell Biochem 2002;234-235:239-48.

Raines EW, Ferri N. Thematic review series: The immune system and atherogenesis. Cytokines affecting endothelial and smooth muscle cells in vascular disease. J Lipid Res 2005;46:1081-92.

Rao DD, Vorhies JS, Senzer N, Nemunaitis J. siRNA vs. shRNA: similarities and differences. Adv Drug Deliv Rev 2009;61:746-59.

Rauscher FJ 3rd. The WT1 Wilms tumor gene product: a developmentally regulated transcription factor in the kidney that functions as a tumor suppressor. FASEB J 1993;7:896-903.

Rauscher FJ 3rd, Morris JF, Tournay OE, Cook DM, Curran T. Binding of the Wilms' tumor locus zinc finger protein to the EGR-1 consensus sequence. Science 1990;250:1259-62.

Reitsma PH, Versteeg HH, Middeldorp S. Mechanistic view of risk factors for venous thromboembolism. Arterioscler Thromb Vasc Biol 2012;32:563-8.

Rittenhouse J, Marcus F. Peptide mapping by polyacrylamide gel electrophoresis after cleavage at aspartyl-prolyl peptide bonds in sodium dodecyl sulfate-containing buffers. Anal Biochem 1984;138:442-8.

Roberts SG. Transcriptional regulation by WT1 in development. Curr Opin Genet Dev 2005;15:542-7.

Roh TY, Cuddapah S, Zhao K. Active chromatin domains are defined by acetylation islands revealed by genome-wide mapping. Genes Dev 2005;19:542-52.

Ross R. Atherosclerosis--an inflammatory disease. N Engl J Med 1999;340:115-26.

Ross R. Cell biology of atherosclerosis. Annu Rev Physiol 1995;57:791-804.

Ross R. The pathogenesis of atherosclerosis: a perspective for the 1990s. Nature 1993;362:801-9.

Saha P, Humphries J, Modarai B, Mattock K, Waltham M, Evans CE, Ahmad A, Patel AS, Premaratne S, Lyons OT, Smith A. Leukocytes and the natural history of deep vein thrombosis: current concepts and future directions. Arterioscler Thromb Vasc Biol 2011;31:506-12.

Sambrook J, Russell DW. Molecular cloning: a laboratory manual. CSHL Press, Cold Spring Harbor, New York 2001.

Saxonov S, Berg P, Brutlag DL. A genome-wide analysis of CpG dinucleotides in the human genome distinguishes two distinct classes of promoters. Proc Natl Acad Sci U S A 2006;103:1412-7.

Scalia R, Gooszen ME, Jones SP, Hoffmeyer M, Rimmer DM 3rd, Trocha SD, Huang PL, Smith MB, Lefer AM, Lefer DJ. Simvastatin exerts both anti-inflammatory and cardioprotective effects in apolipoprotein E-deficient mice. Circulation 2001;103:2598-603.

Schmitz ML, dos Santos Silva MA, Baeuerle PA. Transactivation domain 2 (TA2) of p65 NF-kappa B. Similarity to TA1 and phorbolester-stimulated activity and phosphorylation in intact cells. J Biol Chem 1995;270:15576-84.

Schreiber E, Matthias P, Müller MM, Schaffner W. Rapid detection of octamer binding proteins with 'mini-extracts', prepared from a small number of cells. Nucleic Acids Res 1989;17:6419.

Schunkert H, König IR, Kathiresan S, Reilly MP, Assimes TL, Holm H, Preuss M, Stewart AF, Barbalic M, Gieger C, Absher D, Aherrahrou Z, Allayee H, Altshuler D, Anand SS, Andersen K, Anderson JL, Ardissino D, Ball SG, Balmforth AJ, Barnes TA, Becker DM, Becker LC, Berger K, Bis JC, Boekholdt SM, Boerwinkle E, Braund PS, Brown MJ, Burnett MS, Buysschaert I; Cardiogenics, Carlquist JF, Chen L, Cichon S, Codd V, Davies RW, Dedoussis G, Dehghan A, Demissie S, Devaney JM, Diemert P, Do R, Doering A, Eifert S, Mokhtari NE, Ellis SG, Elosua R, Engert JC, Epstein SE, de Faire U, Fischer M, Folsom AR, Freyer J, Gigante B, Girelli D, Gretarsdottir S, Gudnason V, Gulcher JR, Halperin E, Hammond N, Hazen SL, Hofman A, Horne BD, Illig T, Iribarren C, Jones GT, Jukema JW, Kaiser MA, Kaplan LM, Kastelein JJ, Khaw KT, Knowles JW, Kolovou G, Kong A, Laaksonen R, Lambrechts D, Leander K, Lettre G, Li M, Lieb W, Loley C, Lotery AJ, Mannucci PM, Maouche S, Martinelli N, McKeown PP, Meisinger C, Meitinger T, Melander O, Merlini PA, Mooser V, Morgan T, Mühleisen TW, Muhlestein JB, Münzel T, Musunuru K, Nahrstaedt J, Nelson CP, Nöthen MM, Olivieri O, Patel RS, Patterson CC, Peters A, Peyvandi F, Qu L, Quyyumi AA, Rader DJ, Rallidis LS, Rice C, Rosendaal FR, Rubin D, Salomaa V, Sampietro ML, Sandhu MS, Schadt E, Schäfer A, Schillert A, Schreiber S, Schrezenmeir J, Schwartz SM, Siscovick DS, Sivananthan M, Sivapalaratnam S, Smith A, Smith TB, Snoep JD, Soranzo N, Spertus JA, Stark K, Stirrups K, Stoll M, Tang WH, Tennstedt S, Thorgeirsson G, Thorleifsson G, Tomaszewski M, Uitterlinden AG, van Rij AM, Voight BF, Wareham NJ, Wells GA, Wichmann HE, Wild PS, Willenborg C, Witteman JC, Wright BJ, Ye S, Zeller T, Ziegler A, Cambien F, Goodall AH, Cupples LA, Quertermous T, März W, Hengstenberg C, Blankenberg S, Ouwehand WH, Hall AS, Deloukas P, Thompson JR, Stefansson K, Roberts R, Thorsteinsdottir U, O'Donnell CJ, McPherson R, Erdmann J; CARDIoGRAM Consortium, Samani NJ. Large-scale association analysis identifies 13 new susceptibility loci for coronary artery disease. Nat Genet 2011;43:333-8.

Seeler JS, Muchardt C, Suessle A, Gaynor RB. Transcription factor PRDII-BF1 activates human immunodeficiency virus type 1 gene expression. J Virol 1994;68:1002-9.

Seshasayee D, Geiger JN, Gaines P, Wojchowski DM. Intron 1 elements promote erythroid-specific GATA-1 gene expression. J Biol Chem 2000;275:22969-77.

Shah PK. Mechanisms of plaque vulnerability and rupture. J Am Coll Cardiol 2003;41:15S-22S.

Shaw G, Kamen R. A conserved AU sequence from the 3' untranslated region of GM-CSF mRNA mediates selective mRNA degradation. Cell 1986;46:659-67.

Sheppard KA, Rose DW, Haque ZK, Kurokawa R, McInerney E, Westin S, Thanos D, Rosenfeld MG, Glass CK, Collins T. Transcriptional activation by NF-kappaB requires multiple coactivators. Mol Cell Biol 1999;19:6367-78.

Silverman ES, Collins T. Pathways of Egr-1-mediated gene transcription in vascular biology. Am J Pathol 1999;154:665-70.

Simionescu M. Implications of early structural-functional changes in the endothelium for vascular disease. Arterioscler Thromb Vasc Biol 2007;27:266-74.

Skerka C, Decker EL, Zipfel PF. A regulatory element in the human interleukin 2 gene promoter is a binding site for the zinc finger proteins Sp1 and EGR-1. J Biol Chem 1995;270:22500-6.

Smale ST. Hierarchies of NF-κB target-gene regulation. Nat Immunol 2011;12:689-94.

Smale ST, Baltimore D. The "initiator" as a transcription control element. Cell 1989;57:103-13.

Smale ST, Kadonaga JT. The RNA polymerase II core promoter. Annu Rev Biochem 2003;72:449-79.

Smale ST, Schmidt MC, Berk AJ, Baltimore D. Transcriptional activation by Sp1 as directed through TATA or initiator: specific requirement for mammalian transcription factor IID. Proc Natl Acad Sci U S A 1990;87:4509-13.

Smith JD, Trogan E, Ginsberg M, Grigaux C, Tian J, Miyata M. Decreased atherosclerosis in mice deficient in both macrophage colony-stimulating factor (op) and apolipoprotein E. Proc Natl Acad Sci U S A 1995;92:8264-8.

Sposito AC, Chapman MJ. Statin therapy in acute coronary syndromes: mechanistic insight into clinical benefit. Arterioscler Thromb Vasc Biol 2002;22:1524-34.

Srinivasan L, Atchison ML. YY1 DNA binding and PcG recruitment requires CtBP. Genes Dev 2004;18:2596-601.

Tang D, Park HJ, Georgescu SP, Sebti SM, Hamilton AD, Galper JB. Simvastatin potentiates tumor necrosis factor alpha-mediated apoptosis of human vascular endothelial cells via the inhibition of the geranylgeranylation of RhoA. Life Sci 2006;79:1484-92.

Takemoto M, Liao JK. Pleiotropic effects of 3-hydroxy-3-methylglutaryl coenzyme a reductase inhibitors. Arterioscler Thromb Vasc Biol 2001;21:1712-9.

Tedgui A, Mallat Z. Cytokines in atherosclerosis: pathogenic and regulatory pathways. Physiol Rev 2006;86:515-81.

Telgmann R, Dördelmann C, Brand E, Nicaud V, Hagedorn C, Pavenstädt H, Cambien F, Tiret L, Paul M, Brand-Herrmann SM. Molecular genetic analysis of a human insulin-like growth factor 1 promoter P1 variation. FASEB J 2009;23:1303-13.

Thomas MC, Chiang CM. The general transcription machinery and general cofactors. Crit Rev Biochem Mol Biol 2006;41:105-78.

Towbin H, Staehelin T, Gordon J. Electrophoretic transfer of proteins from polyacrylamide gels to nitrocellulose sheets: procedure and some applications. Proc Natl Acad Sci USA 1979;76:4350-4.

Trégouët DA, Heath S, Saut N, Biron-Andreani C, Schved JF, Pernod G, Galan P, Drouet L, Zelenika D, Juhan-Vague I, Alessi MC, Tiret L, Lathrop M, Emmerich J, Morange PE. Common susceptibility alleles are unlikely to contribute as strongly as the FV and ABO loci to VTE risk: results from a GWAS approach. Blood 2009;113:5298-303.

Undas A, Brummel KE, Musial J, Mann KG, Szczeklik A. Simvastatin depresses blood clotting by inhibiting activation of prothrombin, factor V, and factor XIII and by enhancing factor Va inactivation. Circulation 2001;103:2248-53.

Venter JC, Adams MD, Myers EW, Li PW, Mural RJ, Sutton GG, Smith HO, Yandell M, Evans CA, Holt RA, Gocayne JD, Amanatides P, Ballew RM, Huson DH, Wortman JR, Zhang Q, Kodira CD, Zheng XH, Chen L, Skupski M, Subramanian G, Thomas PD, Zhang J, Gabor Miklos GL, Nelson C, Broder S, Clark AG, Nadeau J, McKusick VA, Zinder N, Levine AJ, Roberts RJ, Simon M, Slayman C, Hunkapiller M, Bolanos R, Delcher A, Dew I, Fasulo D, Flanigan M, Florea L, Halpern A, Hannenhalli S, Kravitz S, Levy S, Mobarry C, Reinert K, Remington K, Abu-Threideh J, Beasley E, Biddick K, Bonazzi V, Brandon R, Cargill M, Chandramouliswaran I, Charlab R, Chaturvedi K, Deng Z, Di Francesco V, Dunn P, Eilbeck K, Evangelista C, Gabrielian AE, Gan W, Ge W, Gong F, Gu Z, Guan P, Heiman TJ, Higgins ME, Ji RR, Ke Z, Ketchum KA, Lai Z, Lei Y, Li Z, Li J, Liang Y, Lin X, Lu F, Merkulov GV, Milshina N, Moore HM, Naik AK, Narayan VA, Neelam B, Nusskern D, Rusch DB, Salzberg S, Shao W, Shue B, Sun J, Wang Z, Wang A, Wang X, Wang J, Wei M, Wides R, Xiao C, Yan C, Yao A, Ye J, Zhan M, Zhang W, Zhang H, Zhao Q, Zheng L, Zhong F, Zhong W, Zhu S, Zhao S, Gilbert D, Baumhueter S, Spier G, Carter C, Cravchik A, Woodage T, Ali F, An H, Awe A, Baldwin D, Baden H, Barnstead M, Barrow I, Beeson K, Busam D, Carver A, Center A, Cheng ML, Curry L, Danaher S, Davenport L, Desilets R, Dietz S, Dodson K, Doup L, Ferriera S, Garg N, Gluecksmann A, Hart B, Haynes J, Haynes C, Heiner C, Hladun S, Hostin D, Houck J, Howland T, Ibegwam C, Johnson J, Kalush F, Kline L, Koduru S, Love A, Mann F, May D, McCawley S, McIntosh T, McMullen I, Moy M, Moy L, Murphy B, Nelson K, Pfannkoch C, Pratts E, Puri V, Qureshi H, Reardon M, Rodriguez R, Rogers YH, Romblad D, Ruhfel B, Scott R, Sitter C, Smallwood M, Stewart E, Strong R, Suh E, Thomas R, Tint NN, Tse S, Vech C, Wang G, Wetter J, Williams S, Williams M, Windsor S, Winn-Deen E, Wolfe K, Zaveri J, Zaveri K, Abril JF, Guigó R, Campbell MJ, Sjolander KV, Karlak B, Kejariwal A, Mi H, Lazareva B, Hatton T, Narechania A, Diemer K, Muruganujan A, Guo N, Sato S, Bafna V, Istrail S, Lippert R, Schwartz R, Walenz B, Yooseph S, Allen D, Basu A, Baxendale J, Blick L, Caminha M, Carnes-Stine J, Caulk P, Chiang YH, Coyne M, Dahlke C, Mays A, Dombroski M, Donnelly M, Ely D, Esparham S, Fosler C, Gire H, Glanowski S, Glasser K, Glodek A, Gorokhov M, Graham K, Gropman B, Harris M, Heil J, Henderson S, Hoover J, Jennings D, Jordan C, Jordan J, Kasha J, Kagan L, Kraft C, Levitsky A, Lewis M, Liu X, Lopez J, Ma D, Majoros W, McDaniel J, Murphy S, Newman M, Nguyen T, Nguyen N, Nodell M, Pan S, Peck J, Peterson M, Rowe W, Sanders R, Scott J, Simpson M, Smith T, Sprague A, Stockwell T, Turner R, Venter E, Wang M, Wen M, Wu D, Wu M, Xia A, Zandieh A, Zhu X. The sequence of the human genome. Science 2001;291:1304-51.

Vermeulen L, De Wilde G, Van Damme P, Vanden Berghe W, Haegeman G. Transcriptional activation of the NF-kappaB p65 subunit by mitogen- and stress-activated protein kinase-1 (MSK1). EMBO J 2003;22:1313-24.

Viemann D, Goebeler M, Schmid S, Nordhues U, Klimmek K, Sorg C, Roth J. TNF induces distinct gene expression programs in microvascular and macrovascular human endothelial cells. J Leukoc Biol 2006;80:174-85.

Vilar JM, Saiz L. DNA looping in gene regulation: from the assembly of macromolecular complexes to the control of transcriptional noise. Curr Opin Genet Dev 2005;15:136-44.

Wakefield TW, Myers DD, Henke PK. Mechanisms of venous thrombosis and resolution. Arterioscler Thromb Vasc Biol 2008;28:387-91.

Weis M, Heeschen C, Glassford AJ, Cooke JP. Statins have biphasic effects on angiogenesis. Circulation 2002;105:739-45.

Wierstra I. Sp1: emerging roles--beyond constitutive activation of TATA-less housekeeping genes. Biochem Biophys Res Commun 2008;372:1-13.

Wilkinson IB, Franklin SS, Cockcroft JR. Nitric oxide and the regulation of large artery stiffness: from physiology to pharmacology. Hypertension 2004;44:112-6.

Wu KK, Thiagarajan P. Role of endothelium in thrombosis and hemostasis. Annu Rev Med 1996;47:315-31.

Wu LC, Liu Y, Strandtmann J, Mak CH, Lee B, Li Z, Yu CY. The mouse DNA binding protein Rc for the kappa B motif of transcription and for the V(D)J recombination signal sequences contains composite DNA-protein interaction domains and belongs to a new family of large transcriptional proteins. Genomics 1996;35:415-24.

Yao J, Mackman N, Edgington TS, Fan ST. Lipopolysaccharide induction of the tumor necrosis factor-alpha promoter in human monocytic cells. Regulation by Egr-1, c-Jun, and NF-kappaB transcription factors. J Biol Chem 1997;272:17795-801.

Yin MJ, Yamamoto Y, Gaynor RB. The anti-inflammatory agents aspirin and salicylate inhibit the activity of I(kappa)B kinase-beta. Nature 1998;396:77-80.

Yu B, Mitchell GA, Richter A. Cirhin up-regulates a canonical NF-kappaB element through strong interaction with Cirip/HIVEP1. Exp Cell Res 2009;315:3086-98.

Yuan GC, Liu YJ, Dion MF, Slack MD, Wu LF, Altschuler SJ, Rando OJ. Genome-scale identification of nucleosome positions in S. cerevisiae. Science 2005;309:626-30.

Zee RY, Glynn RJ, Cheng S, Steiner L, Rose L, Ridker PM. An evaluation of candidate genes of inflammation and thrombosis in relation to the risk of venous thromboembolism: The Women's Genome Health Study. Circ Cardiovasc Genet 2009;2:57-62.

Zhan Q, Chen IT, Antinore MJ, Fornace AJ Jr. Tumor suppressor p53 can participate in transcriptional induction of the GADD45 promoter in the absence of direct DNA binding. Mol Cell Biol 1998;18:2768-78.

Zhang HG, Hyde K, Page GP, Brand JP, Zhou J, Yu S, Allison DB, Hsu HC, Mountz JD. Novel tumor necrosis factor alpha-regulated genes in rheumatoid arthritis. Arthritis Rheum 2004;50:420-31.

Zhong H, May MJ, Jimi E, Ghosh S. The phosphorylation status of nuclear NF-kappa B determines its association with CBP/p300 or HDAC-1. Mol Cell 2002;9:625-36.

Zhong H, SuYang H, Erdjument-Bromage H, Tempst P, Ghosh S. The transcriptional activity of NF-kappaB is regulated by the IkappaB-associated PKAc subunit through a cyclic AMP-independent mechanism. Cell 1997;89:413-24.

Electronic sources

ALGGEN – PROMO 3.0.2
http://alggen.lsi.upc.es/cgi-bin/promo_v3/promo/promoinit.cgi?dirDB=TF_8.3
(last access: 16.02.2012)

AliBaba 2.1
http://www.generegulation.com/pub/programs/alibaba2/index.html
(last access: 16.02.2012)

Catalog of Published Genome-Wide Association Studies
http://www.genome.gov/gwastudies/
(last access: 25.02.2012)

Gene Expression Ominbus (GEO, Microarray Database)
http://www.ncbi.nlm.nih.gov/geo/info/linking.html
(last access: 28.09.2011)

National Center for Biotechnology Information (NCBI):
http://www.ncbi.nlm.nih.gov/guide/
(last access: 07.04.2012)

ParAlign
http://www.paralign.org/
(last access: 17.11.2011)

siRNA at WHITEHEAD
http://sirna.wi.mit.edu/
(last access: 17.11.2011)

UCSC Genome Browser
http://genome.ucsc.edu/
(last access: 27.02.2012)

8 APPENDIX

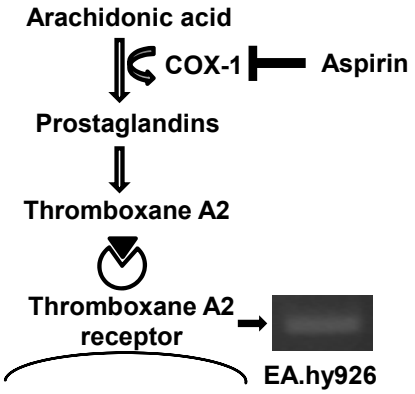

Figure A1: Endogenous expression of the *TXA2* receptor in EA.hy926 cells Aspirin inhibits COX-1 leading to inhibition of TXA2 synthesis, a mediator of platelet aggregation and vasoconstriction. We observed endogenous expression of *TXA2* in EA.hy926 cells, confirming that the components necessary for the aspirin pathway are present in EA.hy926 cells. PCR was performed after RNA isolation and cDNA generation using primers for both *TXA2 receptor type α* and *β*.

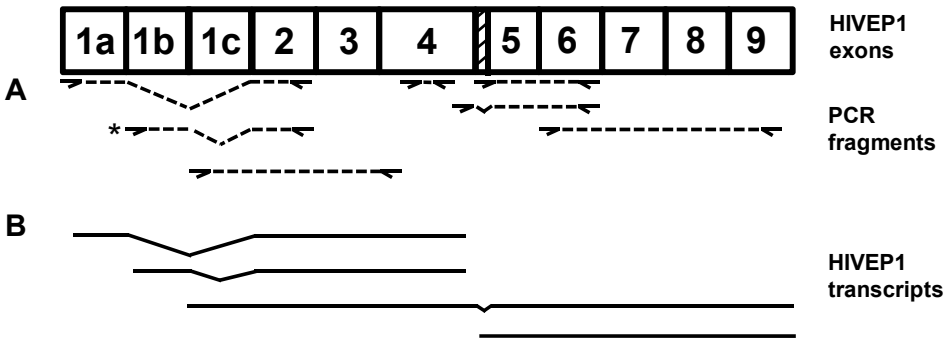

Figure A2: Schematic representation of sequential detection of HIVEP1 transcripts in EA.hy926 and THP1 cells A) PCR fragments (dashed lines) were generated using sequence-specific primers based on HIVEP1 mRNA (NM_002114.2). B) HIVEP1 transcripts in EA.hy926 and THP1 cells deduced from sequential detection of *HIVEP1* exons (white boxes) (A) and ENSEMBL database. Shaded box: alternative part of exon 5; *: exclusively in EA.hy926 cells.

Table A1: Oligonucleotides* used for sequential analysis of HIVEP1 transcripts

Exons	Sequence 5'-3'	Amplicon size (bp)
1a - 2	SS: CACTTCCAACCTAGGAGGC AS: CTCTTAGATTTCTGGGATGAATTTG	243
1b - 2	SS: GCC CCA AAG ACG CTA AAC G AS: CTCTTAGATTTCTGGGATGAATTTG	192
1c - 4[♣$]	SS: CGCCATCAGCAGCGCAGC AS: GCACTATGAAGAACGGCGAAAG	439
4	SS: GCCTTCAGTTTCAGAATGCTCTG AS: GCTTGGGATCCATGGTCTGC	153
4 - 6	SS: TTGCACTTGCTCTCCTTAATTC AS: CAGTAAGTGCAGTGGTAGGG	411
5 - 6	SS: TTCCTTTCAGAGAGCATTAGG AS: CTTTAGTCTTAAAGGAGAAGTTAC	325
6 - 9	SS: GAGTATGTATATGTCCGAGGC AS: GCTATCACAAGCCTGTCCTCG	1948
8[$]	SS: CAGAGATTCAGTTATGAGCGATC AS: GTTATAGCAACAGCTTTTCCTGC	479

* based on NM_002114.2
[♣] used for *HIVEP1* endogenous expression PCR under basic and stimulatory conditions
[$] used for *HIVEP1* knockdown monitoring
SS: sense primer; AS: antisense primer

9 CONFERENCES

Salomon A, Schmitz B, Rötrige A, Bruns F, Brand E, Morange PE, Cambien F, Tiret L, Trégouët D, Brand SM. Characterization and functional analysis of the proximal HIVEP1 promoter. 34. Wissenschaftlicher Kongress der Deutschen Hochdruckliga e.V. DHL® - Deutsche Hypertonie Gesellschaft, Berlin 09.-11. Dezember 2010.

Salomon A, Schmitz B, Rötrige A, Brand E, Morange PE, Cambien F, Tiret L, Trégouët D, Brand SM. Characterization of the 5´-flanking region promoting human immunodeficiency virus type 1 enhancer binding protein 1 (HIVEP1) gene expression. 77. Jahrestagung der DGPT, Frankfurt a. M. 30. März - 01. April 2011.

Salomon A, Schmitz B, Rötrige A, Brand E, Morange PE, Cambien F, Tiret L, Trégouët D, Brand SM. Functional analysis of the 5´-flanking region promoting HIVEP1 gene expression. 77. Jahrestagung der Deutschen Gesellschaft für Kardiologie, Mannheim 27.-30. April 2011.

Salomon A, Schmitz B, Rötrige A, Brand E, Morange PE, Cambien F, Tiret L, Trégouët D, Brand SM. Analysis of 5´-flanking regulatory elements of the human immunodeficiency virus type 1 enhancer binding protein 1 (HIVEP1). 21st European Meeting on Hypertension, Mailand 17.-20. Juni 2011. Oral presentation.

Salomon A, Schmitz B, Herrmann M, Rötrige A, Brand E, Morange PE, Cambien F, Tiret L, Trégouët D, Brand SM. Transcriptional regulation of the human immunodeficiency virus type 1 enhancer binding protein 1 (HIVEP1). 3. Jahrestagung der Deutschen Gesellschaft für Nephrologie, Berlin 10.-13. September 2011.

Salomon A, Schmitz B, Herrmann M, Rötrige A, Brand E, Morange PE, Cambien F, Tiret L, Trégouët D, Brand SM. Identification of regulatory elements promoting *human immunodeficiency virus type 1 enhancer binding protein 1 (HIVEP1)* gene expression. Basic Science Meeting der Deutschen Gesellschaft für Kardiologie – Herz-Kreislaufforschung e.V., Düsseldorf 06.-08. Oktober 2011.

Salomon A, Schmitz B, Herrmann M, Rötrige A, Brand E, Morange PE, Cambien F, Tiret L, Trégouët D, Brand SM. Transcriptional control of the human immunodeficiency virus type 1 enhancer binding protein 1 (HIVEP1). 35. Wissenschaftlicher Kongress der Deutschen Hochdruckliga e.V. DHL® - Deutsche Hypertonie Gesellschaft, Köln 24.-26. November 2011.

Salomon A, Schmitz B, Rötrige A, Brand E, Morange PE, Cambien F, Tiret L, Trégouët D, Brand SM. The human immunodeficiency virus type 1 enhancer binding protein 1 (HIVEP1) is regulated by proinflammatory stimuli and statins. 78. Jahrestagung der DGPT, Dresden 19.-22. März 2012. Oral presentation.

Salomon A, Schmitz B, Rötrige A, Brand E, Morange PE, Cambien F, Tiret L, Trégouët D, Brand SM. Regulation of transcription factor HIVEP1 by simvastatin and inflammatory stimuli. 22st European Meeting on Hypertension, London 26.-29. April 2012. Oral presentation.

10 PUBLICATIONS

Schmitz B, Salomon A, Rötrige A, Fischer JW, Paul M, Brand E and Brand SM. Inter-individual transcriptional regulation of the human *biglycan* gene involves three common molecular haplotypes (MolHaps). Submitted.

Salomon A, Schmitz B, Herrmann M, Rötrige A, Fabritius C, Morange PE, Cambien F, Tiret L, Trégouët DA, Pap T, Brand E and Brand SM. Regulation of transcription factor HIVEP1 by inflammatory cytokines and statins. Manuscript ready for submission.

Danksagung

Mein besonderer Dank gilt Herrn Univ.-Prof. Dr. Dr. Stefan-Martin Brand für die Bereitstellung des interessanten Promotionsthemas und das Vertrauen in meine Arbeit und Person, insbesondere zu Beginn der Dissertation. Außerdem danke ich Ihm für die Möglichkeit, meine Arbeit auf nationalen und internationalen Kongressen vorzustellen und daraus profitieren zu können. Ebenso danke ich Herrn Univ.-Prof. Dr. Bruno Moerschbacher, meinem Betreuer der biologischen Fakultät der WWU.

Ein ausdrücklicher Dank geht an alle KollegInnen der Arbeitsgruppen von Frau Univ.-Prof. Dr. Dr. Eva Brand und Herrn Univ.-Prof. Dr. Dr. Stefan-Martin Brand. Eure Hilfe war Gold wert, Eure Unterstützung in allen Phasen der Promotion hat zu dem Gelingen und Vollenden der Arbeit beigetragen. Mein Dank gilt Dr. Boris Schmitz für die gute Einführung ins Labor und die Betreuung meiner Dissertation. Den technischen AssistentInnen Christine Fabritius, Karin Tegelkamp, Margit Käse und Alois Rötrige danke ich sehr, ohne Euch läuft das Labor einfach nicht! Hierbei danke ich besonders Christine Fabritius und Alois Rötrige, Eure Unterstützung in jeglicher Hinsicht hat mich jeden Tag motiviert! Meinen Mitstreitern, den DoktorandInnen Katrin Guske, Mareike Herrmann und Michael Schelleckes danke ich für die gute Zusammenarbeit, die anregenden Diskussionen und die schöne Zeit. Mareike Herrmann danke ich besonders für die sehr gute Teamarbeit während der gesamten drei Jahre!

Bei meiner „Hammer-Clique“ und besonders bei meinen „Bonner-Mädels“ möchte ich mich bedanken. Die Telefonate und Treffen mit Euch waren eine wunderbare Ablenkung und gaben mir stets neue Kraft!

Meiner Familie kann ich nicht genug danken. Ich danke meinem Bruder Richard, Deine ganz eigenen Tipps waren sehr wichtig für mich. Oma und Opa danke ich für das unermüdliche Daumendrücken und Mitfiebern. Vor allem danke ich meinen Eltern für die stetige grenzenlose Unterstützung mit allen Mitteln und in allen Lebenslagen! Ebenso danke ich Dir, Christopher, für die unermüdliche Unterstützung jeden Tag und dafür, dass Du immer schon an mich geglaubt hast!